



## Interfacial-engineering-enabled high-performance Li-rich cathodes



Quanxin Ma<sup>a</sup>, Mengqian Yang<sup>a</sup>, Junxia Meng<sup>b,\*</sup>, Lingfei Zhou<sup>a</sup>, Lishuang Xu<sup>b</sup>, Fangrui Wang<sup>a</sup>, Tiankai Sun<sup>a</sup>, Ruihong Li<sup>c</sup>, Shengwen Zhong<sup>a</sup>, Qian Zhang<sup>a</sup>, Xianfa Rao<sup>a</sup>, Tiefeng Liu<sup>d</sup>

<sup>a</sup> Key Laboratory of Power Battery and Materials, Faculty of Materials Metallurgy and Chemistry, Jiangxi University of Science and Technology, Ganzhou 341000, China

<sup>b</sup> School of Physics and Electronics, Gannan Normal University, Ganzhou 341000, China

<sup>c</sup> ZJU-Hangzhou Global Scientific and Technological Innovation Center, Zhejiang University, Hangzhou 311215, China

<sup>d</sup> College of Chemical and Biological Engineering, Zhejiang University, Hangzhou, 310027, China

### ARTICLE INFO

#### Keywords:

Li-rich layered oxides  
Oxygen vacancies  
OVs-spinel layer  
Voltage fading  
Cycling stability

### ABSTRACT

Li-rich layered oxides (LLOs) with high energy density and low cost are regarded as the most promising cathode materials for the next generation Li-ion batteries (LIBs). However, the rapid capacity decline and voltage fading impede their practical application. Herein, an OVs(oxygen vacancies)-spinel functional layer with rich-OVs and surface spinel phase is constructed on the surface of  $\text{Li}_{1.2}\text{Mn}_{0.56}\text{Ni}_{0.16}\text{Co}_{0.08}\text{O}_2$  (LLMO) through  $\text{Y}_2\text{O}_3$  and  $\text{ZrO}_2$  co-modification. The interface OVs effectively stabilize lattice oxygen evolution and suppress structural distortion by storing  $\text{O}_2$  or  $\text{O}^{(2-n)}$  released from LLMO within these OVs, while the formation of spinel phase in the subsurface motivates rapid  $\text{Li}^+$  transfer. The comprehensive effect of this OVs-spinel layer synergistically inhibits irreversible oxygen release, mitigates electrolyte decomposition, and accelerates  $\text{Li}^+$  ions diffusion kinetics. The corresponding cathode with  $\text{Y}_2\text{O}_3$  and  $\text{ZrO}_2$  co-modification (Y&Zr-LLMO) exhibits an average attenuation voltage of 2.5 mV per cycle (vs. 3.3 mV), and a capacity retention rate of 95.4 % after 100 cycles at 1C (vs. 86.5 %). Remarkably, the pouch cell (Y&Zr-LLMO/graphite) also demonstrates excellent cycling stability, retaining 71.4 % capacity after 600 cycles at 0.5C. This finding pioneers multifunctional interface layer designs for high energy density LIBs.

### 1. Introduction

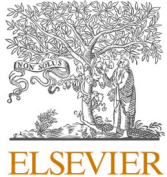
To meet the booming energy storage and conversion fields, developing high energy density, low cost, and environmental friendliness cathodes become urgent [1,2]. Among the various advanced cathode materials, Li-rich Mn-based layered oxides (LLOs), depicted as  $(1-x)\text{Li}_2\text{MnO}_3 \bullet x\text{LiMO}_2$  ( $M = \text{Mn, Co, and Ni}$ ), have garnered significant attention due to their potential to deliver both high energy density ( $1000\text{Wh kg}^{-1}$ ) and high specific capacity ( $>250\text{mAh g}^{-1}$ ) [3,4]. However, they still suffer from poor rate performance and detrimental voltage/capacity decay, which hinder their practical applications. These obstacles are mainly attributable to the irreversible oxygen release from the activation of  $\text{Li}_2\text{MnO}_3$  phase during the charging process, which is the result of the redox reaction involving both cations and anions, leading to irreversible oxygen release and phase transitions [5,6]. Therefore, it is essential to inhibit the irreversible oxygen release for the practical application of LLOs.

LLOs are generally perceived as solid solution materials, composed of

rhombohedral  $\text{LiMO}_2$  with  $R-3m$  space group and monoclinic  $\text{Li}_2\text{MnO}_3$  with  $C2/m$  space group [7,8]. Complex solid solution structure leads to its confusing electrochemical mechanism. Typically, the anionic redox reaction concludes a reversible anodic redox ( $\text{O}^{2-}$  to  $\text{O}^{n-}$ ) and an irreversible lattice oxygen loss ( $\text{O}^{2-}$  to  $\text{O}_2$ ) [9,10]. However, the continuous irreversible lattice oxygen loss usually causes the generation of some oxygen vacancies (OVs) on the surface of LLOs. These surface OVs exhibit dual characteristics. On one hand, the formation of OVs leads to the structural evolution from a layered into spinel-like phase and accelerates the electrolyte decomposition at the cathode surface and makes it unsafe [11–13], thereby destroying the crystal structure and aggravating voltage and capacity fading of the LLOs. On the other hand, OVs can significantly enhance intrinsic electronic conductivity and  $\text{Li}^+$  ions diffusion kinetics [14,15], making them valuable for applications in energy conversion and storage [16–18]. To stabilize the lattice oxygen and mitigate surface side reactions of electrode, surface coating and element doping has been studied to ameliorate these deficiencies [19–21]. However, most coating materials and doping elements are non-

\* Corresponding author.

E-mail address: [jxmeng@buaa.edu.cn](mailto:jxmeng@buaa.edu.cn) (J. Meng).



## Naming entity recognition of citrus pests and diseases based on the BERT-BiLSTM-CRF model

Yafei Liu, Siqi Wei, Haijun Huang, Qin Lai, Mengshan Li<sup>\*</sup>, Lixin Guan<sup>\*</sup>

*College of Physics and Electronic Information, Gannan Normal University, Ganzhou 341000, Jiangxi, China*

### ARTICLE INFO

**Keywords:**

Citrus pests and diseases  
Named entity recognition  
BERT  
BiLSTM  
CRF

### ABSTRACT

In the agricultural industry, there is still a need for improved systematic integration of knowledge related to citrus pests and diseases. Creating a knowledge base focused on citrus pests and diseases and developing a knowledge map would enable the formation of a system providing accurate and convenient prevention and control methods for citrus growers. However, the majority of existing data on citrus pests and diseases is unstructured, making identifying named entities from large volumes of unstructured text data particularly important for creating a knowledge map. In this paper, we propose a training model based on Bidirectional Encoder Representation from Transformers (BERT), combined with Bidirectional Long and Short Term Memory Networks (BiLSTM) and Conditional Random Field (CRF), to extract specific entity categories from unstructured data. When tested on a created dataset, the model achieved an accuracy rate of 0.9423 and an f1 value of 0.8048. The results demonstrate that the proposed method can be applied to extract specific entity categories from text data related to citrus pests and diseases, laying a solid foundation for the subsequent construction of a knowledge map. This paper introduces a method for named entity recognition in the field of citrus pests and diseases, which could serve as a reference for constructing knowledge maps in other fields and improving the utilization of domain knowledge.

### 1. Introduction

Citrus is an important economic crop worldwide and is also among the agricultural and processed products traded internationally, occupying a significant proportion of the fruit trade. However, the harm caused by pests and diseases to citrus trees should not be underestimated. The variety and symptoms of citrus pests and diseases are numerous. Some of them seriously affect the entire growth cycle of citrus and not only impact the yield and quality of citrus but also can even lead to plant death (Guo et al., 2020). If the normal growth of citrus trees is affected, the economic benefits of the citrus industry will decrease (Yin, 2022). Therefore, it is crucial to integrate the prevention and control methods and technical knowledge related to citrus pests and diseases into a complete system and provide convenient, efficient, and accurate prevention and control methods for growers. Currently, there is no complete systematic knowledge base available for growers (Zhao et al., 2022). Some scattered pest and disease control information can be searched on various web pages, and much-related information is also recorded in books. The purpose of this paper is to integrate this

information, extract the important parts, and establish a foundation for building and utilizing a knowledge map (Zhang et al., 2022).

The collected unstructured text data covers a wealth of information on citrus pests and diseases including citrus diseases, citrus pests, distribution areas, prevention and control drugs, transmission methods, etc. The entity names for citrus diseases and pests are complex and varied, such as citrus whitefly also known as citrus yellow whitefly, common grass whitefly, naked citrus whitefly, powdery whitefly, etc., while brown rot disease is also known as foot rot, brown decay rot, skirt rot disease, and phytophthora brown rot. At the same time, there is also the phenomenon of nested entities, such as "Phytophthora mainly damages the seedlings of sour citrus and the grafted seedlings of sweet orange in Guangdong", which includes three types of entities, namely citrus disease (Phytophthora), transmission method (seedling, grafting), and affected part (seedling). Currently, there is no publicly available dataset for citrus pests and diseases, which makes named entity recognition in this field challenging.

Based on the collected text data characteristics and research on named entity recognition, this study aims to conduct named entity

\* Corresponding authors.

E-mail addresses: [jcimsli@163.com](mailto:jcimsli@163.com) (M. Li), [lxguan@gnnu.edu.cn](mailto:lxguan@gnnu.edu.cn) (L. Guan).

RESEARCH ARTICLE

[View Article Online](#)  
[View Journal](#) | [View Issue](#)



Cite this: *Inorg. Chem. Front.*, 2023,  
10, 984

## Electrochemically induced amorphous and porous VO<sub>x</sub>/N-doped carbon spheres as a cathode for advanced aqueous zinc-ion batteries†

Jujun Yuan,<sup>a</sup> Yunfei Gan,<sup>a,b</sup> jirong Mou,<sup>a</sup> Xiangdong Ma,<sup>a</sup> Xiaokang Li,<sup>a,b</sup> Junxia Meng,<sup>a</sup> Lishuang Xu,<sup>a</sup> Xianke Zhang,<sup>a\*</sup> Haishan He<sup>a,b</sup> and Jun Liu <sup>b\*</sup><sup>a,c</sup>

Vanadium-based oxides have captured considerable attention as ZIB cathodes benefiting from their rich valences and superior theoretical capacity. However, vanadium-based oxides still suffer from structural instability, low electronic conductivity, and slow reaction dynamics, which will lead to poor zinc ion storage performance. Herein, amorphous VO<sub>x</sub>/NC porous spheres were fabricated by *in situ*, electrochemically-induced vanadium-polydopamine-derived crystalline V<sub>2</sub>O<sub>3</sub>/NC porous spheres. As a zinc-ion battery cathode, the VO<sub>x</sub>/NC porous spheres exhibit a sustainable capacity of 233 mA h g<sup>-1</sup> at 5 A g<sup>-1</sup> upon 1500 cycles and superior rate property. The excellent electrochemical performance of the VO<sub>x</sub>/NC porous-sphere electrode is ascribed to its distinctive architecture. The VO<sub>x</sub>/NC porous spheres possess amorphous VO<sub>x</sub> with a higher oxidation states of V<sup>5+</sup>/V<sup>4+</sup>, which can increase the theoretical energy density, provide more active sites, and improve Zn<sup>2+</sup> diffusion kinetics. Furthermore, VO<sub>x</sub>/NC porous spheres with a porous core-shell architecture can enhance electrical conductivity and ensure electrolyte accessibility. This synthesis strategy can be potentially extended to fabricate other VO<sub>x</sub>/carbon composites with high valence states (V<sup>5+</sup> and V<sup>4+</sup>).

Received 5th October 2022,  
Accepted 3rd December 2022

DOI: 10.1039/d2qi02144g

rsc.li/frontiers-inorganic

## 1. Introduction

Lithium-ion batteries are widely utilized in the current battery market because of their high specific energy.<sup>1–4</sup> Nevertheless, the high cost of lithium raw materials and safety issues limit the development of lithium-ion batteries in large-scale energy storage. As a competitive candidate, rechargeable aqueous zinc-ion batteries (ZIBs) show high theoretical capacity (820 mA h g<sup>-1</sup>), rich zinc storage resources, and high safety.<sup>5–12</sup> Recently, typical ZIB cathode materials such as vanadium-based compounds,<sup>13–15</sup> manganese oxides,<sup>16,17</sup> and Prussian blue analogues<sup>18,19</sup> have been intensively explored on the basis of different electrochemical reaction mechanisms, involving conversion and intercalation/deintercalation processes. Particularly, vanadium-based oxides have captured con-

siderable attention for ZIB cathodes benefiting from their rich valences and superior theoretical capacity.<sup>20–26</sup> For example, Yang *et al.* reported that VO<sub>2</sub> (B) nanofibers with tunnel-like frameworks displayed a reversible capacity (357 mA h g<sup>-1</sup> at 0.25 C upon 50 cycles).<sup>7</sup> Cheng *et al.* reported that porous V<sub>2</sub>O<sub>5</sub> nanofibers exhibited a sustainable capacity (166 mA h g<sup>-1</sup> at 2 C upon 500 cycles).<sup>24</sup> Mai *et al.* also reported that VO<sub>2</sub> nanorods exhibited reversible capacity (75 mA h g<sup>-1</sup> at 3 A g<sup>-1</sup> upon 5000 cycles).<sup>25</sup> However, vanadium-based oxides still suffer from structural instability, low electronic conductivity, and slow reaction dynamics, which will lead to poor zinc ion storage performance.

For overcoming the above issues, carbon materials are usually introduced to improve the electrochemical performance of vanadium-based oxide electrodes. In particular, vanadium-based oxides/C nanomaterials with the advantages of superior electrical conductivity, good structural stability, and short ion diffusion length are proven for highly reversible ZIBs.<sup>27–31</sup> For instance, Chen *et al.* synthesized porous V<sub>2</sub>O<sub>3</sub>@C microspheres using V-MOF as the template. The V<sub>2</sub>O<sub>3</sub>@C electrode exhibited a reversible capacity of 175 mA h g<sup>-1</sup> at 5 A g<sup>-1</sup> upon 4000 cycles.<sup>27</sup> Wang *et al.* synthesized 3D spongy VO<sub>2</sub>/graphene nanocomposites using hydrothermal and chemical reduction methods. The VO<sub>2</sub>/graphene electrode exhibited 186 mA h g<sup>-1</sup> at 10 A g<sup>-1</sup> upon 5000 cycles.<sup>28</sup> Zhou

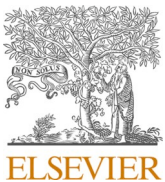
<sup>a</sup>Key Laboratory of New Energy Materials and Low Carbon Technologies, College of Physics and Electronics, Gannan Normal University, Ganzhou 341000, PR China.

E-mail: lixiaokang@gnnu.edu.cn, zhangxianke77@163.com

<sup>b</sup>College of Chemistry and Chemical Engineering, Gannan Normal University, Ganzhou 341000, PR China

<sup>c</sup>School of Materials Science and Engineering, South China University of Technology, Guangzhou 510641, P. R. China. E-mail: msjliu@scut.edu.cn

† Electronic supplementary information (ESI) available. See DOI: <https://doi.org/10.1039/d2qi02144g>



# Three-dimensional porous FeS@N doped carbon nanosheets for high-rate and high-stable sodium/potassium storage

Jujun Yuan<sup>a</sup>, Meiqi Mu<sup>a</sup>, Xijun Xu<sup>b,c,\*</sup>, Yunfei Gan<sup>a,d</sup>, Haishan He<sup>a,d</sup>, Xianke Zhang<sup>a</sup>, Xiaokang Li<sup>a,d,\*\*</sup>, Fanguang Kuang<sup>a</sup>, Haixia Li<sup>a</sup>, Jun Liu<sup>a,c,\*\*\*</sup>

<sup>a</sup> Key Laboratory of New Energy Materials and Low Carbon Technologies, College of Physics and Electronics, Gannan Normal University, Ganzhou, 341000, PR China

<sup>b</sup> School of Chemical Engineering and Light Industry, Guangdong University of Technology, Guangzhou, 510006, PR China

<sup>c</sup> School of Materials Science and Engineering, South China University of Technology, Guangzhou, 510641, PR China

<sup>d</sup> College of Chemistry and Chemical Engineering, Gannan Normal University, Ganzhou, 341000, PR China

## ARTICLE INFO

### Keywords:

Anode material  
3D FeS@NC nanosheets  
Sodium ion battery  
Potassium ion battery  
High capacity

## ABSTRACT

The three-dimensional (3D) FeS@N doped Carbon (NC) nanosheets are successfully synthesized using a simple sol-gel method followed by a solid sulfidation process. As SIBs anode, the 3D FeS@NC nanosheets exhibit a maintainable capacity ( $254 \text{ mAh g}^{-1}$  at  $1.5 \text{ A g}^{-1}$  upon 1100 cycles) and outstanding rate behaviour. As PIBs anode, the 3D FeS@NC nanosheets also exhibit a maintainable capacity ( $120 \text{ mAh g}^{-1}$  at  $1 \text{ A g}^{-1}$  upon 1100 cycles) and outstanding rate behaviour. The excellent electrochemical performance can be attributed to the distinctive 3D porous FeS@NC nanosheets, which can inhibit the aggregation and pulverization of FeS, enhance electronic/ionic conductivity, firmly immobilize the dissolved polysulfides, and provide a larger contact area between active materials and electrolytes. Moreover, the N-doped carbon framework can also provide substantial active sites for  $\text{Na}^+(\text{K}^+)$  storage. Our synthesizing strategy can be potentially utilized for fabricating other 3D metal sulfide@C composites for SIB (PIB) anodes.

## 1. Introduction

As effective power sources, lithium-ion batteries(LIBs) are universally used for portable electronic devices and electronic vehicles, and are regarded as prospective candidates in emerging smart grid technology [1–6]. However, the scarcity and high price of lithium resources block their going a step further development. In the quest for superseding LIBs in large-scale energy storage equipment, sodium (potassium) ion batteries (S(P)IBs) show giant latent capacity, because of sufficient natural resources and low price for Na (K), along with their analogous chemistry characteristics to those of Li [7–16]. The larger ionic radius ( $1.02 \text{ \AA}$  ( $1.38 \text{ \AA}$ ) of  $\text{Na}^+(\text{K}^+)$ ), nevertheless, bring about large volumetric expansion and sluggish reaction kinetics for electrode materials within charge/discharge processes. To meet the practical application of large-scale energy storage equipment, it is significant to search for efficient electrode materials with superior maintainable capacities as

### SIBs(PIBs) anodes.

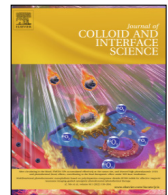
In recent years, Fe-related sulfides (e.g.,  $\text{FeS}$ ,  $\text{FeS}_2$ ,  $\text{Fe}_7\text{S}_8$ ,  $\text{Fe}_{1-x}\text{S}$ ) [17–23] have captured considerable attention for SIBs(PIBs) anode materials, which are benefited from their high theoretical capacities and oxidation-reduction invertibility. For instance, Chen and coworkers reported that  $\text{FeS}_2$  microspheres showed excellent rate properties ( $170 \text{ mA h g}^{-1}$  at  $20 \text{ A g}^{-1}$ ) for SIBs anode [18]. Sun and coworkers researched  $\text{FeS}_2$  nanotubes with sustainable capacity ( $360 \text{ mAh g}^{-1}$  at  $179 \text{ mA g}^{-1}$ ) for SIBs anode. Xu and coworkers also reported that  $\text{Fe}_{1-x}\text{S}$  microcubes exhibited a capacity of  $418 \text{ mAh g}^{-1}$  at  $50 \text{ mA g}^{-1}$  for PIBs anode [23]. Nevertheless, pure Fe-related sulfides generally meet with dissatisfied electrochemical behaviour as a result of delayed reaction kinetics, the larger volumetric change, and dissolution of the polysulfide intermediates in the charge/discharge processes. To overcome these problems, designing Fe-related sulfides/C nanocomposites has been regarded as a promising strategy, which can not only inhibit volumetric

\* Corresponding author. School of Chemical Engineering and Light Industry, Guangdong University of Technology, Guangzhou, 510006, PR China.

\*\* Corresponding author. Key Laboratory of New Energy Materials and Low Carbon Technologies, College of Physics and Electronics, Gannan Normal University, Ganzhou, 341000, PR China.

\*\*\* Corresponding author. Key Laboratory of New Energy Materials and Low Carbon Technologies, College of Physics and Electronics, Gannan Normal University, Ganzhou, 341000, PR China.

E-mail addresses: [xuxijun2022@gdut.edu.cn](mailto:xuxijun2022@gdut.edu.cn) (X. Xu), [lixiaokang@gnnu.edu.cn](mailto:lixiaokang@gnnu.edu.cn) (X. Li), [msjliu@scut.edu.cn](mailto:msjliu@scut.edu.cn) (J. Liu).



# Pomegranate-like structured Nb<sub>2</sub>O<sub>5</sub>/Carbon@N-doped carbon composites as ultrastable anode for advanced sodium/potassium-ion batteries

Jujun Yuan <sup>a,1</sup>, Xiaofan Li <sup>a,c,1</sup>, Jun Liu <sup>a,b,\*</sup>, Shiyong Zuo <sup>b</sup>, Xiaokang Li <sup>a,c,\*</sup>, Fangkun Li <sup>b</sup>, Yunfei Gan <sup>a,c</sup>, Haishan He <sup>a,c</sup>, Xijun Xu <sup>b</sup>, Xianke Zhang <sup>a,\*</sup>, Junxia Meng <sup>a</sup>

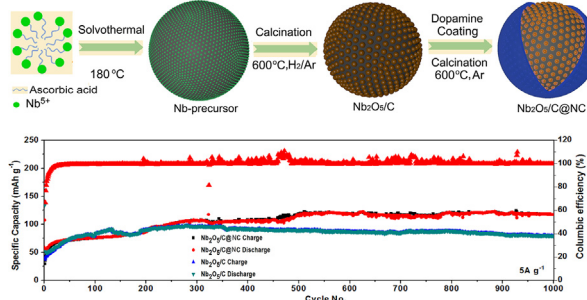
<sup>a</sup> School of Physics and Electronics, Gannan Normal University, Ganzhou 341000, PR China

<sup>b</sup> School of Materials Science and Engineering, South China University of Technology, Guangzhou 510641, PR China

<sup>c</sup> College of Chemistry and Chemical Engineering, Gannan Normal University, Ganzhou 341000, PR China



## GRAPHICAL ABSTRACT



## ARTICLE INFO

### Article history:

Received 14 November 2021

Revised 3 January 2022

Accepted 4 January 2022

Available online 7 January 2022

### Keywords:

Anode

Nb<sub>2</sub>O<sub>5</sub>/C@NC composites

Na-ion batteries

K-ion batteries

High rate and stable

## ABSTRACT

The distinctive pomegranate-like Nb<sub>2</sub>O<sub>5</sub>/Carbon@N-doped carbon (Nb<sub>2</sub>O<sub>5</sub>/C@NC) composites are fabricated using hydrothermal method integrated with nitrogen doped carbon coating procedure. For the SIBs anode, the Nb<sub>2</sub>O<sub>5</sub>/C@NC composites present superior rate character and sustainable capacity (117 mAh g<sup>-1</sup> upon 1000 cycles at 5 A g<sup>-1</sup>). The in-situ X-ray diffraction (XRD) is utilized to research its sodium storage mechanism. Furthermore, for PIBs, the Nb<sub>2</sub>O<sub>5</sub>/C@NC composites present sustainable capacity (81 mAh g<sup>-1</sup> upon 1000 cycles at 1 A g<sup>-1</sup>). The outstanding performance of Nb<sub>2</sub>O<sub>5</sub>/C@NC composites is ascribed to its unique architecture, in which Nb<sub>2</sub>O<sub>5</sub> nanocrystals embedded in porous carbon can restrain agglomeration of Nb<sub>2</sub>O<sub>5</sub> nanocrystals, enhance electron/ion diffusion kinetics, and ensure electrolyte accessibility, and moreover, NC shell layer can provide effective active sites and further increase ions/electrons transfer.

© 2022 Elsevier Inc. All rights reserved.

## 1. Introduction

As potential candidate for large-scale energy storage device, SIBs (PIBs) has got sustainable attention due to sufficiency of sodium (potassium) on earth [1–5]. But the large Na<sup>+</sup>(K<sup>+</sup>) radius (1.09 Å (1.38 Å)) bring about sluggish kinetics and larger volume variation in the process of discharge/charge cycle. Thus, seeking

\* Corresponding authors at: School of Physics and Electronics, Gannan Normal University, Ganzhou 341000, PR China.

E-mail addresses: msjliu@scut.edu.cn (J. Liu), gnnulxk@163.com (X. Li), zhangxianke77@163.com (X. Zhang).

<sup>1</sup> These authors contributed equally to this work.

# Modulating Crystal and Interfacial Properties by W-Gradient Doping for Highly Stable and Long Life Li-Rich Layered Cathodes

**Junxia Meng, Lishuang Xu, Quanxin Ma,\* Mengqian Yang, Yuzhong Fang, Guangying Wan, Ruhong Li,\* Jujun Yuan, Xianke Zhang, Huajun Yu, Lingli Liu, and Tiefeng Liu\***

**Stabilizing Li-rich layered oxides without capacity/voltage fade upon cycling is a prerequisite for a successful commercialization. Although the inhibition of structural and interfacial changes is identified as an effective strategy, the battery community always seeks for a technologically flexible method to make it really competitive among the cathode. Herein, the gradient W-doping within  $\text{Li}_{1.2}\text{Mn}_{0.56}\text{Ni}_{0.16}\text{Co}_{0.08}\text{O}_2$  (LLMO) is proposed to relieve crystal disintegration and simultaneously enhance interfacial stability because of the formation of  $\text{Li}_2\text{WO}_4$  coating layer on the material surface. This is mainly attributed to the scenario that partial Mn replacement by W can stabilize the LLMO structure and regulate the electrochemical activity of Mn element. The W-doped LLMO (W@LLMO) possesses improved specific capacity and voltage stability (83.2% capacity retention and voltage retention of 94.9% after 200 cycles at 0.5 C). Besides, a practical pouch cell based on the W@LLMO cathode presents sufficient gravimetric energy density ( $318 \text{ Wh kg}^{-1}$ ) and cycling stability (capacity retention of 87.7% after 500 cycles at 1.0 C). This study presents an effective method to design robust Li-rich layered cathodes for next-generation Li-ion batteries.**

## 1. Introduction

The use of Li-rich layered oxides (LLOs) with a formula of  $x\text{Li}_2\text{MnO}_3 \cdot (1-x)\text{LiMO}_2$  (M = Mn, Co, Ni, Fe, etc.) has been always projected from the battery community because of its capacity and cost advantages over other conventional cathodes<sup>[1]</sup> as part of the development of Li-ion battery (LIB) applications

requiring high-energy-density, sustainable, and affordable properties,<sup>[2]</sup> such as electric vehicles and grid storage.<sup>[3]</sup> Regrettably, cycling instability and capacity fade of LLOs stemming from irreversible structural distortion and pernicious oxygen redox seriously retard their large-scale practical applications.<sup>[4]</sup> Presently, the clear consensus has emphasized that the structural instability of LLOs mainly occurs in the initial charge process as accessing high states of delithiation,<sup>[5]</sup> while such a necessary pathway to activate high capacity undoubtedly renders the partial Li extraction<sup>[6]</sup> and irreversible oxygen loss ( $\text{O}^{2-} \rightarrow \text{O}_2$ ).<sup>[2b,7]</sup> Specifically, the release of lattice oxygen ( $\text{O}_L$ ) on particle surface causes the cation migration between transition metal (TM) layers and neighboring Li layers,<sup>[8]</sup> subsequently resulting in phase transformation from layered to spinel and then to rock salt phase.<sup>[9]</sup> Furthermore, during extended cycles, oxygen deficiency partially penetrates into the bulk of active particles and thus are detrimental for structural stability.<sup>[10]</sup>

To overcome above issues, modulating crystal and interfacial properties on the surface of LLOs has surfaced as a highly researched topic presumably because of their effects in mitigating oxygen release and enhancing structural/interfacial stability of LLOs materials.<sup>[11]</sup> Typically, using heterogeneous ions

J. Meng, L. Xu, Y. Fang, J. Yuan, X. Zhang, H. Yu, L. Liu  
 School of Physics and Electronics  
 Gannan Normal University  
 Ganzhou 341000, China

Q. Ma, M. Yang  
 Key Laboratory of Power Battery and Materials  
 Faculty of Materials Metallurgy and Chemistry  
 Jiangxi University of Science and Technology  
 Ganzhou 341000, China  
 E-mail: maquanxin@jxust.edu.cn

 The ORCID identification number(s) for the author(s) of this article can be found under <https://doi.org/10.1002/adfm.202113013>.

DOI: 10.1002/adfm.202113013

Q. Ma  
 Far East Battery  
 FEB Research Institute  
 Yichun 336000, China  
 G. Wan, T. Liu  
 College of Materials Science and Engineering  
 Zhejiang University of Technology  
 Hangzhou 310014, China  
 E-mail: tiefengliu@zjut.edu.cn  
 R. Li  
 School of Materials Science and Engineering  
 Zhejiang University  
 Hangzhou 310027, China  
 E-mail: ruhong@zju.edu.cn



# Construction of Fe<sub>7</sub>Se<sub>8</sub>@Carbon nanotubes with enhanced sodium/potassium storage

Jujun Yuan <sup>a</sup>, Yunfei Gan <sup>a,c</sup>, Xijun Xu <sup>b,d,\*</sup>, Meiqi Mu <sup>a</sup>, Haishan He <sup>a,c</sup>, Xiaokang Li <sup>a,c,\*</sup>, Xianke Zhang <sup>a</sup>, Jun Liu <sup>a,b,\*</sup>

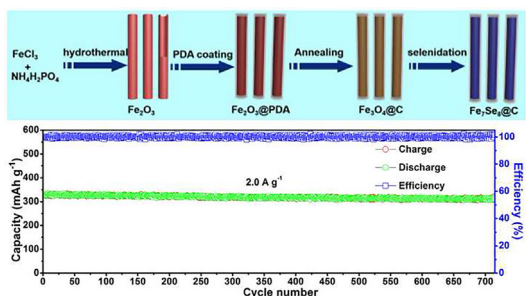
<sup>a</sup> Key Laboratory of New Energy Materials and Low Carbon Technologies, College of Physics and Electronics, Gannan Normal University, Ganzhou 341000, PR China

<sup>b</sup> School of Materials Science and Engineering, South China University of Technology, Guangzhou 510641, PR China

<sup>c</sup> College of Chemistry and Chemical Engineering, Gannan Normal University, Ganzhou 341000, PR China

<sup>d</sup> School of Chemical Engineering and Light Industry, Guangdong University of Technology, Guangzhou 510006, PR China

## GRAPHICAL ABSTRACT



## ARTICLE INFO

### Article history:

Received 1 May 2022

Revised 13 June 2022

Accepted 25 June 2022

Available online 28 June 2022

### Keywords:

Anode

Fe<sub>7</sub>Se<sub>8</sub>@C nanotubes

Sodium ion batteries

Potassium ion batteries

Electrochemical performance

## ABSTRACT

The Fe<sub>7</sub>Se<sub>8</sub>@Carbon (C) nanotubes are successfully synthesized using Fe<sub>3</sub>O<sub>4</sub>@C nanotubes as sacrificial templates. Fe<sub>7</sub>Se<sub>8</sub>@C nanotubes exhibit excellent rate behaviour and maintainable capacity (319 mAh g<sup>-1</sup> at 2 A g<sup>-1</sup> upon 720 cycles), when utilized as SIBs anode. Moreover, for PIBs anode, Fe<sub>7</sub>Se<sub>8</sub>@C nanotubes also exhibit outstanding rate behaviour and maintainable capacity 222 mAh g<sup>-1</sup> at 2 A g<sup>-1</sup> upon 500 cycles). The superior electrochemical performance of Fe<sub>7</sub>Se<sub>8</sub>@C nanotubes is ascribed to the unique structure, where the hierarchical hollow tubular characteristic of Fe<sub>7</sub>Se<sub>8</sub>@C composites can mitigate the volume expansion of Fe<sub>7</sub>Se<sub>8</sub> and supply effective transmission paths for both Na<sup>+(K<sup>+</sup>)</sup> and electrons within repeated cycle processes, and additionally, N-doped carbon layer can further protect the integrality of Fe<sub>7</sub>Se<sub>8</sub>@C nanotubes from destruction within the cycle processes, and enhance electronic conductivity.

© 2022 Elsevier Inc. All rights reserved.

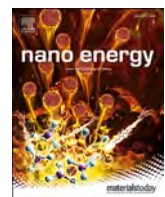
## 1. Introduction

As a high-energy storage device, lithium-ion batteries(LIBs) are universally utilized for daily electronic equipment and electric automobile [1–5]. Nevertheless, the shortage of lithium resources

brings about high costs, and it is urgent need to explore low-price energy storage devices with the aim for meeting secondary applications in the future. Because of sufficient natural resource of sodium (potassium), sodium (potassium) ion batteries (S(P) IBs) are regarded as appealing alternatives to LIBs [6–12]. Although

\* Corresponding authors at: Key Laboratory of New Energy Materials and Low Carbon Technologies, College of Physics and Electronics, Gannan Normal University, Ganzhou 341000, PR China (X. Li, J. Liu) and School of Materials Science and Engineering, South China University of Technology, Guangzhou 510641, PR China (X. Xu).

E-mail addresses: xuxijun2022@gdt.edu.cn (X. Xu), lixiaokang@gnnu.edu.cn (X. Li), msjliu@scut.edu.cn (J. Liu).



## Full paper

## Na-substitution induced oxygen vacancy achieving high transition metal capacity in commercial Li-rich cathode



Quanxin Ma<sup>a</sup>, Zaijun Chen<sup>a</sup>, Shengwen Zhong<sup>a,\*</sup>, Junxia Meng<sup>b,\*</sup>, Fulin Lai<sup>a</sup>, Zhifeng Li<sup>a</sup>, Chen Cheng<sup>c</sup>, Liang Zhang<sup>c</sup>, Tiefeng Liu<sup>d</sup>

<sup>a</sup> Key Laboratory of Power Battery and Materials, Faculty of Materials Metallurgy and Chemistry, Jiangxi University of Science and Technology, Ganzhou 341000, China

<sup>b</sup> School of Physics and Electronics, Gannan Normal University, Ganzhou 341000, China

<sup>c</sup> Institute of Functional Nano & Soft Materials (FUNSOM), Jiangsu Key Laboratory for Carbon-Based Functional Materials & Devices, Soochow University, Suzhou 215123, China

<sup>d</sup> Department of Materials Science and Engineering, Zhejiang University of Technology, Hangzhou 310014, China

## ARTICLE INFO

## Keywords:

Li-rich layered oxide

Sodium doping

Oxygen vacancy

Structure stability

First principles calculations

## ABSTRACT

High-capacity and low-cost Li-rich layered Mn-based oxides (LLMOs) hold the great promise for next-generation lithium ion battery cathode but LLMOs still encounter grand challenges in voltage decay and gas release. Here, we proposed a simple but effective as well as scalable approach of creating surface oxygen vacancies (OVs) and simultaneously enhancing structural stability. A series of  $\text{Li}_{1.2-2x}\text{Na}_x\text{Mn}_{0.56}\text{Ni}_{0.16}\text{Co}_{0.08}\text{O}_2$  ( $x = 0, 0.05, 0.1$  and  $0.2$ ) cathode materials are synthesized, based on Na-pre-embedded precursor and nonstoichiometric lithiation processes, to render the OVs confirmed by synchrotron radiation analysis. First-principles calculations suggest that the architecture induced by surface OVs obviously affects the local Mn coordination environments and enhances the structural stability. Meanwhile, enlarged Li layer spacing by Na doping enables increased Li diffusion, decreased voltage polarization, and enhanced structural stability. Accordingly, the optimized  $\text{Na}_{0.1}$ -LLMO cathode delivers highly initial coulombic efficiency of 84.2% compared to the pristine one (79.9%) and remarkable electrochemical behaviors in terms of cycling stability, voltage retention and rate performance. Pouch cell investigation further verifies the practical applicability of Na-doped LLMO cathode materials to scale up.

## 1. Introduction

In the search for ideal cathode materials for realizing high-energy-density lithium-ion batteries (LIBs), the class of Li-rich layered Mn-based oxides with a general formula of  $x\text{Li}_2\text{MnO}_3\cdot(1-x)\text{LiMO}_2$  ( $\text{M}=\text{Ni}, \text{Co}, \text{Mn}$ , etc.) (LLMO) has gained significant interest due to their high specific capacity and low material cost [1,2]. However, their practical applications are still plagued by the problems in terms of irreversible capacity loss, severe voltage fading, inferior rate capability, and extensive oxygen release [3–5]. Their potential origins have been identified and typically fall into two categories [6–8]: One is that transition metal (TM) ions migrate from octahedral sites of the TM layer to tetrahedral sites of the Li layer at high charge states [9–11]. Once all three adjacent sites in the Li layer are vacant, TM ions will easily migrate to these Li sites. This process is only partially reversible. The other is due to the participation of oxygen anions of the LLMOs into the redox reaction

[12], causing surface oxygen loss upon electrochemical cycling, eventually resulting in irreversible  $\text{O}_2$  release for battery swollen and structural collapse for performance degradation [13,14]. Therefore, recent research into the LLMOs has placed a spotlight on their precise structural modifications.

As for anionic redox for LLMOs, it is well recognized that the oxygen oxidation in LLMOs mainly occurs by extracting unstable electrons from orphaned unhybridized  $\text{O}$   $2p$  states locating on Li-O-Li configurations, essentially coinciding with charge compensation, leading to the aggregation of adjacent oxygen atoms and the formation of O-O dimer. Subsequently, the O-O dimer to release as  $\text{O}_2$  causes surface oxygen vacancies (OVs) and structural collapse. Although the former is believed to promote  $\text{Li}^+$  diffusion, improve the capacity and rate performance of LLMOs, the latter inevitably induces the deterioration of electrochemical behaviors and battery safety [3,15–18]. Therefore, a promising strategy of pre-introducing OVs into the LLMOs during the synthesis process have

\* Corresponding authors.

E-mail addresses: [zhongshw@jxust.edu.cn](mailto:zhongshw@jxust.edu.cn) (S. Zhong), [jxmeng@buaa.edu.cn](mailto:jxmeng@buaa.edu.cn) (J. Meng), [liangzhang2019@suda.edu.cn](mailto:liangzhang2019@suda.edu.cn) (L. Zhang), [tiefengliu@zjut.edu.cn](mailto:tiefengliu@zjut.edu.cn) (T. Liu).



# MOF derived ZnSe–FeSe<sub>2</sub>/RGO Nanocomposites with enhanced sodium/potassium storage



Jujun Yuan <sup>a,1</sup>, Wen Liu <sup>b,1</sup>, Xianke Zhang <sup>a</sup>, Yaohui Zhang <sup>c, \*\*</sup>, Wentao Yang <sup>b</sup>, Weidong Lai <sup>a</sup>, Xiaokang Li <sup>a</sup>, Jiujun Zhang <sup>b,d</sup>, Xifei Li <sup>b,e,\*</sup>

<sup>a</sup> School of Physics and Electronics, Gannan Normal University, Ganzhou, 341000, PR China

<sup>b</sup> Xi'an Key Laboratory of New Energy Materials and Devices, Institute of Advanced Electrochemical Energy & School of Materials Science and Engineering, Xi'an University of Technology, Xi'an, Shaanxi, 710048, PR China

<sup>c</sup> School of Physics, Harbin Institute of Technology, Harbin, Heilongjiang, 150001, PR China

<sup>d</sup> Institute for Sustainable Energy, Shanghai University, Shanghai, 200444, PR China

<sup>e</sup> Center for International Cooperation on Designer Low-carbon & Environmental Materials (CDLCEM), Zhengzhou University, Zhengzhou, Henan, 450001, China

## ARTICLE INFO

### Keywords:

ZnSe–FeSe<sub>2</sub>/RGO nanocomposites

Anode material

Sodium ion batteries

Potassium ion batteries

Fe/Zn-MOF-5 template

## ABSTRACT

ZnSe–FeSe<sub>2</sub>/reduced graphene oxide (RGO) composites are synthesized through a rational strategy using Fe/Zn-MOF-5 as a template. Compared with the ZnSe/RGO or FeSe<sub>2</sub>/RGO composites, the ZnSe–FeSe<sub>2</sub>/RGO anode electrode exhibits a higher reversible capacity (439 mAh g<sup>-1</sup> after 100 cycles at 100 mA g<sup>-1</sup>) for sodium ion batteries (SIBs). The excellent electrochemical performance of ZnSe–FeSe<sub>2</sub>/RGO composites can be attributed to the synergistic effects of the unique architecture, where ZnSe is responsible for providing a high capacity, FeSe<sub>2</sub> improves the electrochemical stability, and RGO is beneficial for enhancing the charge transfer behavior. Furthermore, the ZnSe–FeSe<sub>2</sub>/RGO anode reveals stable reversible capacity (363 mAh g<sup>-1</sup> after 100 cycles at 50 mA g<sup>-1</sup>) for potassium ion batteries (KIBs).

## 1. Introduction

As a green and effective energy storage device, lithium-ion batteries (LIBs) have been successfully applied to the fields of portable electronics and electric vehicles [1–5]. However, the limited lithium salt resources and its high price have been an obstacle for large-scale energy storage. In contrast to LIBs, SIBs [6–8] and KIBs [9,10] have received considerable attention owing to abundant resources of sodium (potassium) and their similar electrochemical principles with LIBs. However, compared with the radius of Li<sup>+</sup> (0.76 Å), Na<sup>+</sup>(K<sup>+</sup>) shows larger radius of 1.09 Å (1.38 Å), which will lead to a larger volume variation and severe structure pulverization of electrode materials during the charge/discharge processes. Therefore, developing effective electrode materials for NIBs (KIBs) has been challenging [11,12].

Recently, metal selenide-based electrode materials (M<sub>x</sub>Se<sub>y</sub>, M = Fe, Zn, Co, Mo, Sn, Sb) have been reported as promising anodes of NIBs (KIBs) owing to their high capacity, chemical stability, and

environmental friendliness [13–21]. For example, Fe<sub>7</sub>Se<sub>8</sub>@C nanorods anode displayed a stable capacity of 360 mAh g<sup>-1</sup> after 100 cycles at 300 mA g<sup>-1</sup> for SIBs anode [14]. For the ZnSe microsphere/CNT composites, it delivered the capacity of 362 mAh g<sup>-1</sup> at 200 mA g<sup>-1</sup> after 80 cycles [15]. Amazingly, the CoSe<sub>2</sub>/carbon nanofiber as an SIBs anode showed a high reversible capacity (371.8 mAh g<sup>-1</sup> at 200 mA g<sup>-1</sup>) [17]. In addition, MoSe<sub>2</sub>/N-doped carbon exhibited 258 mAh g<sup>-1</sup> after 300 cycles at 100 mA g<sup>-1</sup> [19] when used as KIBs anode. Although attractive results of metal selenide materials were previously reported, how to further enhance the battery performance of anode materials has been challenging since the electrochemical conversion and alloying reactions are usually accompanied by large volume variation and continuous growth of solid electrolyte interface (SEI) films.

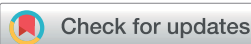
To address this barrier, great efforts have been devoted by designing the composites of mixed-metal selenide and conductive carbon for improving the electrochemical performance of energy-related devices [22–27]. Particularly, two different metal cations in the mixed-metal

\* Corresponding author. Xi'an Key Laboratory of New Energy Materials and Devices, Institute of Advanced Electrochemical Energy & School of Materials Science and Engineering, Xi'an University of Technology, Xi'an, Shaanxi, 710048, PR China.

\*\* Corresponding author.

E-mail addresses: [hitcrazyzyh@hit.edu.cn](mailto:hitcrazyzyh@hit.edu.cn) (Y. Zhang), [xli2011@hotmail.com](mailto:xli2011@hotmail.com) (X. Li).

<sup>1</sup> Authors Jujun Yuan and Wen Liu make the same contribution to this work.



Cite this: *J. Mater. Chem. A*, 2020, **8**, 23395

## Heterogeneous structured MoSe<sub>2</sub>–MoO<sub>3</sub> quantum dots with enhanced sodium/potassium storage†

Wen Liu,<sup>a,c</sup> Jujun Yuan,<sup>\*b</sup> Youchen Hao,<sup>a,c</sup> Hirbod Maleki Kheimeh Sari,<sup>b</sup> Jingjing Wang,<sup>a,c</sup> Alibek Kakimov,<sup>a,c</sup> Wei Xiao,<sup>a,c</sup> Jian Qin,<sup>a,c</sup> Wenbin Li,<sup>a,c</sup> Chong Xie,<sup>a,c</sup> Junhua Hu,<sup>b,d</sup> Jianhong Peng<sup>\*e</sup> and Xifei Li<sup>b,f\*</sup>

Herein, quantum dot-assisted self-assembled MoSe<sub>2</sub>–MoO<sub>3</sub> with a porous structure is synthesized via a MOF-directed strategy involving a thermal-induced reaction with Se. As an anode material for sodium ion batteries, due to inheriting the chemical activity of quantum dots and physical stability of the porous heterogeneous structure, it exhibits an outstanding electrochemical performance (*i.e.*, 400 mA h g<sup>-1</sup> after 500 cycles at a current density of 0.1 A g<sup>-1</sup> with a capacity retention of 90% and 218.5 mA h g<sup>-1</sup> after 2000 cycles at 3.0 A g<sup>-1</sup> with a capacity retention of almost 100%) superior to that of MoSe<sub>2</sub>–MoO<sub>3</sub> with different ratios and the traditional bulk MoSe<sub>2</sub>. Moreover, the improved potassium-ion storage of the anode is obtained (*i.e.*, 308.7 mA h g<sup>-1</sup> with a capacity retention of 97.9% after 300 cycles at 0.05 A g<sup>-1</sup>). This work paves the way for developing high-performance anode materials with a large reversible capacity and a long cycle-life for sodium/potassium ion batteries.

Received 3rd September 2020  
Accepted 14th October 2020

DOI: 10.1039/d0ta08674f  
[rsc.li/materials-a](http://rsc.li/materials-a)

## Introduction

Recently, metal selenides (such as CoSe<sub>2</sub>, FeSe<sub>2</sub>, MoSe<sub>2</sub>, NiSe<sub>2</sub>, etc.) have been frequently suggested as promising anode materials with a suitable redox voltage as well as intrinsically high electrical conductivity for high-performance sodium ion batteries (SIBs) and potassium ion batteries (PIBs).<sup>1,2</sup> Specifically, MoSe<sub>2</sub> has been recognized as a competitive anode resulting from a sandwich structure composed of stacked atom layers (Se–Mo–Se) with a large interlayer space and a small band gap.<sup>3,4</sup> However, its insufficient

electrical conductivity and ion diffusion rate, and large volume expansion/shrinkage upon cycling may result in a rapid capacity degradation.<sup>5–7</sup> In this regard, considerable attempts have been made by innovative design of the electrode materials including fabricating porous structures, making hybrid composites, surface modification, doping, *etc.*<sup>8–11</sup>

To this end, nanomaterials with excellent electrolyte accessibility and short ion diffusion paths are more desirable because of their capability to buffer volume expansion/shrinkage and accelerate the electrochemical process in a considerable way.<sup>12,13</sup> Hence, downsizing electrode materials to zero-dimensional quantum dots (QDs), might be a promising strategy.<sup>14–17</sup> QDs possess various striking advantages: (1) the small size immensely shortens the diffusion length, boosting charge/mass transfer, (2) the large surface-to-volume ratio facilitates intimate contact current collector/electrode materials/electrolyte, providing rapid charge/electron transfer kinetics, and (3) the high proportion of surface atoms with more activity greatly improves the electrochemical reactions.<sup>18–20</sup> As a result, QDs have been employed in various advanced applications such as light-emitting devices, catalysis, solar cells, *etc.*, however, their utilization as electrochemically active materials in Na<sup>+</sup>/K<sup>+</sup> storage has remained a tough challenge owing to the poor electrical conductivities of most available QDs.<sup>21–23</sup> Meanwhile, the increased interfaces between active nanoparticles and electrolyte may produce more exposed surfaces for the repeated formation/decomposition of the solid electrolyte interphase (SEI) layer, which significantly increases the electrochemical resistance.<sup>12,24</sup> These disadvantages severely limit their application in various fields and particularly in batteries.

<sup>a</sup>Institute of Advanced Electrochemical Energy, School of Materials Science and Engineering, Xi'an University of Technology, Xi'an 710048, Shaanxi, China. E-mail: [xjli2011@hotmail.com](mailto:xjli2011@hotmail.com)

<sup>b</sup>School of Physics and Electronics, Gannan Normal University, Ganzhou, 341000, PR China. E-mail: [juanjijun123@163.com](mailto:juanjijun123@163.com)

<sup>c</sup>Shaanxi International Joint Research Center of Surface Technology for Energy Storage Materials, Xi'an 710048, Shaanxi, China

<sup>d</sup>State Center for International Cooperation on Designer Low-carbon & Environmental Materials (CDLCEM), Zhengzhou University, Zhengzhou, China

<sup>e</sup>School of Physical and Electronic Information Engineering, Qinghai Nationalities University, Xining, China. E-mail: [pjhjh@sohu.com](mailto:pjhjh@sohu.com)

† Electronic supplementary information (ESI) available: Electrochemical impedance spectroscopy (EIS) analysis and the galvanostatic intermittent titration technique (GITT); XRD spectrum and SEM images of the synthesized molybdenum-based MOF (Mo-MOF); HRTEM images of MoSe<sub>2</sub>-1 and MoSe<sub>2</sub>-4; adsorption/desorption isotherms and the pore size distribution of MoSe<sub>2</sub>-1, MoSe<sub>2</sub>-2, MoSe<sub>2</sub>-3, and MoSe<sub>2</sub>-4; TEM image of MoSe<sub>2</sub>-3; XPS spectra of MoSe<sub>2</sub>-1, MoSe<sub>2</sub>-2, MoSe<sub>2</sub>-3, and MoSe<sub>2</sub>-4; the XPS full spectra for C 1s, and O 2p; the molar proportion of Mo from MoSe<sub>2</sub> in the total Mo content of samples; TGA curves of MoSe<sub>2</sub>-1, MoSe<sub>2</sub>-2, MoSe<sub>2</sub>-3, and MoSe<sub>2</sub>-4; the equivalent circuit for the fitting electrochemical impedance spectroscopy; the loading of MoO<sub>3</sub>, MoSe<sub>2</sub> and C in the four samples. See DOI: [10.1039/d0ta08674f](https://doi.org/10.1039/d0ta08674f)



# A decision support system using hybrid AI based on multi-image quality model and its application in color design



Mengshan Li <sup>\*</sup>, Suyun Lian, Fan Wang, Yanying Zhou, Bingsheng Chen, Lixin Guan, Yan Wu

College of Physics and Electronic Information, Gannan Normal University, Ganzhou, Jiangxi 341000, China

## ARTICLE INFO

### Article history:

Received 6 March 2020

Received in revised form 20 June 2020

Accepted 23 June 2020

Available online 3 July 2020

### Keywords:

Decision support system

Artificial intelligence

Product design

Multi-users' images

## ABSTRACT

The product-color image conveys consumers' color demands through emotion cognition. In this paper, a decision support system is proposed based on the hybrid artificial intelligence algorithm. The proposed system explores the internal correlation between the color image and demand of users. In the proposed system, an artificial neural network based on the radial basis function is employed. The network model is trained with an improved particle swarm optimization combined with the weight-adaptive strategy and chaos theory. The proposed model predicts the multi-uses' color images. Then, the decision colors are extracted from the predicted colors by K-harmonic means clustering. The experimental results show that the proposed color decision support system is promising in designing the color scheme and providing theoretical guidance for the product-color design.

© 2020 Published by Elsevier B.V.

## 1. Introduction

The product-color image is defined as consumers' intuitive association with product-color, which fully conveys consumer's demand for the color. The product-color image is of theoretical and practical value because it affects consumer's decisions in the purchase, and designers can understand customers' color emotion cognition by it [1]. The design of a product-color has been transformed from the traditional experience-based strategy to the user-centered decision strategy. Before the designers grasp users' image preference and cognition to product-color and reduce the perception gap with the users in the color image, they cannot design the products conforming to users' images or improve the design [2,3].

Previous studies on product-color design were based on color harmony theory, knowledge-engineering theory, and customers' images obtained with intelligent computation. Traditional color design methods failed to meet diverse and changeable demands since the fuzzy perceptual description of the color image was not considered. Thus, understanding the consumer's complex perceptual images of product-color has become a significant element in product-color design [4].

In recent years, many product-color design methods were proposed based on intelligent computation, such as gray theory [5,6], fuzzy theory, support vector machine (SVM) [7,8], artificial neural network (ANN) [9–13], and imperialist competitive algorithm.

Also, several methods were proposed based on the various swarm intelligence algorithms, such as tabu search algorithm, ant colony algorithm, genetic algorithm, and particle swarm optimization algorithm, which were successfully applied in various product designs [14–16]. As a novel design method imitating color evolution under the influence of the law of survival of the fittest in biological evolution, the swarm intelligence-based product-color design has played an important role [17,18]. For example, Hsiao et al. used the gray theory and backpropagation artificial neural network (BP ANN) to study the color of baby walker, proving that the gray theory prediction model can be applied in the color design of all kinds of products [19–21]. In [6,19,22–25], the double-color system for the product-color design was proposed based on the gray theory, color harmony method, and genetic algorithm. The genetic algorithm was applied and verified in the product-color selection [20,21,26–29]. Shiu [30] used the artificial neural network to establish the color prediction model in the study of the color of children's toys. Chen et al. [31] established the color image base by using user preference as the input value.

However, previous studies mostly focused on the application of intelligent computing algorithms only in the development process of the color scheme. Users' color image was not considered as the main factor in the studies on color selection. The only single-user rather than mass-users was considered in the design process, leading the dotted distribution problem. Also, intelligent computation algorithms had problems, such as the artificial neural network might lead to unstable results because of the uncertainty of the initial values of parameters and the weight. Swarm intelligence algorithms also had some problems, such as

<sup>\*</sup> Corresponding author.

E-mail address: [jcimsl@163.com](mailto:jcimsl@163.com) (M. Li).



# Hollow spheres constructed by ZnS-CoS<sub>2</sub> @N-doped carbon@N-doped carbon as anodes for high-performance sodium-ion batteries

Haishan He <sup>a,b</sup>, Mingquan Li <sup>a,b</sup>, Yunfei Gan <sup>a,b</sup>, Jirong Mou <sup>b</sup>, Jujun Yuan <sup>b,\*</sup>, Xianke Zhang <sup>b</sup>, Bin Li <sup>c,\*</sup>, Jing Yu <sup>b</sup>, Chao Zhang <sup>b</sup>, Xiaokang Li <sup>a,b,\*\*</sup>, Jun Liu <sup>b,d</sup>

<sup>a</sup> College of Chemistry and Chemical Engineering, Gannan Normal University, Ganzhou 341000, PR China

<sup>b</sup> School of Physics and Electronics, Gannan Normal University, Ganzhou 341000, PR China

<sup>c</sup> Ganzhou Jirui New Energy Technology Co., Ltd, Ganzhou 341000, PR China

<sup>d</sup> School of Materials Science and Engineering, South China University of Technology, Guangzhou 510641, PR China



## ARTICLE INFO

### Keywords:

ZnS  
CoS<sub>2</sub>  
Hollow spheres  
N-doped Carbon  
Sodium ion battery  
Anode

## ABSTRACT

Hollow spheres constructed by ZnS-CoS<sub>2</sub> @N-doped Carbon@N-doped carbon (ZnS-CoS<sub>2</sub> @NC@NC) are successfully synthesized using template method combined with NC coating procedure. For SIBs anode, ZnS-CoS<sub>2</sub> @NC@NC electrode exhibits excellent rate property and sustainable capacity of 164 mAh g<sup>-1</sup> at 5 A g<sup>-1</sup> after 1000 cycles. The superior sodium storage performance for ZnS-CoS<sub>2</sub> @NC@NC composites is benefited from its distinctive structure, in which the hollow architecture for ZnS/CoS<sub>2</sub> @NC@NC composites can buffer the volume change of ZnS/CoS<sub>2</sub> and enhance electronic/ionic conductivity within charge/discharge processes. Furthermore, the NC shell layer can further alleviate structural degradation of ZnS/CoS<sub>2</sub> @NC@NC hollow spheres, and supply more effective active sites.

## 1. Introduction

Because of the problem of the environment contamination and the rapidly increased requirement of energy storage, renewable secondary batteries have gained widespread attention in the past years [1–3]. Sodium-ion batteries (SIBs) are deemed as promising candidates due to low cost, rich sodium storage in the earth's crust, and similar characteristics to lithium-ion batteries (LIBs) [4–7]. Nevertheless, the larger sodium ion radius (1.02 Å) and sluggish sodium ion diffusion kinetics will lead to large volume changes and inferior cyclic stability for electrode materials in the discharge/charge processes. Therefore, it is a urgent task to exploit ideal electrode materials for SIBs with high capacity and superior cyclic stability.

Recently, metal sulfides (e.g., MnS<sub>x</sub>, MoS<sub>2</sub>, NiS<sub>x</sub>, FeS<sub>x</sub>, ZnS, CoS<sub>x</sub>) [8–15] have been reported as competitive SIBs anode materials owing to their high capacities. Especially, mixed-metal sulfides have drawn increasing attentions for sodium storage benefiting from the improvement of conversion reaction kinetics in the discharge/charge process. It has been demonstrated that the heterointerface in the mixed-metal sulfides heterostructure can effectively reduce sodium ion diffusion

barrier and promote charge-transfer kinetics, thereby improving cycling stability [16–18]. In this regard, Yan et al. reported Co<sub>9</sub>S<sub>8</sub>/MoS<sub>2</sub> yolk-shell spheres displayed good cycling stability (430 mAh g<sup>-1</sup> at 1 A g<sup>-1</sup> after 105 cycles) [17]. Lou et al. studied CuS@CoS<sub>2</sub> nanobox, which owned a maintainable capacity of 400 mAh g<sup>-1</sup> at 0.5 A g<sup>-1</sup> [18]. However, mixed-metal sulfides commonly suffer severe capacity degradation owing to larger volumetric change and poor electronic conductivity within charge/discharge processes.

One method for solving above issues is to design hollow (porous) mixed-metal sulfides/C composites, which can alleviate structural degradation of mixed-metal sulfides and enhance electronic/ionic conductivity in the charging/discharging procedures [19–23]. For example, Yin et al. confirmed that hollow ZnS-Sb<sub>2</sub>S<sub>3</sub>@C polyhedron structure can maintain a sustainable capacity of 630 mAh g<sup>-1</sup> at 0.1 A g<sup>-1</sup> after 120 cycles [20]. Zhu et al. reported that Ni-Co-MOF derived hollow Ni<sub>3</sub>S<sub>2</sub>/Co<sub>9</sub>S<sub>8</sub>/NC composite possessed a stable capacity of 420 mAh g<sup>-1</sup> at 0.1 A g<sup>-1</sup> after 100 cycles [21]. Cai et al. designed hierarchical MoS<sub>2</sub>-NiS nanotube@NC by template-assisted hydrothermal treatment and followed by a subsequent sulfidation strategy. The hierarchical MoS<sub>2</sub>-NiS nanotube@NC electrode delivered a retainable capacity of

\* Corresponding authors.

\*\* Corresponding author at: College of Chemistry and Chemical Engineering, Gannan Normal University, Ganzhou 341000, PR China.

E-mail addresses: [yuanjijun123@163.com](mailto:yuanjijun123@163.com) (J. Yuan), [wpslibin@163.com](mailto:wpslibin@163.com) (B. Li), [lixiaokang@gznu.edu.cn](mailto:lixiaokang@gznu.edu.cn) (X. Li).

RESEARCH

Open Access



# Essential genes identification model based on sequence feature map and graph convolutional neural network

Wenxing Hu<sup>1</sup>, Mengshan Li<sup>1\*</sup>, Haiyang Xiao<sup>1</sup> and Lixin Guan<sup>1</sup>

## Abstract

**Background** Essential genes encode functions that play a vital role in the life activities of organisms, encompassing growth, development, immune system functioning, and cell structure maintenance. Conventional experimental techniques for identifying essential genes are resource-intensive and time-consuming, and the accuracy of current machine learning models needs further enhancement. Therefore, it is crucial to develop a robust computational model to accurately predict essential genes.

**Results** In this study, we introduce GCNN-SFM, a computational model for identifying essential genes in organisms, based on graph convolutional neural networks (GCNN). GCNN-SFM integrates a graph convolutional layer, a convolutional layer, and a fully connected layer to model and extract features from gene sequences of essential genes. Initially, the gene sequence is transformed into a feature map using coding techniques. Subsequently, a multi-layer GCN is employed to perform graph convolution operations, effectively capturing both local and global features of the gene sequence. Further feature extraction is performed, followed by integrating convolution and fully-connected layers to generate prediction results for essential genes. The gradient descent algorithm is utilized to iteratively update the cross-entropy loss function, thereby enhancing the accuracy of the prediction results. Meanwhile, model parameters are tuned to determine the optimal parameter combination that yields the best prediction performance during training.

**Conclusions** Experimental evaluation demonstrates that GCNN-SFM surpasses various advanced essential gene prediction models and achieves an average accuracy of 94.53%. This study presents a novel and effective approach for identifying essential genes, which has significant implications for biology and genomics research.

**Keywords** Essential genes, Graphical convolutional neural networks, Machine learning, Gene sequences, Bioinformatics

## Introduction

Essential genes, which are currently a hot topic in genomics and bioinformatics research, are indispensable for supporting cellular life [1]. Their coding functions are crucial for the survival of organisms. These genes constitute a set that must be present in an organism and are vital for maintaining its life activities under specific environmental conditions. They encode key proteins or RNA molecules that are essential for life, and their functions are considered fundamental for the organism's survival

\*Correspondence:

Mengshan Li  
mssl@gnnu.edu.cn

<sup>1</sup> College of Physics and Electronic Information, Gannan Normal University, Ganzhou, Jiangxi 341000, China



© The Author(s) 2024. **Open Access** This article is licensed under a Creative Commons Attribution 4.0 International License, which permits use, sharing, adaptation, distribution and reproduction in any medium or format, as long as you give appropriate credit to the original author(s) and the source, provide a link to the Creative Commons licence, and indicate if changes were made. The images or other third party material in this article are included in the article's Creative Commons licence, unless indicated otherwise in a credit line to the material. If material is not included in the article's Creative Commons licence and your intended use is not permitted by statutory regulation or exceeds the permitted use, you will need to obtain permission directly from the copyright holder. To view a copy of this licence, visit <http://creativecommons.org/licenses/by/4.0/>. The Creative Commons Public Domain Dedication waiver (<http://creativecommons.org/publicdomain/zero/1.0/>) applies to the data made available in this article, unless otherwise stated in a credit line to the data.

RESEARCH

Open Access



# A miRNA-disease association prediction model based on tree-path global feature extraction and fully connected artificial neural network with multi-head self-attention mechanism

Hou Biyu<sup>1</sup>, Li Mengshan<sup>1\*</sup>, Hou Yuxin<sup>2</sup>, Zeng Ming<sup>1</sup>, Wang Nan<sup>3</sup> and Guan Lixin<sup>1</sup>

## Abstract

**Background** MicroRNAs (miRNAs) emerge in various organisms, ranging from viruses to humans, and play crucial regulatory roles within cells, participating in a variety of biological processes. In numerous prediction methods for miRNA-disease associations, the issue of over-dependence on both similarity measurement data and the association matrix still hasn't been improved. In this paper, a miRNA-Disease association prediction model (called TP-MDA) based on tree path global feature extraction and fully connected artificial neural network (FANN) with multi-head self-attention mechanism is proposed. The TP-MDA model utilizes an association tree structure to represent the data relationships, multi-head self-attention mechanism for extracting feature vectors, and fully connected artificial neural network with 5-fold cross-validation for model training.

**Results** The experimental results indicate that the TP-MDA model outperforms the other comparative models, AUC is 0.9714. In the case studies of miRNAs associated with colorectal cancer and lung cancer, among the top 15 miRNAs predicted by the model, 12 in colorectal cancer and 15 in lung cancer were validated respectively, the accuracy is as high as 0.9227.

**Conclusions** The model proposed in this paper can accurately predict the miRNA-disease association, and can serve as a valuable reference for data mining and association prediction in the fields of life sciences, biology, and disease genetics, among others.

**Keywords** Association tree, Multi-head self-attention mechanism, miRNA-disease association, Deep learning, Cancer

\*Correspondence:

Li Mengshan  
mengl@gnnu.edu.cn

<sup>1</sup> College of Physics and Electronic Information, Gannan Normal University, Ganzhou, Jiangxi 341000, China

<sup>2</sup> College of Computer Science and Engineering, Shanxi Datong University, Datong, Shanxi 037000, China

<sup>3</sup> College of Life Sciences, Jiaying University, Meizhou, Guangdong 514000, China



© The Author(s) 2024. **Open Access** This article is licensed under a Creative Commons Attribution 4.0 International License, which permits use, sharing, adaptation, distribution and reproduction in any medium or format, as long as you give appropriate credit to the original author(s) and the source, provide a link to the Creative Commons licence, and indicate if changes were made. The images or other third party material in this article are included in the article's Creative Commons licence, unless indicated otherwise in a credit line to the material. If material is not included in the article's Creative Commons licence and your intended use is not permitted by statutory regulation or exceeds the permitted use, you will need to obtain permission directly from the copyright holder. To view a copy of this licence, visit <http://creativecommons.org/licenses/by/4.0/>. The Creative Commons Public Domain Dedication waiver (<http://creativecommons.org/publicdomain/zero/1.0/>) applies to the data made available in this article, unless otherwise stated in a credit line to the data.



# Multi-scale model integrated particle dynamics and evolutionary algorithm with the coarse-grained particle partitioning ratio strategy for calculating the dissolution behaviors of supercritical carbon dioxide in polymer fluids

Li Mengshan <sup>a,\*</sup>, Wu Wei <sup>a</sup>, Chen Bingsheng <sup>a</sup>, Guan Lixin <sup>a</sup>, Wu Yan <sup>a</sup>, Wang Nan <sup>b,\*</sup>

<sup>a</sup> College of Physics and Electronic Information, Gannan Normal University, Ganzhou, 341000, Jiangxi, China

<sup>b</sup> College of Life Sciences, Jiaying University, Meizhou 514015, Guangdong, China

## ARTICLE INFO

### Keywords:

Multi-scale  
Dissolution  
Evolutionary calculation  
Particle dynamics  
Coarse-grained transfixion

## ABSTRACT

Supercritical carbon dioxide is widely applied in the preparation, extraction, and modifications of novel advanced materials. The dissolution behavior of supercritical carbon dioxide in polymer fluids is an important physicochemical property of foamed materials and its multi-scale research is significant in revealing the essence of dissolution at different spatial and temporal scales. In multi-scale models, scale transfixion methods and computational complexity need to be explored urgently. Inspired by the principle of evolutionary computing and particle dynamics, in this paper, the molecular diffusion motion in the dissolution process is simulated with the iterative motion of evolutionary particles in the dynamic potential energy field and the micro- to meso-scale transfixion is realized with the coarse-grained partitioning ratio strategy. Based on the above methods, a multi-scale computational model based on the chaotic accelerated double-population particle dynamics evolution algorithm (CADPPD-EA) is proposed. The calculation results of the dissolution behaviors of supercritical carbon dioxide in Poly (D, L-lactide-co-glycolide), Poly (L-lactide), and Poly (butylene succinate) show that the CADPPD-EA model has good computational effects. The calculation error and correlation coefficients at micro- and meso-scales are 0.3651, 0.3912 and 0.9244, 0.9098 respectively. Compared with similar models, CADPPD-EA shows significant advantages in accuracy, efficiency, and correlation. Its average calculation time was 7.143% of that of other dynamics models. CADPPD-EA model provides the theoretical basis for multi-scale modeling and scale transfixion methods and can be applied in the property calculation, computational fluid, the prediction of dynamics structure and performance of complex multi-component systems in chemical and chemical engineering, material energy, biomedicine, and computer.

## 1. Introduction

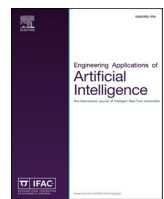
Microporous foam materials are a new type of advanced materials formed based on the principle that the dissolution behavior of a gas in a polymer is rapidly weakened with the instantaneous decrease in temperature and pressure and have many superior comprehensive properties [1–6]. In the continuous molding process of microcellular foam materials, the dissolution behaviors of supercritical CO<sub>2</sub> in polymer fluids are significant and generally explored through experiments and computer simulation. In recent years, multi-scale simulations have been extensively performed at different temporal and spatial scales from micro-scale to meso- and macro-scale and from femtosecond to nanosecond and millisecond scales [7–12]. Undoubtedly, multi-scale

research on dissolution behaviors can efficiently reveal the essence of dissolution and can be widely applied in molecular self-assembly, phase rheology, and kinetic analysis in chemistry, materials, and physics.

Great achievements have been made in multi-scale simulation for exploring the physical, chemical, mechanical, and rheological properties of materials at different temporal or spatial scales [13–17]. In the previous study we also proposed a dissolution calculation model based on the combination of particle dynamics and intelligent algorithms and achieved good results [18–20]. However, the multi-scale study on dissolution behaviors was seldom reported. The multi-scale problems of dissolution behaviors in various fields such as materials and chemicals remain to be solved urgently. The temporal and spatial scales in multi-scale simulation are limited because many molecular details need to

\* Corresponding authors.

E-mail addresses: [jcimsli@163.com](mailto:jcimsli@163.com) (L. Mengshan), [201401018@jyu.edu.cn](mailto:201401018@jyu.edu.cn) (W. Nan).



## Achieving accurate trajectory predicting and tracking for autonomous vehicles via reinforcement learning-assisted control approaches

Tan Guangwen, Li Mengshan\*, Hou Biyu, Zhu Jihong, Guan Lixin

*College of Physics and Electronic Information, Gannan Normal University, Ganzhou, Jiangxi, 341000, China*



### ARTICLE INFO

**Index Terms:**

Autonomous driving  
Reinforcement learning  
Vehicle lane-change  
Tracking control

### ABSTRACT

In complex urban traffic scenarios, autonomous vehicles face significant challenges in adapting to diverse and dynamic traffic conditions. Reward-based reinforcement learning has emerged as an effective approach to tackle these challenges. This paper presents a novel method that combines deep reinforcement learning with automotive dynamics systems. Building upon the Double Deep Q-learning algorithm, our approach integrates a Recurrent Neural Network with Gated Recurrent Units to enhance the environmental exploration capabilities of autonomous vehicles. To obtain more precise reward values, we introduce a trajectory tracking algorithm based on a combination of proportional-integral-derivative control and feedforward control within the automotive dynamics system. The proportional-integral-derivative controller is utilized for longitudinal control, while the Error-Optimized feedforward controller enhances lateral control, thereby improving trajectory tracking accuracy. Finally, extensive simulation experiments are conducted to evaluate the proposed method, comparing it against other baseline methods in terms of vehicle following and lane-changing scenarios. The results demonstrate that our approach significantly improves both the reward values and control performance of the algorithm.

### 1. Introduction

Autonomous driving technology has created a new wave of innovation in the automotive field. Although various methods exist for detecting and alerting drivers to traffic accidents, such as the automatic traffic accident alarm system of Volvo and Lexus, and the traffic accident detection function of the iPhone 14 series, these do not address the issue of improper driving, which is often the root cause of accidents. The advent of autonomous driving has transformed the usual patterns of accidents caused by improper driving (Bimbra et al., 2015). Autonomous driving algorithms process environmental data and provide actionable instructions to the vehicle through the control system. Therefore, precise vehicle trajectory planning, as well as accurate lateral and longitudinal control of the vehicle, are critical to achieving optimal autonomous driving performance (Xu et al., 2015; Kala and Warwick, 2013).

The field of autonomous driving has been revolutionized by various machine-learning models, leading to more intelligent autonomous vehicle algorithms. Reinforcement learning (Sutton and Barto, 1999; Sun et al., 2023) is a widely employed machine-learning model that uses a reward-punishment system to imbue behavioral norms through

excellent strategy formulation. Due to its high effectiveness and scalability, it has been extensively applied in autonomous driving technologies. For instance, the deep reinforcement learning algorithm (Li et al., 2021; Xu et al., 2021), which combines reinforcement learning with a neural network, has solved the slow-data-processing limitation of traditional reinforcement learning. Based on this algorithm, numerous reinforcement learning-related models have been developed (Fu et al., 2021; Cai et al., 2022; Wu et al., 2021), such as the automatic driving guidance model that combines deep reinforcement learning with an expert system, the safe and efficient automatic driving model based on deep Q-learning and graph attention network, and the deep reinforcement learning model for autonomous driving based on auxiliary critical networks. These models demonstrate the advantages of reinforcement learning in various aspects and can be used to modulate various behaviors of autonomous vehicles.

For instance (Wang et al., 2017), proposed a reinforcement learning architecture for autonomous vehicles to achieve ramp merging and an automatic lane-change maneuver model for autonomous vehicles. However, they did not address the lateral control of the vehicle, even though they considered a continuous action space in their reinforcement learning model (Tammewar et al., 2023). compared Proximal Policy

\* Corresponding author.

E-mail address: [msli@gnnu.edu.cn](mailto:msli@gnnu.edu.cn) (L. Mengshan).

# Trumpet-Like ZnS@C Composite for High-Performance Potassium Ion Battery Anode

Yunfei Gan,<sup>[a, b]</sup> Meiqi Mu,<sup>[b]</sup> Mingquan Li,<sup>[a, b]</sup> Xiangdong Ma,<sup>[b]</sup> Jujun Yuan,<sup>\*[b]</sup> Haishan He,<sup>[a, b]</sup> Xiaokang Li,<sup>\*[a, b]</sup> Jirong Mou,<sup>[b]</sup> Chao Zhang,<sup>[b]</sup> Xianke Zhang,<sup>[b]</sup> and Jun Liu<sup>\*[b, c]</sup>

**Abstract:** ZnS has acquired increasing attention for high-performance PIBs anode because of its remarkable theoretical capacity, and redox reversibility for conversion reaction. However, the larger volume variation and delayed reaction kinetics for the ZnS in the discharge/charge processes lead to pulverization and severe capacity degradation. Herein, the trumpet-like ZnS@C composite was synthesized by template method by using sodium citrate as carbon source followed by vulcanization process. As potassium ion batteries (PIB) anode, ZnS@C composite exhibits good rate performance and long life (stable reversible capacity of 107.8 mAh/g over

2000 charge-discharge cycles at 5 A/g and high reversible capacity of 310 mAh/g at 0.1 A/g). The outstanding electrochemical performance of the ZnS@C composite is ascribed to its unique structure, which can mitigate the volume expansion of ZnS in the charge discharge process, expand the contact area between the electrode and electrolyte, and improve the conductivity of electrode materials by the introduction of carbon layer. This method of synthesizing trumpet-like ZnS@C composite provides an important strategy for obtaining potassium ion batteries anode with long cycle.

## Introduction

Lithium-ion batteries have been successfully commercialized and commonly used in movable electronic appliances since 1991.<sup>[1–4]</sup> However, for large-scale renewable energy storage, the scarcity and uneven distribution of lithium resources and high cost limit its application.<sup>[5,6]</sup> This has prompted scientists to focus on the development of other cheaper and suitable alkali metal ion batteries such as sodium ion batteries and potassium ion batteries. Sodium ion batteries (SIBs) and potassium ion batteries (PIBs) have the same “rocking chair” detachment/insertion mechanism as lithium ion batteries (LIBs).<sup>[7,8]</sup> In the Periodic Table of elements, potassium is in the same main group as lithium and sodium, and they have similar chemical properties. Potassium ion batteries (PIBs) has a few benefits such as abundant resources, low price, low reduction potential

and high energy density.<sup>[9–11]</sup> However, owing to the larger ion radius ( $K^+$ , 2.76 Å) and the larger molecular weight, the transmission speed is slower and the volume fluctuation of the electrode is larger, which leads to the poor cyclic stability for potassium ion battery. Therefore, it is very important to explore new potassium ion electrode materials with high performance and long cycle stability.<sup>[12–14]</sup>

As a typical conversion electrode material, transition metal sulfide has the advantages of high capacity and excellent stability. These advantages make layered transition metal sulfides to be a good choice for scientists.<sup>[15–19]</sup> For instance, Geng et al. reported a carbon coated  $WS_2$  nanosheet supported by carbon nanofibers(C- $WS_2$ @CNFs) with high reversible capacity (247 mAh/g at 0.5 A/g after 300 cycles) for PIBs.<sup>[20]</sup> Cheng et al. adopted one-step hydrothermal strategy for synthesizing rGO@ $Fe_3S_4$ . When the composite material was applied to the negative electrode for PIBs, it provided excellent electrochemical performance (355 mAh/g at 0.1 A/g after 300 charge-discharge cycles).<sup>[21]</sup> Yang et al. used a simple method to synthesize bifunctional carbon modified  $NiS_2$ ( $NiS_2$ @C@C). This anode exhibited good potassium storage performance (302.7 mAh/g at 0.05 A/g).<sup>[22]</sup> However, volume expansion from the conversion reactions in the electrochemical process is still intractable, as it will result in damaging electrode material and making stability worse. Therefore, it is very important to design an effective anode material for PIBs to achieve the better electrochemical performance.

It is worth mentioning that ZnS has aroused the interest of scientists in the area of potassium ion battery energy reserves due to its non-toxic, environment-friendly, low price and great theoretical capacity (550 mAh/g).<sup>[23–28]</sup> For example, Qi et al. designed a evenly dispersed and shape controllable ZnS quantum dot loaded on graphene. When it was used as the

[a] Y. Gan, M. Li, H. He, Prof. X. Li  
College of Chemistry and Chemical Engineering  
Gannan Normal University  
Ganzhou 341000 (P.R. China)  
E-mail: lixiaokang@gznu.edu.cn

[b] Y. Gan, M. Mu, M. Li, X. Ma, Prof. J. Yuan, H. He, Prof. X. Li, J. Mou, C. Zhang, Prof. X. Zhang, Prof. J. Liu  
College of Physics and Electronics  
Gannan Normal University  
Ganzhou 341000 (P.R. China)  
E-mail: yuanjujun123@163.com  
msjliu@scut.edu.cn

[c] Prof. J. Liu  
School of Materials Science and Engineering  
South China University of Technology  
Guangzhou 510641 (P.R. China)

Supporting information for this article is available on the WWW under  
<https://doi.org/10.1002/chem.202300373>

## RESEARCH ARTICLE

# Prediction of DNA Methylation based on Multi-dimensional feature encoding and double convolutional fully connected convolutional neural network

Wenxing Hu, Lixin Guan, Mengshan Li\*

College of Physics and Electronic Information, Gannan Normal University, Ganzhou, Jiangxi, China

\* [msli@gnnu.edu.cn](mailto:msli@gnnu.edu.cn)



## OPEN ACCESS

**Citation:** Hu W, Guan L, Li M (2023) Prediction of DNA Methylation based on Multi-dimensional feature encoding and double convolutional fully connected convolutional neural network. PLoS Comput Biol 19(8): e1011370. <https://doi.org/10.1371/journal.pcbi.1011370>

**Editor:** Piero Fariselli, Universita degli Studi di Torino, ITALY

**Received:** May 16, 2023

**Accepted:** July 18, 2023

**Published:** August 28, 2023

**Peer Review History:** PLOS recognizes the benefits of transparency in the peer review process; therefore, we enable the publication of all of the content of peer review and author responses alongside final, published articles. The editorial history of this article is available here: <https://doi.org/10.1371/journal.pcbi.1011370>

**Copyright:** © 2023 Hu et al. This is an open access article distributed under the terms of the [Creative Commons Attribution License](#), which permits unrestricted use, distribution, and reproduction in any medium, provided the original author and source are credited.

**Data Availability Statement:** The codes, architecture, parameters, dataset, functions, usage and output of the proposed model are available free

## Abstract

DNA methylation takes on critical significance to the regulation of gene expression by affecting the stability of DNA and changing the structure of chromosomes. DNA methylation modification sites should be identified, which lays a solid basis for gaining more insights into their biological functions. Existing machine learning-based methods of predicting DNA methylation have not fully exploited the hidden multidimensional information in DNA gene sequences, such that the prediction accuracy of models is significantly limited. Besides, most models have been built in terms of a single methylation type. To address the above-mentioned issues, a deep learning-based method was proposed in this study for DNA methylation site prediction, termed the MEDCNN model. The MEDCNN model is capable of extracting feature information from gene sequences in three dimensions (i.e., positional information, biological information, and chemical information). Moreover, the proposed method employs a convolutional neural network model with double convolutional layers and double fully connected layers while iteratively updating the gradient descent algorithm using the cross-entropy loss function to increase the prediction accuracy of the model. Besides, the MEDCNN model can predict different types of DNA methylation sites. As indicated by the experimental results, the deep learning method based on coding from multiple dimensions outperformed single coding methods, and the MEDCNN model was highly applicable and outperformed existing models in predicting DNA methylation between different species. As revealed by the above-described findings, the MEDCNN model can be effective in predicting DNA methylation sites.

## Author summary

DNA methylation is an important DNA modification form associated with a wide range of biological processes. Identifying accurately methylation sites on a genomic scale is crucial for understanding of biological functions. This study proposes an algorithm based on Multi-dimensional feature encoding and double convolutional fully connected



## Fabrication of CeO<sub>2</sub>/Co/C composites for high-efficiency electromagnetic wave absorption

Meiqi Mu <sup>a</sup>, Jing Yu <sup>a</sup>, Zhiqian Yao <sup>a</sup>, Suqiong Xu <sup>a</sup>, Chucai Rong <sup>a</sup>, Xianke Zhang <sup>a,\*</sup>,  
Zuzhou Xiong <sup>a</sup>, Xingquan Wang <sup>a</sup>, Xiaokang Li <sup>a,b,\*\*</sup>, Jujun Yuan <sup>a,\*</sup>

<sup>a</sup> College of Physics and Electronics, Gannan Normal University, Ganzhou 341000, PR China

<sup>b</sup> College of Chemistry and Chemical Engineering, Gannan Normal University, Ganzhou 341000, PR China



### ARTICLE INFO

#### Article history:

Received 27 January 2023

Received in revised form 3 April 2023

Accepted 25 April 2023

Available online 26 April 2023

#### Keywords:

Electromagnetic wave absorption

CeO<sub>2</sub>/Co/C composites

Synergistic effect

Heterogeneous interface

Polarization

### ABSTRACT

CeO<sub>2</sub>/Co/C composites have been successfully prepared by a template method. When being applied as electromagnetic (EM) wave absorbers, CeO<sub>2</sub>/Co/C composites exhibit stronger EM wave absorption properties than Co/C and CeO<sub>2</sub>/C composites. The enhanced performance can be attributed to the unique structures of CeO<sub>2</sub>/Co/C composites, in which the synergistic effect of conductance loss, polarization loss together with magnetic loss play an important role for improving the EM wave absorption properties. Additionally, the CeO<sub>2</sub>/Co/C composites own more heterogeneous interfaces and high porosity, which promotes the continuous occurrence of interface polarization and dipole polarization, resulting in increased multiple scattering. The CeO<sub>2</sub>/Co/C composites show a RL<sub>min</sub> of -55.02 dB and an EAB of 3.29 GHz at the matching thickness of 2.82 mm. This work provides an effective strategy for constructing CeO<sub>2</sub>/Co/C composites for microwave absorbing material with high performances.

© 2023 Elsevier B.V. All rights reserved.

## 1. Introduction

Nowadays, with the rapid and ceaseless development of wireless communication technology and high-frequency electronic equipment, electromagnetic interference (EMI) and electromagnetic wave (EMW) radiation pollution have brought great harm to people's health and national information security [1,2]. Microwave absorbing materials (MAMs) are able to convert the incident electromagnetic energy into thermal energy, thereby reducing electromagnetic interference and electromagnetic radiation [3,4]. Therefore, for solving the impact of electromagnetic pollution on humans, much effort has been paid to seek new and efficient microwave absorbing materials with thin matching thickness, wide efficient bandwidth and strong absorption capacity [5–7].

According to the absorption mechanism, MAMs are chiefly divided into magnetic loss materials, dielectric loss materials, and conduction loss materials [8,9]. Among the various candidate materials, ferromagnetic materials (Fe, Co, Ni elements, etc) [10–13]

have already attracted great attraction because of their advantages such as low price, thin matching thickness, and Snoek limit [14]. However, due to the poor impedance matching of a single magnetic material, the electromagnetic wave absorption performance is poor [15,16]. To solve this problem, an effective strategy is to combine magnetic materials with carbon materials (porous carbon, graphene, carbon nanotubes) to improve microwave absorption performance [16–18]. The impedance matching of magnetic materials/carbon composites can be effectively improved owing to the mutually reinforcing of magnetic loss of the magnetic material and the conduction loss of carbon material. For instance, Li et al. [19] synthesized rod-shaped Ni@C composites using a simple hydrothermal method. The Ni@C composites showed a good wave absorbing performance with the RL<sub>min</sub> of -58.7 dB at 13.9 GHz and an EAB of 4.40 GHz at the matching thickness 1.66 mm. Wang et al. [20] prepared nanoporous Co/C composites using a thermal carbonization process. At the optimal carbonization temperature of 700 °C, the RL<sub>min</sub> of -30.31 dB at 11.03 GHz and an EAB of 4.93 GHz at the matching thickness 3.0 mm. Zeng et al. [21] prepared uniformly distributed CoFe@C core-shell composite nanoparticles with the RL<sub>min</sub> of -43.50 dB at 9.92 GHz and an EAB of 4.30 GHz at the matching thickness 2.50 mm.

Additionally, the introduction of metal oxides (SiO<sub>2</sub>, TiO<sub>2</sub>, etc.) with dielectric loss to construct metal oxide/carbon/magnetic

\* Corresponding authors.

\*\* Corresponding author at: College of Physics and Electronics, Gannan Normal University, Ganzhou 341000, PR China.

E-mail addresses: zhangxianke77@163.com (X. Zhang), lixiaokang@gnnu.edu.cn (X. Li), yuanjyun123@163.com (J. Yuan).

## Article

# DCCaps-UNet: A U-Shaped Hyperspectral Semantic Segmentation Model Based on the Depthwise Separable and Conditional Convolution Capsule Network

Siqi Wei, Yafei Liu, Mengshan Li , Haijun Huang, Xin Zheng and Lixin Guan <sup>\*</sup>

College of Physics and Electronic Information, Gannan Normal University, Ganzhou 341000, China; 1210880010@gnnu.edu.cn (S.W.); 1210880014@gnnu.edu.cn (Y.L.); msli@gnnu.edu.cn (M.L.)

\* Correspondence: lxguan@gnnu.edu.cn; Tel.: +86-797-839-3668

**Abstract:** Traditional hyperspectral image semantic segmentation algorithms can not fully utilize the spatial information or realize efficient segmentation with less sample data. In order to solve the above problems, a U-shaped hyperspectral semantic segmentation model (DCCaps-UNet) based on the depthwise separable and conditional convolution capsule network was proposed in this study. The whole network is an encoding–decoding structure. In the encoding part, image features are firstly fully extracted and fused. In the decoding part, images are then reconstructed by upsampling. In the encoding part, a dilated convolutional capsule block is proposed to fully acquire spatial information and deep features and reduce the calculation cost of dynamic routes using a conditional sliding window. A depthwise separable block is constructed to replace the common convolution layer in the traditional capsule network and efficiently reduce network parameters. After principal component analysis (PCA) dimension reduction and patch preprocessing, the proposed model was experimentally tested with Indian Pines and Pavia University public hyperspectral image datasets. The obtained segmentation results of various ground objects were analyzed and compared with those obtained with other semantic segmentation models. The proposed model performed better than other semantic segmentation methods and achieved higher segmentation accuracy with the same samples. Dice coefficients reached 0.9989 and 0.9999. The OA value can reach 99.92% and 100%, respectively, thus, verifying the effectiveness of the proposed model.

**Keywords:** hyperspectral image; semantic segmentation; capsule network; depthwise separable convolution; dynamic routing; encoding–decoding



**Citation:** Wei, S.; Liu, Y.; Li, M.; Huang, H.; Zheng, X.; Guan, L. DCCaps-UNet: A U-Shaped Hyperspectral Semantic Segmentation Model Based on the Depthwise Separable and Conditional Convolution Capsule Network. *Remote Sens.* **2023**, *15*, 3177. <https://doi.org/10.3390/rs15123177>

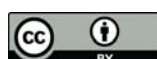
Academic Editors: Federico Santini and Sen Jia

Received: 15 May 2023

Revised: 16 June 2023

Accepted: 16 June 2023

Published: 19 June 2023



**Copyright:** © 2023 by the authors. Licensee MDPI, Basel, Switzerland. This article is an open access article distributed under the terms and conditions of the Creative Commons Attribution (CC BY) license (<https://creativecommons.org/licenses/by/4.0/>).

## 1. Introduction

In recent years, with the continuous development of hyperspectral image technology [1], the analysis and processing of hyperspectral data [2–5] have become a research hotspot in many fields. Hyperspectral image is a kind of image with hundreds to thousands of spectral bands for a single pixel, which can obtain a large amount of spatial and spectral information, so it has important application value in many fields such as remote sensing [6,7], environmental monitoring [8,9], agriculture [10–12], and medicine [13,14]. Semantic segmentation is one of the main tasks in hyperspectral image application research. The semantic segmentation of hyperspectral images is mainly to classify each pixel in the image into a specific feature category according to its spatial semantic information. However, the complex data structure and high information redundancy of hyperspectral images make this task challenging. Although the operation of traditional image segmentation [15–21] is relatively simple, it is difficult to obtain satisfactory performance because it mostly relies on handmade features. Therefore, it is of great research significance to establish an efficient semantic segmentation model for hyperspectral images.

With the rapid development of deep learning, convolutional neural networks (CNN) have been widely used in semantic segmentation [22,23]. In 2015, Hu et al. [24] first tried to



## Research Article

Fabrication of  $\text{Bi}_2\text{Se}_3/\text{Mo}_3\text{Se}_4$  composite for efficient sodium storage

Yunfei Gan<sup>a,b</sup>, Haishan He<sup>a,b</sup>, Meiqi Mu<sup>b</sup>, Jujun Yuan<sup>b,\*</sup>, Hong Liao<sup>b</sup>, Xiaokang Li<sup>a,b,\*\*</sup>, Yi Yu<sup>b</sup>, Xianke Zhang<sup>b</sup>, Jun Liu<sup>b,c,\*</sup>

<sup>a</sup> College of Chemistry and Chemical Engineering, Gannan Normal University, Ganzhou 341000, PR China<sup>b</sup> Key Laboratory of New Energy Materials and Low Carbon Technologies, College of Physics and Electronics, Gannan Normal University, Ganzhou 341000, PR China<sup>c</sup> School of Materials Science and Engineering, South China University of Technology, Guangzhou 510641, PR China

## ARTICLE INFO

## Article history:

Received 20 March 2022

Received in revised form 15 July 2022

Accepted 21 July 2022

Available online 23 July 2022

## Keywords:

 $\text{Bi}_2\text{Se}_3$  $\text{Mo}_3\text{Se}_4$ 

Composite

Sodium ion battery

Anode

## ABSTRACT

In this work, the  $\text{Bi}_2\text{Se}_3/\text{Mo}_3\text{Se}_4$  composite is obtained through electrochemical activation of  $\text{Bi}_2\text{Se}_3/\text{MoSe}_2$  composite, which has been synthesized by an ordinary hydrothermal reaction closely followed by selenization process. The  $\text{Bi}_2\text{Se}_3/\text{Mo}_3\text{Se}_4$  composite appears good electrochemical property as the negative electrode material for sodium ion batteries (the stable reversible capacity is 409 (346) mAh g<sup>-1</sup> at 100 (1000) mA g<sup>-1</sup>). The outstanding electrochemical property can be attributed to the unique  $\text{Bi}_2\text{Se}_3/\text{Mo}_3\text{Se}_4$  composite architecture, in which  $\text{Bi}_2\text{Se}_3$  is responsible for offering a high capacity, and  $\text{Mo}_3\text{Se}_4$  is responsible for improving electrochemical stability. Moreover, the small particle sizes for  $\text{Bi}_2\text{Se}_3/\text{Mo}_3\text{Se}_4$  resulting from the amorphous to crystalline transitions during cycling is also the cause of the increased stability of the electrode. The design of the  $\text{Bi}_2\text{Se}_3/\text{Mo}_3\text{Se}_4$  composite provides a potential tactics to construct other metal selenides composites for sodium-ion battery anode.

© 2022 Elsevier B.V. All rights reserved.

## 1. Introduction

Rechargeable battery technology is regarded as an important part of high-efficiency energy storage systems [1]. Nowadays lithium-ion batteries have been successfully commercially available [2–4]. However, with the consumption of lithium resources, people have begun to look for other types of batteries that can replace lithium-ion batteries [1,5,6]. Sodium-ion batteries (SIBs) has captured increasing attention since its abundant resources, low cost, and electrochemical principles resemble to lithium [7–9]. However, because the atomic radius of sodium ions is larger than lithium ions, the volume change of the electrode material of the sodium ions during the charging and discharging process will be greater, and the structure pulverization will be serious. At present, finding suitable battery electrode materials with excellent performance is a challenge to adapt to wide-range energy storage in the future [10–12].

Transition metal selenides are regarded as a candidate for negative electrode material in sodium storage since its excellent

reversible capacity, stable chemistry and environmental friendliness [13–16]. For instance, the  $\text{Cu}-\text{CoSe}_2$  NFCs [17] anode represented stable reversible capacity of 470 mAh g<sup>-1</sup> at 100 mA g<sup>-1</sup>. And  $\text{FeSe}_2$  [13] nanorods/graphene showed a glorious rate performance and excellent reversible capacity of 459 mAh g<sup>-1</sup> at 100 mA g<sup>-1</sup>. Besides,  $\text{MoSe}_2 @\text{C}@\text{GR}$  [18] nanofiber electrode could provide a discharge capacity of 366.9 mAh g<sup>-1</sup> after 200 charge-discharge cycles at 200 mA g<sup>-1</sup>. Furthermore, the  $\text{Bi}_2\text{Se}_3/\text{C}$  [19] electrode also provided an initial capacity of 527 mAh g<sup>-1</sup> at 100 mA g<sup>-1</sup> while a capacity retention rate of the battery was 89 % after 100 charge-discharge cycles. Despite attractive results had been achieved for many selenide metal materials, how to go a step further improve the property of battery anode materials has been a confusing challenge. It is because electrochemical conversion and alloying reactions are usually accompanied by large volume changes and solid electrolyte interface (SEI) film growth.

Compared with single transition metal selenides/sulfides, binary metal selenides/sulfides composite have more redox sites, higher ion diffusion kinetics, and better electrical conductivity. Numerous studies have shown that bimetallic selenides/sulfides composite can improve the electrochemical performance of the whole material when used as anode materials for sodium/potassium ion batteries due to the synergistic effect of each other [20–24]. Interfacial interactions between materials can also effectively tune their physicochemical properties, considering that charge/mass transfer

\* Corresponding author.

\*\* Corresponding authors at: Key Laboratory of New Energy Materials and Low Carbon Technologies, College of Physics and Electronics, Gannan Normal University, Ganzhou 341000, PR China.

E-mail addresses: [yuanjun123@163.com](mailto:yuanjun123@163.com) (J. Yuan), [lixiaokang@gnnu.edu.cn](mailto:lixiaokang@gnnu.edu.cn) (X. Li), [msjliu@scut.edu.cn](mailto:msjliu@scut.edu.cn) (J. Liu).



# A microscopic computational model based on particle dynamics and evolutionary algorithm for the prediction of gas solubility in polymers



Mengshan Li <sup>a,\*</sup>, Ming Zeng <sup>a</sup>, Bingsheng Chen <sup>a</sup>, Lixin Guan <sup>a</sup>, Yan Wu <sup>a</sup>, Nan Wang <sup>b,\*</sup>

<sup>a</sup>College of Physics and Electronic Information, Gannan Normal University, Ganzhou 341000, Jiangxi, China

<sup>b</sup>College of Life Sciences, Jiaying University, Meizhou 514015, Guangdong, China

## ARTICLE INFO

### Article history:

Received 28 April 2022

Revised 12 August 2022

Accepted 20 August 2022

Available online 25 August 2022

### Keywords:

Dissolution behavior

Evolutionary computation

Particle dynamics

Computational model

## ABSTRACT

Solubility is one of the key physicochemical properties of foaming materials and plastic membrane materials, which are commonly used in the processing, preparation, and modification of various new materials. It is challenging to develop a good dissolution behavior calculation model. A novel particle dynamics evolutionary algorithm (DP-PD-EA) is developed to simulate the movement of molecules in the process of dissolution at the microscopic scale. DP-PD-EA deeply combines particle dynamics with evolutionary algorithm so that particles evolve iteratively under the action of the potential energy field. The prediction experiments of the solubility of supercritical carbon dioxide ( $\text{SCCO}_2$ ) in three polymers confirmed that DP-PD-EA had the better prediction performances than other models. The proposed model can be used in the solubility calculation of foaming materials and has theoretical and practical values in many fields, such as the prediction of physical/chemical properties and the calculation of multi-scale theory.

© 2022 Elsevier B.V. All rights reserved.

## 1. Introduction

Foaming materials have many superior properties due to their unique structures. In the molding process, supercritical carbon dioxide ( $\text{SCCO}_2$ ) enters polymer melt through an air inlet and then goes through three processes of dissolution, nucleation and foaming to obtain foaming material products. The dissolution behavior of  $\text{SCCO}_2$  in polymer melt is the important factor influencing the product performance [1,2]. In addition, it is used in various new materials and has significant values [3–8]. Dissolution behaviors of  $\text{SCCO}_2$  are mainly explored through experiments and simulations. Due to the experimental difficulty under high temperature and high pressure, stirring, vibration, shear and other means are often used to accelerate the dissolution process [9–12]. Dissolution behaviors of  $\text{SCCO}_2$  show some complex characteristics, such as nonlinearity, non-equilibrium, dynamics and criticality under supercritical conditions. The simulation of dissolution behaviors of  $\text{SCCO}_2$  is of great significance in both theoretical studies and applications.

The calculation models of dissolution behaviors mainly include thermodynamic model, empirical model, and computer simulation model [13–16]. The thermodynamic model is mainly composed of equation of state (EOS) and empirical/semi-empirical equation. The

EOS is mainly P-R EOS and S-L EOS, the empirical equation is expanded based on Chrastil's equation [17–20]. Computer simulations mainly contain ab initio simulation, molecular dynamics simulation, and machine learning simulation [21]. Ab initio simulation is a computational method of solving the Schrödinger equation. While, molecular dynamics simulation is based on the calculation strategy of classical Newton mechanics [22–24]. Machine learning simulation uses intelligent algorithm and/or artificial neural network (ANN) to predict dissolution behaviors. For example, Ghargheizi et al. [25–27] indicated that the prediction method of ANN had the higher prediction accuracy than other models. However, the predictive performance of artificial neural networks is highly dependent on the training algorithm. Some researchers explored the application of particle swarm optimization (PSO) in the parameter optimization of the model and achieved the good prediction effect [28]. When the PSO algorithm was applied in ANN training [29], the search process became slow and the local optimization problem occurred near the global value. The hybrid method based on the improved PSO and back propagation ANN (BP ANN) has the better performance [30]. Based on the PSO, clustering algorithm, and diffusion theory, we proposed several macro-scale models for predicting the gas solubility in polymers [31–34]. Compared with other existing models, the proposed models had the better comprehensive performance.

Although the above methods (EOS, MD, and AI) have achieved satisfactory results in some experiments, these methods still have

\* Corresponding authors.

E-mail addresses: [jcimsli@163.com](mailto:jcimsli@163.com) (M. Li), [201401018@jyu.edu.cn](mailto:201401018@jyu.edu.cn) (N. Wang).



# Microstructures constructed by MoSe<sub>2</sub>/C nanoplates sheathed in N-doped carbon for efficient sodium (potassium) storage



Xiaofan Li<sup>a,b,1</sup>, Weidong Lai<sup>a,b,1</sup>, Yunfei Gan<sup>a,b</sup>, Haishan He<sup>a,b</sup>, Jujun Yuan<sup>a,\*</sup>, Xianke Zhang<sup>a</sup>, Huajun Yu<sup>a</sup>, Xiaokang Li<sup>a,b,\*\*</sup>, Jun Liu<sup>a,c,\*\*\*</sup>

<sup>a</sup> College of Physics and Electronics, Gannan Normal University, Ganzhou 341000, PR China

<sup>b</sup> College of Chemistry and Chemical Engineering, Gannan Normal University, Ganzhou 341000, PR China

<sup>c</sup> School of Materials Science and Engineering, South China University of Technology, Guangzhou 510641, PR China

## ARTICLE INFO

### Article history:

Received 7 July 2021

Received in revised form 24 August 2021

Accepted 26 August 2021

Available online 31 August 2021

### Keywords:

MoSe<sub>2</sub>/C nanoplates

Anode material

Sodium ion batteries

Potassium ion batteries

N-doped carbon

## ABSTRACT

Molybdenum diselenide (MoSe<sub>2</sub>) has been drawing increasingly more attention due to its natural abundance, larger interlayer space (~ 6.5 Å) and higher theoretical capacity (422 mA h/g). Nevertheless, the low capacity and the poor cycling stability greatly hinder their application. Here, microstructures constructed by MoSe<sub>2</sub>/C nanoplates sheathed in N-doped carbon (MoSe<sub>2</sub>/C@NC) were synthesized by co-precipitation approach and subsequent annealing treatment with selenium powder. MoSe<sub>2</sub>/C@NC electrode shows the reversible sodium/potassium ion storage capacity of 362 and 310 mA h/g at 0.1 A/g, respectively. In SIBs, the capacity retains 237 mA h/g after a long-term cycling (500 cycles) at 1 A/g. In addition, it is worth noting that the capacity also retains 212 mA h/g at 1 A/g over 100 cycles in PIBs. The excellent performances for sodium and potassium ions storage are credited to the synergistic effect of unique assembly structure of MoSe<sub>2</sub>/C@NC, which can effectively alleviate volume expansion, and improve the electrical conductivity of MoSe<sub>2</sub>.

© 2021 Elsevier B.V. All rights reserved.

## 1. Introduction

Lithium-ion batteries have developed rapidly since their advent in the 1990s and now account for the largest share of the market for small secondary batteries, as well as their popularity in hybrid cars and smart grids [1,2]. Nevertheless, the application of LIBs has been constrained by shortage lithium resources [3,4]. In this case, sodium ion batteries (SIBs) and potassium ion batteries (PIBs) have captured increasing attention because of low prices and richness of the Na and K [5,6]. The physical and chemical properties of sodium and potassium are similar to lithium. However, the ionic radii of sodium (potassium) ion is greater than lithium ion, which greatly increases the diffusion barrier and prevents ion insertion/extraction, inducing the inapplicability of most lithium ion anode materials for SIBs/PIBs

[7–9]. Consequently, it is necessary to explore suitable anode materials for SIBs/PIBs.

Transition-metal dichalcogenides (TMDs) with a layered structure has inspired extensive attention due to their excellent physicochemical characteristics. As a promising candidate for the TMD series, molybdenum diselenide (MoSe<sub>2</sub>) has a large interlayer space (~ 6.5 Å) [10,11] and higher theoretical capacity (~ 422 mA h/g) [12]. However, when MoSe<sub>2</sub> was used as the anode of SIBs/PIBs, it usually displays inferior cycle stability and low specific capacity, mainly owing to its huge volume expansion and poor ionic conductivity. To address above drawbacks, a large number of effective strategies have been put forward, such as formation of a protection layer, preparation of two-dimensional materials [13] and multi-metal organic framework materials [14], preparation of nano/micron MoSe<sub>2</sub> and composite with conductive materials [15–18]. Qian et al. synthesized a MoSe<sub>2</sub>/N,P-rGO composite, which displayed the superior capacity of 378 mA h/g at 0.5 A/g in SIBs [19]. Lu et al. synthesized the carbon-coated MoSe<sub>2</sub> nanosheets, which showed an excellent capacity of 258.02 mA h/g at 0.1 A/g over 300 cycles in PIBs [20]. Guo et al. designed the core-shell structure of MoSe<sub>2</sub>/C, which exhibited the potassium storage capacity of 322 mA h/g at 0.2 A/g over 100 cycles [21]. Zhang et al. designed a MoSe<sub>2</sub>/carbon for SIBs that displayed a

\* Corresponding author.

\*\* Corresponding authors at: College of Physics and Electronics, Gannan Normal University, Ganzhou 341000, PR China.

E-mail addresses: [yuanjijun123@163.com](mailto:yuanjijun123@163.com) (J. Yuan), [gnnulxk@163.com](mailto:gnnulxk@163.com) (X. Li), [msjliu@scut.edu.cn](mailto:msjliu@scut.edu.cn) (J. Liu).

<sup>1</sup> Xiaofan Li and Weidong Lai make the same contribution to this work.



# Local structure modulation *via* cation compositional regulation for durable Li-rich layered cathode materials



Zaijun Chen<sup>a</sup>, Junxia Meng<sup>b</sup>, Yuqin Wang<sup>a</sup>, Quanxin Ma<sup>a,c,\*</sup>, Fulin Lai<sup>a</sup>, Zhifeng Li<sup>a</sup>, Qian Zhang<sup>a</sup>, Dong Li<sup>a</sup>, Shengwen Zhong<sup>a,\*</sup>

<sup>a</sup> Key Laboratory of Power Battery and Materials, Faculty of Materials Metallurgy and Chemistry, Jiangxi University of Science and Technology, Ganzhou 341000, China

<sup>b</sup> School of Physics and Electronics, Gannan Normal University, Ganzhou 341000, China

<sup>c</sup> Far East Battery, FEB Research Institute, Yichun 336000, China

## ARTICLE INFO

### Article history:

Received 8 December 2020

Revised 8 March 2021

Accepted 8 March 2021

Available online 10 March 2021

### Keywords:

Li-ion battery

Li-rich Mn-based layered oxide

Mn/Ni ratio

Local structure regulation

Energy density decay

## ABSTRACT

A series of manganese-based lithium-rich layered oxide (LLO) cathode materials with different local structures have been synthesized by adjusting the stoichiometric ratios of Mn/Ni. One of the as-synthesized cathode materials with an Mn/Ni ratio of 7 to 2 ( $\text{Li}_{1.3}\text{Mn}_{0.7}\text{Ni}_{0.2}\text{Co}_{0.1}\text{O}_{2.4}$ , denoted as MNC-721) showed an appropriate degree of cation mixing, thereby exhibiting superior cycling stability, better rate capability, and much slower voltage decay when compared with the other two cathode materials with different Mn/Ni ratios. More importantly, a full cell was assembled using the MNC-721 cathode material and it rendered mass-energy density retention of 90.0% after 300 cycles. An appropriate amount of mixing of the  $\text{Li}^+$  ions and the transition metal (TM) in the Li layers improved the electrochemical performance of the material. The TM ions in the lithium layers can support the layered structure as well as weaken the repulsion between neighboring oxygen layers during processes of charge and discharge. The proposed method in this project is promising to be used to improve LLO cathode materials' electrochemical performance by modifying their local structures, thereby promoting their further practical applications in Li-ion batteries with high performance.

© 2021 Elsevier Ltd. All rights reserved.

## 1. Introduction

The increasing global interest in electric vehicles has inspired the interest of research on next-generation rechargeable batteries of high energy density and low cost. Therefore, there is an urgency and greater demand to develop lithium-ion battery (LIB) materials with high energy density and durable cycle life [1–5]. Li-rich Mn-based layered oxides (LLOs) are promising cathode materials because the theoretical energy density of this type of cathode materials can reach 1000 Wh kg<sup>-1</sup> and their specific capacity can be higher than 300 mAh g<sup>-1</sup> [6–9]. Unfortunately, LLO cathode materials have not been successfully commercialized because they suffer from several drawbacks, such as energy density decay upon cycling, significant first irreversible loss in capacity and unsatisfactory rate performance [10,11]. Among these problems, the energy

density decay of LLO materials is the most critical issue in their industrialization process. Therefore, one way to promote the application of LLO materials in high-energy LIBs is to enhance energy retention during long-term cycling.

A rock-salt phase transition process from a layered one to a spinel one or an orderly one to a disorderly one has been considered as one of the intrinsic reasons for fast energy density decay [12–14]. Because Li and transition metal (TM) cation arrangement patterns differ in layered and spinel or rock-salt phases, usually TM ion migration is involved in a layered-to-spinel or an order-to-disorder rock salt phase transition process during long-term cycling [15]. To effectively address this issue, a great deal of research has been done on the lattice doping, surface modification or particle size control [6, 16–18]. Although dopants can stabilize the structures of LLO materials, an atomic scale of such doping remains challenging [19]. The surface modification does not cause degradation of electrodes while the bulk structure of an electrode is kept intact. The coating on the surface of a modified material tends to be uneven and spotted, which will impair the specific capacity of cathodes and hinder  $\text{Li}^+$  diffusion [20]. The rate capability of LLO materials can be improved when the particle size of coating ma-

\* Corresponding authors at: Key Laboratory of Power Battery and Materials, Faculty of Materials Metallurgy and Chemistry, Jiangxi University of Science and Technology, Ganzhou 341000, China.

E-mail addresses: [maquanxin321@163.com](mailto:maquanxin321@163.com) (Q. Ma), [zhongshw@126.com](mailto:zhongshw@126.com) (S. Zhong).

# Fabrication of ZnSe/C Hollow Polyhedrons for Lithium Storage

Jujun Yuan,<sup>[a]</sup> Xiaofan Li,<sup>[a, c]</sup> Haixia Li,<sup>[a]</sup> Weidong Lai,<sup>[a, c]</sup> Yunfei Gan,<sup>[a, c]</sup> Jianwen Yang,\*<sup>[b]</sup> Xianke Zhang,<sup>[a]</sup> Jun Liu,\*<sup>[a, d]</sup> Xiurong Zhu,<sup>[a]</sup> and Xiaokang Li\*<sup>[a, c]</sup>

**Abstract:** ZnSe has got extensive attention for high-performance LIBs anode due to its remarkable theoretical capacity and environmental friendliness. Nevertheless, the large volume variation for the ZnSe in the discharge/charge processes brings about rapid capacity fading and poor rate performance. Herein, ZnSe/C hollow polyhedrons are successfully synthesized by selenization of zeolitic imidazolate framework-8 (ZIF-8) with resorcinol-formaldehyde (RF) coating. The protection of C layer derived from RF coating layer and Ostwald ripening during the process of selenization play

important roles in promoting formation of ZnSe/C hollow polyhedrons. The ZnSe/C hollow polyhedrons exhibit good rate performance and long-term cycle stability ( $345 \text{ mAh g}^{-1}$  up to 1000 cycles at  $1 \text{ A g}^{-1}$ ) for lithium ion batteries (LIBs) anode. The improved electrochemical performance is benefit from the unique ZnSe/C hollow structure, in which the hollow structure can effectively avoid terrible volume expansion, and the thin ZnSe/C shell can not only provide adequate diffusion paths of lithium ions and but also enhance the electronic conductivity.

## Introduction

Nowadays, growing requirements of batteries for electric vehicles have promoted the research on electrode materials for LIBs anode with high energy density.<sup>[1,2]</sup> Metal chalcogenide (metal selenides (sulfides)) have unique physicochemical properties (e.g., good electric conductivity, superior thermal stability, earth abundance, etc.).<sup>[3]</sup> Especially, metal selenides (ZnSe, MoSe<sub>2</sub>, FeSe<sub>2</sub> etc)<sup>[4–7]</sup> have been regarded as hopeful candidates for substituting the commercial graphite ( $372 \text{ mAh g}^{-1}$ ) anode because of their high theoretical capacities. For example, ZnSe@C nanocomposite displayed high capacity of  $960 \text{ mAh g}^{-1}$  at  $0.2 \text{ A g}^{-1}$ .<sup>[4]</sup> MoSe<sub>2</sub>/CMK-5 composites showed a reversible capacity of  $788 \text{ mAh g}^{-1}$  at  $0.1 \text{ A g}^{-1}$  and superior rate

performance.<sup>[5]</sup> As one competitive material within metal selenides, ZnSe has got extensive attention for high-performance LIBs anode due to its remarkable theoretical capacity and environmental friendliness.<sup>[8,9]</sup> Nevertheless, similar to other metal selenides, the large volume variation for the ZnSe in the discharge/charge processes bring about rapid capacity fading and poor rate performance.

For the sake of overcoming these problems, one of effective strategy is to design ZnSe/C nanocomposite, which can availablely buffer strain of volume variation in the lithiation/delithiation process and provide adequate diffusion paths of lithium ions.<sup>[10–14]</sup> For example, Ji et al. designed carbon-coated hollow ZnSe sphere by Ostwald ripening method and the ZnSe/C sphere retained a reversible capacity ( $574 \text{ mAh g}^{-1}$  at  $1 \text{ A g}^{-1}$ ).<sup>[10]</sup> Feng et al. demonstrated ZIF-8 derived ZnSe polyhedra/RGO composites could maintain stable capacity of  $464 \text{ mAh g}^{-1}$  at  $2 \text{ A g}^{-1}$ .<sup>[11]</sup> It is also confirmed that ZnSe/C electrospinning nanofiber displayed improved electrochemical properties.<sup>[12]</sup> Based on the above mentioned electrochemical properties of ZnSe/C nanocomposites, it is observed that constitution, morphology, and pore structure for the ZnSe/C nanocomposites can synergistically affect the cyclability of the ZnSe/C anode. Therefore, to further improve electrochemical property of ZnSe/C anode materials for LIBs, it deserves to continue exploring novel ZnSe/C nanocomposites by facile strategy.

Herein, for the first time, ZIF-8@RF derived ZnSe/C hollow polyhedrons have been synthesized through a facile strategy. As LIBs anode, ZnSe/C hollow polyhedrons exhibit better cyclability, compared with ZIF-8 without RF coating derived ZnSe/C nanostructures. The improved electrochemical property is benefit from the unique ZnSe/C hollow architecture, in which the hollow structure can effectively buffer the strain of volume variation, and the thin ZnSe/C shell can not only provide

[a] Prof. J. Yuan, X. Li, H. Li, W. Lai, Y. Gan, Prof. X. Zhang, Prof. J. Liu, Prof. X. Zhu, Prof. X. Li

School of Physics and Electronics  
Gannan Normal University  
Ganzhou 41000 (P. R. China)  
E-mail: msjliu@scut.edu.cn  
gnulxk@163.com

[b] Prof. J. Yang

College of Chemistry and Bioengineering  
Guilin University of Technology  
Guilin (P. R. China)  
E-mail: 2005009@glut.edu.cn

[c] X. Li, W. Lai, Y. Gan, Prof. X. Li

College of Chemistry and Chemical Engineering  
Gannan Normal University  
Ganzhou 341000 (P. R. China)

[d] Prof. J. Liu

School of Materials Science and Engineering  
South China University of Technology  
Guangzhou 510641 (P. R. China)

Supporting information for this article is available on the WWW under  
<https://doi.org/10.1002/chem.202102828>



## Precursor pre-oxidation enables highly exposed plane {010} for high-rate Li-rich layered oxide cathode materials



Junxia Meng <sup>a, b, 1</sup>, Huaizhe Xu <sup>c, 1</sup>, Quanxin Ma <sup>a,\*</sup>, Zhifeng Li <sup>a</sup>, Lishuang Xu <sup>c</sup>, Zaijun Chen <sup>a</sup>, Boming Cheng <sup>a</sup>, Shengwen Zhong <sup>a,\*\*</sup>

<sup>a</sup> School of Materials Science and Engineering, Key Laboratory of Power Battery and Materials, Jiangxi University of Science and Technology, Ganzhou, 341000, China

<sup>b</sup> School of Physics and Electronics, Gannan Normal University, Ganzhou, 341000, PR China

<sup>c</sup> School of Physics and Nuclear Energy Engineering, Beihang University, Beijing, 100191, China

### ARTICLE INFO

#### Article history:

Received 16 February 2019

Received in revised form

7 April 2019

Accepted 7 April 2019

Available online 17 April 2019

#### Keywords:

Li-rich layered oxide

Precursor pre-oxidation

Single-crystal nanoparticle

High-rate performance

Pouch cell

### ABSTRACT

Precursor synthesis technology is a key factor to improve the electrochemical properties of Li-rich layered oxide (LLO) cathode materials. However, the effect of precursor preparation strategies on the morphology and electrochemical properties of cathode materials has not been clearly elucidated. In this work, an LLO cathode material (denoted as LMNC-300) with highly exposed {010} planes and a lower amount of surface residual lithium is reported via pre-oxidation of a precursor at 300 °C. This LMNC-300 cathode material exhibits an initial Coulombic efficiency of 91.7% with a discharge capacity of 277.2 mA h g<sup>-1</sup> at 0.1 C, an excellent high-rate capability with a discharge capacity of 175.1 mA h g<sup>-1</sup> even at 5.0 C and a good cycling performance with a capacity retention of 92.6% after 200 cycles at 0.5 C. In addition, a pouch cell consisted of the LMNC-300 cathode and a commercial graphite anode presented good cycling stability with a capacity retention of 81.6% after 500 cycles at 2.0 C. The outstanding electrochemical performance can be ascribed to an accelerated Li<sup>+</sup> diffusion dynamics. Therefore, the method reported in this work will be significant to understanding the effects of preparation strategies of transition metal precursors on the electrochemical performance of Li-rich layered cathode materials for high-energy density Li-ion batteries.

© 2019 Elsevier Ltd. All rights reserved.

### 1. Introduction

The development of electric vehicles alternative to fossil-fueled cars calls for lithium-ion batteries (LIBs) with high energy and power densities. Generally, exploring high-capacity electrode materials for high energy storage and engineering heterogeneous structures for fast charge transfer are the most effective approaches for enhancing energy and power densities of LIBs [1–7], respectively. Lithium-rich layered oxides (LLO) with a formula of

$x\text{Li}_2\text{MnO}_3 \cdot (1-x)\text{LiMO}_2$  (M = Mn, Ni, Co) are very promising as commercialized cathode materials for LIBs due to their high discharge capacity, high energy density and a lower cost [8–12]. However, LLO cathode materials show a few drawbacks such as their poor rate capability, large first-cycle irreversible capacity loss, and voltage and capacity decay during extended cycling, which have hindered the commercial applications of this type of materials [13–16]. Therefore, it is highly desired to have essential modifications for LLO cathode materials.

To optimize the electrochemical properties of LLO cathode materials, the surface structure and morphology control are two crucial factors that determine the rate of Li<sup>+</sup> ion deintercalation-intercalation [17,18]. In general, the morphology of cathode materials has inheritance to the morphology of the precursor to a certain degree; the structure and the electrochemical properties of LLO cathode materials are closely related to the synthesis technology and the morphology of their precursors [19–21]. According to the study conducted by Zheng et al. [22], the poor rate capability of LLO

\* Corresponding author. School of Materials Science and Engineering, Key Laboratory of Power Battery and Materials, Jiangxi University of Science and Technology, Ganzhou, 341000, China.

\*\* Corresponding author. School of Materials Science and Engineering, Key Laboratory of Power Battery and Materials, Jiangxi University of Science and Technology, Ganzhou, 341000, China.

E-mail addresses: [maquanxin321@163.com](mailto:maquanxin321@163.com) (Q. Ma), [\(S. Zhong\).](mailto:zhongshw@126.com)

<sup>1</sup> Junxia Meng and Huaizhe Xu contributed equally.



## SnO<sub>2</sub>/polypyrrole hollow spheres with improved cycle stability as lithium-ion battery anodes



Jujun Yuan <sup>a,b,\*</sup>, Chunhui Chen <sup>b</sup>, Yong Hao <sup>b</sup>, Xianke Zhang <sup>a,b</sup>, Bo Zou <sup>c</sup>, Richa Agrawal <sup>b</sup>, Chunlei Wang <sup>b,\*\*</sup>, Huajun Yu <sup>a</sup>, Xiurong Zhu <sup>a</sup>, Yi Yu <sup>a</sup>, Zuzhou Xiong <sup>a</sup>, Ying Luo <sup>a</sup>, Haixia Li <sup>a</sup>, Yingmao Xie <sup>a</sup>

<sup>a</sup> School of Physics and Electronics, Gannan Normal University, Ganzhou, 341000, PR China

<sup>b</sup> Department of Mechanical and Materials Engineering, Florida International University, Miami, FL, 33174, USA

<sup>c</sup> State Key Laboratory of Superhard Materials, Jilin University, Changchun, 130012, PR China

### ARTICLE INFO

#### Article history:

Received 2 June 2016

Received in revised form

15 August 2016

Accepted 22 August 2016

Available online 24 August 2016

#### Keywords:

Lithium ion battery

Anode

SnO<sub>2</sub>/polypyrrole hollow spheres

Wet-chemical

### ABSTRACT

SnO<sub>2</sub>/polypyrrole (SnO<sub>2</sub>/PPy) hollow spheres were fabricated by a liquid-phase deposition method using colloidal carbon spheres as templates followed by an in-situ chemical-polymerization route. The obtained SnO<sub>2</sub>/PPy composite particles had a size of 610–730 nm. The thickness of inner shell (SnO<sub>2</sub>) and outer shell (PPy) for composites was about 35 and 90 nm, respectively. As an anode for lithium ion batteries, the SnO<sub>2</sub>/PPy composites electrode showed superior rate capability and excellent long-term cycling performance. After a long-term cycling of 600 cycles at different current densities, a capacity of 899 mAh g<sup>-1</sup> was achieved at the current density of 100 mA g<sup>-1</sup> for SnO<sub>2</sub>/PPy composites. The excellent electrochemical performance was attributed to the synergistic effect between the PPy coating layer and the hollow SnO<sub>2</sub> spheres, which guaranteed vast lithium storage sites, good electronic conductivity, fast lithium ion diffusion, and sufficient void space to buffer the volume expansion.

© 2016 Elsevier B.V. All rights reserved.

## 1. Introduction

Lithium batteries (LIBs), as a main power source or back-up power source for electric and hybrid vehicles have attracted much attention due to their superior properties such as high energy density, long cycle life, and no memory effect [1]. Many metal oxides have been intensively studied as potential high-performance anodes for LIBs due to their high theoretical capacities, and natural abundance [2–5]. Tin oxide (SnO<sub>2</sub>) stands out as one of the attractive anode candidates considering its abundance, environmental benignity, and high theoretical capacity (780 mAh g<sup>-1</sup>) [6,7]. However, the practical implementation of SnO<sub>2</sub> materials is still hindered by its poor cycle life, which is caused from enormous volume expansion and contraction during repeated discharge/charge process [8].

To overcome the problems related with SnO<sub>2</sub> anodes for LIBs, one strategy is to utilize hollow SnO<sub>2</sub> nanostructures, such as nanotube [9], nanobox [10], and hollow sphere [11], to decrease the

absolute volume variation. Among them, SnO<sub>2</sub> hollow spheres have been investigated as a way to improve its electrochemical properties due to the advantages of providing more reaction sites, short Li<sup>+</sup> diffusion lengths and local empty space for partial accommodation of large volume change during cycling [12]. Up to now, the SnO<sub>2</sub> hollow spheres have been fabricated by numerous efficient methods, including either template (hard and soft templates) assisted synthesis or template-free routes. Between them, template assisted synthesis, especially using hard templates (carbon, polystyrene, SiO<sub>2</sub>, etc), is an effective approach for the preparation of controllable SnO<sub>2</sub> hollow spheres [13–15].

Another important strategy is to prepare SnO<sub>2</sub> composite electrodes with other effective conducting materials, such as carbon [16–18], carbon nanofiber [19], graphene [20], and conductive polymers [21,22]. Among these materials, conducting polymers have gained significant attention given its good flexibility and electronic conductivity. For example, Sun et al. reported that Polypyrrole (PPy) coated ZnFe<sub>2</sub>O<sub>4</sub> hollow spheres electrode showed excellent cycling stability for LIBs [23]. So, an appreciable improvement is thus expected upon the integration of SnO<sub>2</sub> hollow spheres with conducting polymers since the pulverization of SnO<sub>2</sub> will be greatly alleviated owing to the hollow interior, the presence of void spaces between the SnO<sub>2</sub> nanoparticles and a superior structural integrity from the

\* Corresponding author. School of Physics and Electronics, Gannan Normal University, Ganzhou, 341000, PR China.

\*\* Corresponding author. Department of Mechanical and Materials Engineering, Florida International University, Miami, FL, 33174, USA.

E-mail addresses: [yuanjvjun@aliyun.com](mailto:yuanjvjun@aliyun.com) (J. Yuan), [Wangc@fiu.edu](mailto:Wangc@fiu.edu) (C. Wang).



## Fabrication of three-dimensional porous ZnMn<sub>2</sub>O<sub>4</sub> thin films on Ni foams through electrostatic spray deposition for high-performance lithium-ion battery anodes



Jujun Yuan <sup>a, b,\*</sup>, Chunhui Chen <sup>b</sup>, Yong Hao <sup>b</sup>, Xianke Zhang <sup>a, b</sup>, Richa Agrawal <sup>b</sup>, Wenyan Zhao <sup>c</sup>, Chunlei Wang <sup>b,\*\*</sup>, Huajun Yu <sup>a</sup>, Xiurong Zhu <sup>a</sup>, Yi Yu <sup>a</sup>, Zuzhou Xiong <sup>a</sup>, Yingmao Xie <sup>a</sup>

<sup>a</sup> School of Physics and Electronics, Gannan Normal University, Ganzhou, 341000, PR China

<sup>b</sup> Department of Mechanical & Materials Engineering, Florida International University, Miami, FL, 33174, USA

<sup>c</sup> School of Materials Science and Engineering, Jingdezhen Ceramic Institute, Jingdezhen, 333000, PR China

### ARTICLE INFO

#### Article history:

Received 8 October 2016

Received in revised form

1 December 2016

Accepted 6 December 2016

Available online 9 December 2016

### ABSTRACT

Three-dimensional (3D) porous ZnMn<sub>2</sub>O<sub>4</sub> thin films have been successfully synthesized through electrostatic spray deposition (ESD) method followed by an annealing process for lithium-ion battery anodes. These films exhibit excellent cycling performance with a reversible capacity of around 982 mAh g<sup>-1</sup> after 100 cycles at 400 mA g<sup>-1</sup>. The ZnMn<sub>2</sub>O<sub>4</sub> films also display good rate capability with 455 mAh g<sup>-1</sup> at 5 A g<sup>-1</sup>. The superior battery performances of ZnMn<sub>2</sub>O<sub>4</sub> films are ascribed to 3D porous ZnMn<sub>2</sub>O<sub>4</sub> film directly deposited on Ni foam, which can offer effective empty space to accommodate the large volume variation during cycling, increase reaction sites, and improve the electron transport. The ESD strategy is facile, cost-effective, which can be potentially utilized to construct other 3D porous mixed transition-metal oxides materials as well.

© 2016 Elsevier B.V. All rights reserved.

#### Keywords:

ZnMn<sub>2</sub>O<sub>4</sub> film

Porous architecture

Electrostatic spray deposition

Lithium-ion battery

Anode

## 1. Introduction

As one of important green energy-storage devices, lithium-ion batteries (LIBs) have been widely applied in numerous portable electronic devices [1–3]. However, in order to meet high energy storage systems for the ever-growing electrical vehicles (EV), it is still a challenge to design and synthesize effective anode materials for LIBs with high capacity, long cycle life, and good rate capability [4,5]. In recent years, simple transition metal oxides (TMO) such as Mn<sub>3</sub>O<sub>4</sub> [6], Co<sub>3</sub>O<sub>4</sub> [7], ZnO [8], and NiO [9], have been widely researched for high-performance LIB anodes. However, simple TMOs usually show intrinsically low electronic conductivity and ionic conductivity, which lead to the serious capacity fading in the cycling processes. To resolve this issue for LIB anodes, one effective

method is to synthesize metal/metal oxide hybrid for improving the electronic conductivity [10–12]. Another important method to fabricate mixed transition-metal oxides (MTMOs, spinel AB<sub>2</sub>O<sub>4</sub>; A, B = Co, Ni, Zn, Mn, Fe, etc.), which exhibit higher specific capacity and improved electronic conductivity [13–18]. Compared with metal/metal oxide hybrid, the MTMOs usually present higher electrochemical activities because of complex chemical compositions with two different metal cations acting as counter “matrix” for each other, which can make contribution to exceptionally high specific capacity of MTMOs for LIB anodes [19,20].

Among the MTMO-based anode materials, ZnMn<sub>2</sub>O<sub>4</sub> has attracted much attention recently for high-performance LIBs due to its superior properties including cost-effective, environmental benignity, and high theoretical capacity (1008 mAh g<sup>-1</sup>) due to both conversion and alloying reaction mechanisms [21–23]. Although attractive, practical application of the ZnMn<sub>2</sub>O<sub>4</sub> is impeded by its fast capacity fading because of large volume variation upon lithiation/delithiation. As a consequence, rational design and construction of ZnMn<sub>2</sub>O<sub>4</sub> nanostructures with different morphologies have been utilized to overcome this issue [24–32].

\* Corresponding author. School of Physics and Electronics, Gannan Normal University, Ganzhou, 341000, PR China.

\*\* Corresponding author. Department of Mechanical & Materials Engineering, Florida International University, Miami, FL, 33174, USA

E-mail addresses: [yuanjyjun@aliyun.com](mailto:yuanjyjun@aliyun.com) (J. Yuan), [Wangc@fiu.edu](mailto:Wangc@fiu.edu) (C. Wang).



## Predicting DNA sequence splice site based on graph convolutional network and DNA graph construction

Luo Rentao, Li Yelin, Guan Lixin\*, Li Mengshan\*

College of Physics and Electronic Information, Gannan Normal University, Ganzhou, 341000 Jiangxi, China

### ARTICLE INFO

**Keywords:**  
Splice Site  
Deep Learning  
Graph convolutional network  
Bioinformatics

### ABSTRACT

Identifying splice sites is essential for gene structure analysis and eukaryotic genome annotation. Recently, computational and deep learning approaches for splice site detection have advanced, focusing on reducing false positives by distinguishing true from pseudo splice sites. This paper introduces GraphSplice, a method using graph convolutional neural networks. It encodes DNA sequences into directed graphs to extract features and predict splice sites. Tested across multiple datasets, GraphSplice consistently achieved high accuracy (91%-94%) and F1Scores (92%-94%), outperforming state-of-the-art models by up to 9.16% for donors and 5.64% for acceptors. Cross-species experiments also show GraphSplice's capability to annotate splice sites in under-trained genomic datasets, proving its wide applicability as a tool for DNA splice site analysis.

### 1. Introduction

The advancement of high-throughput sequencing technologies in recent years has brought about significant opportunities and challenges in the delineation of gene structures within genomes. The task of identifying coding sequences (CDS) within a DNA sequence, also referred to as gene prediction, is pivotal. In the DNA sequences of eukaryotes, genes are often segmented into interspersed fragments, with coding fragments known as exons and non-coding fragments as introns. Exons are retained following DNA splicing and are involved in transcription and replication during the process of protein synthesis, which is termed gene expression. DNA sequences function as repositories of genetic information, orchestrating the synthesis of proteins, ensuring the correct transmission of genetic information to proteins, and facilitating a myriad of biological functions (Dong et al., 2023). The gene expression is depicted in Fig. 1:

The boundaries between exons and introns are known as splice sites, which are specifically recognized by the spliceosome during the transcription process (Matera and Wang, 2014); and significantly contribute to the diversity within the proteome and cancer (Ben-Dov et al., 2008; Cotto, 2023).

Splice sites are differentiated into two varieties, occurring at the connections between exons and introns and vice versa, referred to as the Donor Splice Site (DSS) and the Acceptor Splice Site (ASS), or more commonly, the 3' splice site and the 5' splice site. These sites feature highly conserved nucleotide sequences, with the GT dinucleotide

usually located at the 3' splice site and the AG dinucleotide at the 5' splice site (Mount, 1982; Leader, 2021), with such configurations being identified as canonical splice sites (Burset et al., 2001). The majority of splice sites in animals (98.3 %), fungi (98.7 %), and plants (97.9 %) are canonical (Frey and Pucker, 2020). However, the presence of non-canonical splice sites, including consensus sequences AT-AC and GC-AG (Pucker and Brockington, 2018), poses significant challenges for splice site prediction within genes. GT and AG dinucleotides that do not occur at splice sites can raise the false positive rate, and neglecting non-canonical splice sites may result in false negative predictions (Pucker et al., 2017).

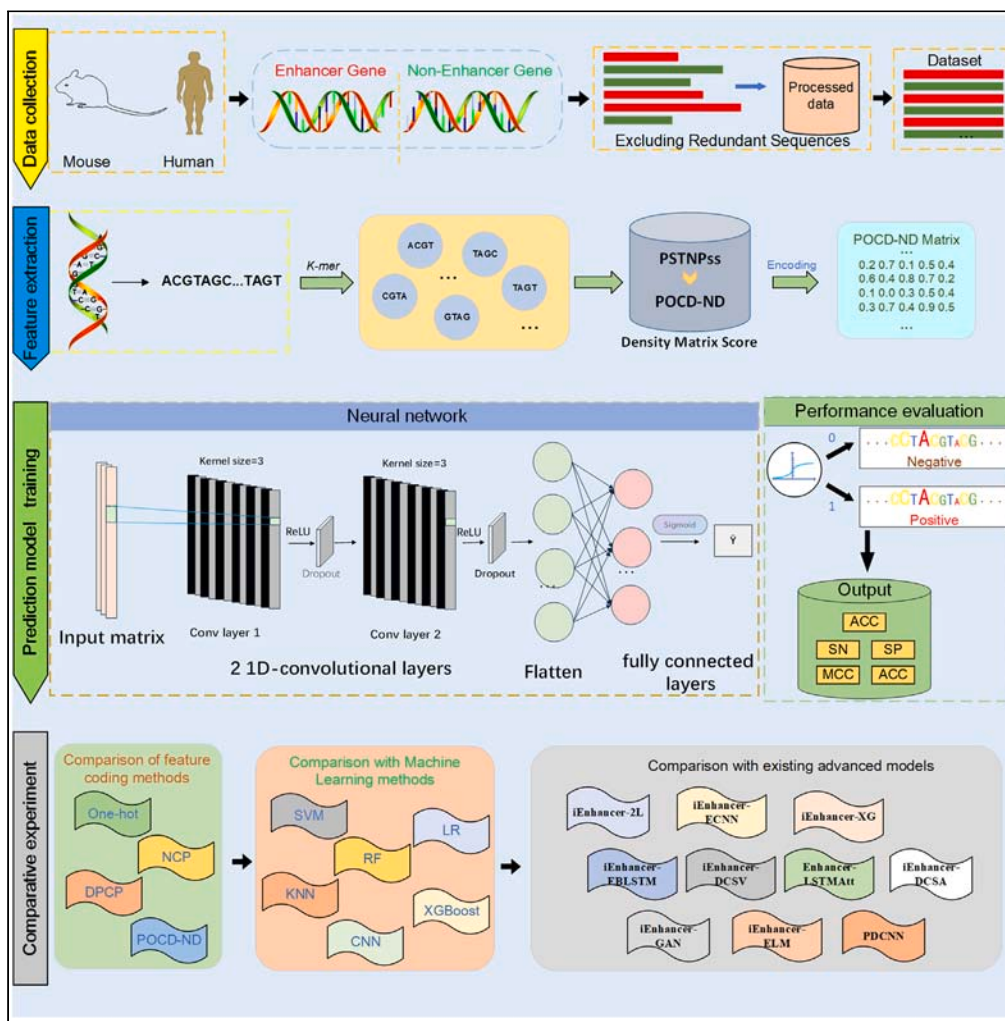
Early efforts to predict splice sites heavily relied on machine learning techniques. Widely used algorithms included Support Vector Machines (SVM) (Sonnenburg et al., 2007; Maji and Garg, 2014), Markov Models (Pashaei et al., 2016; Zhang, 2010); Random Forest (Meher et al., 2016; Pashaei et al., 2017) and Bayesian Network (Chen et al., 2005). For example, GeneSplice (Pertea et al., 2001) applied decision trees along with hidden Markov chains to gather information around splice sites, while SpliceMachine (Degroeve et al., 2005) employed linear SVMs to create predictive models based on high-dimensional local context representations. These machine learning methods required manually crafted features, such as the distribution of mono-, di-, and trinucleotides around splice sites (Wei et al., 2013); nucleotide chemical properties, and data on nucleotide positions and densities (Bari et al., 2013); Additionally, features like dinucleotide linkage, nucleotide dependence,

\* Corresponding authors.

E-mail addresses: [lxguan@gnnu.edu.cn](mailto:lxguan@gnnu.edu.cn) (G. Lixin), [msli@gnnu.edu.cn](mailto:msli@gnnu.edu.cn) (L. Mengshan).

## Article

## A deep learning model for DNA enhancer prediction based on nucleotide position aware feature encoding



Wenxing Hu, Yelin Li, Yan Wu, Lixin Guan, Mengshan Li

mqli@gnnu.edu.cn

### Highlights

A deep learning model PDCNN for identifying DNA enhancers

Improving model performance with position-aware encoders

Comparative studies have shown that PDCNN is superior to existing models



RESEARCH

Open Access



# Cluster energy prediction based on multiple strategy fusion whale optimization algorithm and light gradient boosting machine

Wu Wei<sup>1</sup>, Li Mengshan<sup>1\*</sup>, Wu Yan<sup>2</sup> and Guan Lixin<sup>1</sup>

## Abstract

**Background** Clusters, a novel hierarchical material structure that emerges from atoms or molecules, possess unique reactivity and catalytic properties, crucial in catalysis, biomedicine, and optoelectronics. Predicting cluster energy provides insights into electronic structure, magnetism, and stability. However, the structure of clusters and their potential energy surface is exceptionally intricate. Searching for the global optimal structure (the lowest energy) among these isomers poses a significant challenge. Currently, modelling cluster energy predictions with traditional machine learning methods has several issues, including reliance on manual expertise, slow computation, heavy computational resource demands, and less efficient parameter tuning.

**Results** This paper introduces a predictive model for the energy of a gold cluster comprising twenty atoms (referred to as Au20 cluster). The model integrates the Multiple Strategy Fusion Whale Optimization Algorithm (MSFWOA) with the Light Gradient Boosting Machine (LightGBM), resulting in the MSFWOA-LightGBM model. This model employs the Coulomb matrix representation and eigenvalue solution methods for feature extraction. Additionally, it incorporates the Tent chaotic mapping, cosine convergence factor, and inertia weight updating strategy to optimize the Whale Optimization Algorithm (WOA), leading to the development of MSFWOA. Subsequently, MSFWOA is employed to optimize the parameters of LightGBM for supporting the energy prediction of Au20 cluster.

**Conclusions** The experimental results show that the most stable Au20 cluster structure is a regular tetrahedron with the lowest energy, displaying tight and uniform atom distribution, high geometric symmetry. Compared to other models, the MSFWOA-LightGBM model excels in accuracy and correlation, with MSE, RMSE, and R<sup>2</sup> values of 0.897, 0.947, and 0.879, respectively. Additionally, the MSFWOA-LightGBM model possesses outstanding scalability, offering valuable insights for material design, energy storage, sensing technology, and biomedical imaging, with the potential to drive research and development in these areas.

**Keywords** Cluster, LightGBM, Energy prediction, Machine Learning

\*Correspondence:

Li Mengshan  
msli@gnnu.edu.cn

Full list of author information is available at the end of the article



© The Author(s) 2024. **Open Access** This article is licensed under a Creative Commons Attribution 4.0 International License, which permits use, sharing, adaptation, distribution and reproduction in any medium or format, as long as you give appropriate credit to the original author(s) and the source, provide a link to the Creative Commons licence, and indicate if changes were made. The images or other third party material in this article are included in the article's Creative Commons licence, unless indicated otherwise in a credit line to the material. If material is not included in the article's Creative Commons licence and your intended use is not permitted by statutory regulation or exceeds the permitted use, you will need to obtain permission directly from the copyright holder. To view a copy of this licence, visit <http://creativecommons.org/licenses/by/4.0/>. The Creative Commons Public Domain Dedication waiver (<http://creativecommons.org/publicdomain/zero/1.0/>) applies to the data made available in this article, unless otherwise stated in a credit line to the data.



## Research Papers

## Three-dimensional porous C/CoS nanocomposites for a long-life and high-rate potassium storage



Meiqi Mu<sup>a</sup>, Haishan He<sup>b</sup>, Yunfei Gan<sup>b</sup>, Jing Yu<sup>a</sup>, Jirong Mou<sup>a</sup>, Jujun Yuan<sup>a,\*</sup>, Fangkun Li<sup>c</sup>, Xingquan Wang<sup>a</sup>, Xiaokang Li<sup>a,b,\*</sup>, Xianke Zhang<sup>a</sup>, Jun Liu<sup>c</sup>

<sup>a</sup> College of Physics and Electronics, Gannan Normal University, Ganzhou, 341000, PR China

<sup>b</sup> College of Chemistry and Chemical Engineering, Gannan Normal University, Ganzhou, 341000, PR China

<sup>c</sup> School of Materials Science and Engineering, South China University of Technology, Guangzhou, 510641, PR China

## ARTICLE INFO

## ABSTRACT

## Keywords:

Potassium ion battery  
CoS  
3D porous carbon  
Anode  
High stability

The three-dimensional (3D) porous C/CoS nanocomposites were successfully synthesized using a spontaneous template method followed by a subsequent vulcanization process. As potassium ion battery anode, the 3D porous C/CoS nanocomposites exhibited a reversible capacity of  $165 \text{ mAh g}^{-1}$  at  $5 \text{ A g}^{-1}$  after 2000 cycles and superior rate performance. The excellent electrochemical performance of 3D porous C/CoS nanocomposites is ascribed to its distinctive architecture, which can alleviate the volume variation of CoS in the cyclic processes, improve electronic/ionic conductivity, and provide more chances of contact between electrode material and electrolyte. It is promising that our fabricating method can be expanded for synthesizing other 3D porous C/metal sulfides composites as high-performance PIB anodes.

## 1. Introduction

Lithium-ion batteries (LIBs) are recognized as a great success as effective storage devices for portable electronics, and electric vehicles [1–4]. Nevertheless, the scarcity of lithium reserves and crazily rising price for lithium require the development of alternative energy storage devices. Potassium-ion batteries (PIBs) provide immense hope because of rich resource utilization and low cost of the potassium. Particularly, potassium-ion-based graphite intercalation compounds can keep good stability, which offers a promising energy storage application of PIBs [5]. Additionally, the low standard hydrogen potential ( $E_{\text{o}}$ ) for potassium ( $-2.93 \text{ V vs } E_{\text{o}}$ ) similar with the hydrogen potential for lithium ( $-3.05 \text{ V vs } E_{\text{o}}$ ) implies the high voltage and high power density of the PIBs [6,7]. Hence, PIBs are regarded as potentially effective storage devices for large-scale energy storage [8–12]. Although attractive, the larger potassium ion radius ( $1.38 \text{ \AA}$ ) will cause sluggish ion diffusion kinetics and large volumetric change of electrode materials in the repeated  $\text{K}^+$  insertion/extraction processes, leading to inferior cyclic stability and poor rate performance. So, it is essential for acquiring the effective electrodes which own the outstanding electrochemical performance as PIBs anodes.

As promising candidates, transition metal sulfide ( $\text{FeS}_2$ ,  $\text{FeS}$ ,  $\text{CoS}_2$ ,

$\text{CoS}$ ,  $\text{NiS}_2$ ,  $\text{NiS}$ , et al.) [13–19] anode materials for PIBs have been intensively researched due to their high theoretical capacities. Particularly, Co-based sulfides have attracted increasing attention as competitive anode materials for PIBs because of their remarkable theoretical capacities, and redox reversibility for conversion reactions [20–25]. Nevertheless, the practical application for Co-based sulfides still faces similar problems with transition metal sulfides in the charge/discharge processes, such as larger volume variation and delayed reaction kinetics, which will lead to pulverization and severe capacity degradation for Co-based sulfide electrode materials. An effective strategy for solving the above issues is the construction of Co-based sulfides/C nanocomposites, benefiting from their synergistic effect of accommodating volume variation of Co-based sulfides, and enhancing electronic/ionic conductivity in the charge-discharge cycle processes [26–33]. For example, Guo et al. fabricated CoS quantum dot nanoclusters@graphene nanosheet composites by a two-step hydrothermal strategy. The CoS quantum dot nanoclusters@graphene electrode exhibited a reversible capacity of  $311 \text{ mAh g}^{-1}$  at  $500 \text{ mA g}^{-1}$  upon 100 cycles [26]. Wang et al. reported core-shell  $\text{CoS}_2@\text{NC}$  nanofibers using a hydrothermal method combined with carbon coating, and followed by a vulcanization process. As PIBs anode, the  $\text{CoS}_2@\text{NC}$  nanofiber electrode showed a good long cycle performance stability ( $285 \text{ mAh g}^{-1}$  at  $1 \text{ A g}^{-1}$  upon 800

\* Corresponding author.

E-mail addresses: [yuanjujun123@163.com](mailto:yuanjujun123@163.com) (J. Yuan), [lxxiaokang@gnnu.edu.cn](mailto:lxxiaokang@gnnu.edu.cn) (X. Li), [msjliu@scut.edu.cn](mailto:msjliu@scut.edu.cn) (J. Liu).

# Electrochemical Restoration of Battery Materials Guided by Synchrotron Radiation Technology for Sustainable Lithium-Ion Batteries

*Lei Wang, Yihao Shen, Yuanlong Liu, Pan Zeng, Junxia Meng,\* Tiefeng Liu,\* and Liang Zhang\**

Lithium-ion batteries (LIBs) have been ubiquitous in modern society, especially in the fields of electronic devices, electric vehicles and grid storage, while raising concerns about a tremendous number of spent batteries in the next five to ten years. As environmental awareness and resource security is gaining increasingly extensive attention, how to effectively deal with spent LIBs has become a challenging issue academically and industrially.

Accordingly, the development of battery recycling has surfaced as a highly researched topic in the battery community. Recently, the structural and electrochemical restoration of recycled electrode materials have been proposed as a non-destructive method to save more energy and chemical agents compared with mature metallurgical methods. Such a refurbishment process of electrode materials is also regarded as a reverse process of their degradation in the working condition. Notably, synchrotron radiation technology, which is previously applied to diagnose battery degrade, has started to play major roles in gaining more insight into the structural restoration of electrode materials. Here, the contribution of synchrotron radiation technology to reveal the underlying degradation and regeneration mechanisms of LIBs cathodes is highlighted, providing a theoretical basis and guidance for the direct recycling and reuse of degraded cathodes.

electronics and further into electrified transportation and grid storage.<sup>[1]</sup> As with any commercially available product, there will be an end-of-life scenario and the same is true for LIBs. Thus, the interests on the battery sustainability are recently rising in both academia and industry.<sup>[2]</sup> On the one hand, as the battery production continues to increase, the state-of-the-art LIB technologies are struggling with the scarcity of metal resources (Co, Ni, Li, etc.), safety issues, and high costs.<sup>[3]</sup> On the other hand, a large amount of end-of-life LIBs increasingly become a serious threat to the environmental healthy because damaged batteries inevitably release toxic organic electrolyte and various transition metal elements, such as Co and Ni, into the soil and water sources.<sup>[4]</sup> In this context, recent researches have placed a larger emphasis on what is known as a close-loop battery recycling, which is in fact expected to alleviate the shortage of key metal source together with securing the ecological safety.<sup>[5]</sup>

Currently, the most dominant recycling strategies for end-of-life LIBs originate from metallurgical industrials.<sup>[6]</sup> The corresponding methods are pyrometallurgy, hydrometallurgy, or

## 1. Introduction

Lithium-ion batteries (LIBs) have been an extremely successful commercial product in modern society, being ubiquitous in

L. Wang, Y. Shen, L. Zhang  
Institute of Functional Nano & Soft Materials (FUNSOM)  
Soochow University  
Suzhou, Jiangsu 215123, China  
E-mail: liangzhang2019@suda.edu.cn

Y. Liu  
Zhejiang Tianneng New Materials Co. Ltd.  
Huzhou, Zhejiang 313103, China

P. Zeng  
Institute for Advanced Study  
School of Mechanical Engineering  
Chengdu University  
Chengdu 610106, China

J. Meng  
School of Physics and Electronics  
Gannan Normal University  
Ganzhou 341000, China  
E-mail: jxmeng@buaa.edu.cn

T. Liu  
College of Materials Science and Engineering  
Zhejiang University of Technology  
Hangzhou 310014, China  
E-mail: tiefengliu@zjut.edu.cn

L. Zhang  
Jiangsu Key Laboratory of Advanced Negative Carbon Technologies  
Soochow University  
Suzhou, Jiangsu 215123, China

 The ORCID identification number(s) for the author(s) of this article can be found under <https://doi.org/10.1002/smtd.202201658>

DOI: 10.1002/smtd.202201658

## Classical-driving-assisted quantum synchronization in non-Markovian environments

Xing Xiao<sup>1</sup>, Tian-Xiang Lu<sup>1</sup>, Wo-Jun Zhong<sup>1</sup>, and Yan-Ling Li<sup>2,\*</sup>

<sup>1</sup>College of Physics and Electronic Information, Gannan Normal University, Ganzhou 341000, China

<sup>2</sup>School of Information Engineering, Jiangxi University of Science and Technology, Ganzhou 341000, China



(Received 21 September 2022; revised 17 January 2023; accepted 7 February 2023; published 21 February 2023)

We study the quantum phase synchronization of a driven two-level system (TLS) coupled to a structured environment and demonstrate that quantum synchronization can be enhanced by the classical driving field. We use the Husimi  $Q$  function to characterize the phase preference and find the in-phase and anti-phase locking phenomenon in the phase diagram. Remarkably, we show that the in-phase classical driving enables a TLS to reach stable anti-phase locking in the Markovian regime. However, we find that the synergistic action of classical driving and non-Markovian effects significantly enhances the initial in-phase locking. By introducing the  $S$  function and its maximal value to quantify the strength of synchronization and sketch the synchronization regions, we observe the typical signatures of the hollowed Arnold tongue in the parameter regions of synchronization. In the hollowed Arnold tongue, the synchronization regions exist both inside and outside the tongue while unsynchronized regions only lie on the boundary line. We also provide an intuitive interpretation of the above results by using the quasimode theory.

DOI: [10.1103/PhysRevA.107.022221](https://doi.org/10.1103/PhysRevA.107.022221)

### I. INTRODUCTION

Because of the direct or indirect interactions, the components of a system may adjust their own local dynamics to a common rhythm. This phenomenon is well known as synchronization [1]. The original study about synchronization could be dated back to 1657 when Christian Huygens found “the sympathy of two clocks,” i.e., two pendulums always swung at the same frequency albeit in opposite directions to each other [2]. Examples of synchronization are widespread in multidisciplinary studies and in particular in physics, such as the coupled oscillators [3]. At present, the study of synchronization behavior in various kinds of real complex systems has become one of the active topics in different disciplines [4].

Unlike the ubiquity of synchronization in the classical world, the study of synchronization in the quantum regime has garnered increasing interest only recently [5–35]. Important advances have been made toward understanding quantum synchronization by considering the quantum version of classically synchronous systems, for instance, Van der Pol oscillators [36,37]. Following this, the extension of synchronization to genuinely quantum systems without classical counterparts has been considered in atomic system [38], spin system [17], Bose-Einstein condensates [39], and superconducting circuit system [40]. The studies of quantum synchronization generally fall into two categories: Spontaneous synchronization (or mutual synchronization) and forced synchronization. In the case of spontaneous synchronization, the interested system becomes synchronized in the transient evolution of dynamical systems due to the interaction between the subsystems or an external environment. There-

fore, environmental noise plays a significant role in enabling spontaneous synchronization in open quantum systems. Surprisingly, noise-induced synchronization has been reported in Refs. [41–43]. This phenomenon highlights the constructive role of environmental noise in synchronization. In contrast to spontaneous synchronization, forced synchronization usually emerges with externally driven forces. This was considered in Refs. [44,45], in which the behavior of one and two superconducting qubits coupled to a driven dissipative oscillator is demonstrated, and in Refs. [16,24], where the forced phase synchronization in low-dimensional quantum systems is investigated. It is worth noting that whether a two-level system (TLS) could be synchronized has experienced a theoretical debate. The main disagreement is whether there is a valid limit cycle in TLSs [16]. In Ref. [24], the authors predicted that such a valid limit cycle indeed exists in the stationary mixed state of the TLS because each of those possible pure states that make up the mixed state would precess around the  $z$  axis in the Bloch sphere. This theoretical prediction was subsequently confirmed by experiments in a trapped-ion system [31].

Any realistic quantum system inevitably interacts with external environments. Therefore, the influence of environmental noise on forced synchronization is an intriguing problem that should be evaluated. Recently, non-Markovian environments have drawn particular attention in quantum science and technology since the relevant environment’s correlation time is not too small compared with the system’s relaxation time in many physical systems, in particular, artificial synthesis of materials [46–48]. In fact, the valuable research of non-Markovian environments is the existence of information backflow from the environment (named as non-Markovian effects) [49–53]. The influence of non-Markovian effects on the dynamics of entanglement, quantum discord, and quantum Fisher information has been extensively

\*liyanling0423@gmail.com

# Ca<sup>2+</sup> enhanced far-red emission performance and efficiency of SrGd<sub>2</sub>Al<sub>2</sub>O<sub>7</sub>:Mn<sup>4+</sup> phosphor for the potential application in plant growth lighting

Cite as: J. Chem. Phys. 158, 234703 (2023); doi: 10.1063/5.0149120

Submitted: 3 March 2023 • Accepted: 30 May 2023 •

Published Online: 15 June 2023



View Online



Export Citation



CrossMark

Yi Yu,<sup>1,2,a)</sup> Kai Shao,<sup>1,2</sup> Chonghui Niu,<sup>1,2</sup> Mingjie Dan,<sup>1,2</sup> Zhibin Wang,<sup>1</sup> Yingying Wang,<sup>1</sup> Jie Chen,<sup>1</sup> Jiani Luo,<sup>1</sup> Shiying Liu,<sup>1</sup> and Zhi Xie<sup>3</sup>

## AFFILIATIONS

<sup>1</sup> School of Physics and Electronic Information, Gannan Normal University, Ganzhou 341000, China

<sup>2</sup> Advanced Energy Storage and Photoelectric Materials Research Center, Gannan Normal University, Ganzhou 341000, China

<sup>3</sup> College of Mechanical and Electronic Engineering, Fujian Agriculture and Forestry University, Fuzhou 350002, China

<sup>a)</sup> Author to whom correspondence should be addressed: [yuyignnu@163.com](mailto:yuyignnu@163.com); Present address: Shida south road, Gannan Normal University, Rongjiang District, Ganzhou City, Jiangxi Province, China.

## ABSTRACT

Mn-based phosphors with the wavelength of 700–750 nm are an important category of far-red phosphors that have promising potential in the application of plant lighting, and the higher ability of the far-red light emitting of the phosphors is beneficial to plant growth. Herein, a series of Mn<sup>4+</sup>- and Mn<sup>4+</sup>/Ca<sup>2+</sup>-doped double perovskite SrGd<sub>2</sub>Al<sub>2</sub>O<sub>7</sub> red-emitting phosphors with wavelengths centered at about 709 nm were successfully synthesized by means of a traditional high-temperature solid-state method. First-principles calculations were conducted to explore the intrinsic electronic structure of SrGd<sub>2</sub>Al<sub>2</sub>O<sub>7</sub> for a better understanding of the luminescence behavior in this material. Extensive analysis demonstrates that the introduction of Ca<sup>2+</sup> ions into the SrGd<sub>2</sub>Al<sub>2</sub>O<sub>7</sub>:Mn<sup>4+</sup> phosphor has significantly boosted the emission intensity, internal quantum efficiency, and thermal stability by 170%, 173.4%, and 113.7%, respectively, which are superior to those of most other Mn<sup>4+</sup>-based far-red phosphors. The mechanism of the concentration quench effect and the positive effect of co-doping Ca<sup>2+</sup> ions in the phosphor were extensively explored. All studies suggest that the SrGd<sub>2</sub>Al<sub>2</sub>O<sub>7</sub>:0.1%Mn<sup>4+</sup>, 11%Ca<sup>2+</sup> phosphor is a novel phosphor that can be used to effectively promote the growth of plants and regulate the flowering cycle. Therefore, promising applications can be anticipated from this new phosphor.

Published under an exclusive license by AIP Publishing. <https://doi.org/10.1063/5.0149120>

## I. INTRODUCTION

It is well known that light is one of the most important factors for plant growth and that light with different wavelengths has different effects on the plants' growth and development. For instance, red light ranging from 640 to 660 nm is beneficial to the synthesis of carbohydrates in plants, which can promote the growth of plants; the far-red light over a range of 700–750 nm is mainly absorbed by the photoreceptor in plants, which relates to the height of plants and the flowering cycle.<sup>1–3</sup> Thus, it plays an extremely vital role in the growth and reproduction of plants. Moreover, researchers had pointed out that the shade avoidance syndrome, which is determined

by the concentration of photosensitive pigments, has a strong correlation with the rapid growth of stems and leaf veins for sun plants and the concentration of photosensitive pigments depends on the ratio of far-red light (FR) to the red light (R) and the larger the ratio, the higher the concentration is.<sup>4–6</sup> As such, a relatively higher intensity of far-red light is advantageous to the increase in the photosensitive pigments' concentration and, consequently, to the growth and production of plants. However, the sunlight is a little bit lack of far-red light, leading to a low efficiency for the planting industry. To overcome this problem, a viable strategy is using far-red phosphors to compensate for the shortage of far-red light in the sunlight. In this regard, indoor planting has made a great breakthrough in

# Induction and Maintenance of Local Structural Durability for High-Energy Nickel-Rich Layered Oxides

Quanxin Ma, Yuqin Wang, Fulin Lai, Junxia Meng,\* Sydorov Dmytro, Lingfei Zhou, Mengqian Yang, Qian Zhang, and Shengwen Zhong\*

Nickel-rich layered oxides are one of the most promising cathode candidates for next-generation high-energy-density lithium-ion batteries. However, due to similar ion radius between  $\text{Li}^+$  and  $\text{Ni}^{2+}$ (0.76 and 0.69 Å), the  $\text{Li}^+/\text{Ni}^{2+}$  mixing phenomenon seriously hinders the migration of  $\text{Li}^+$  and increases kinetic barrier of  $\text{Li}^+$  diffusion, resulting in limited rate capability. In this work, the introduction of  $\text{Ce}^{4+}$  to effectively improve electrochemical properties of Ni-rich cathode materials is proposed. The  $\text{LiNi}_{0.8}\text{Co}_{0.15}\text{Al}_{0.05}\text{O}_2$  (LNCA) is modified with an additional precursor oxidization process using an appropriate amount of  $(\text{NH}_4)_2\text{Ce}(\text{NO}_3)_6$ . The  $\text{Ce}(\text{NO}_3)_6^{2-}$  easily obtains electrons and generates reduction reactions, while  $\text{Ni}(\text{OH})_2$  is prone to electron loss and oxidation reaction. The participation of  $(\text{NH}_4)_2\text{Ce}(\text{NO}_3)_6$  can promote the oxidation of  $\text{Ni}^{2+}$  to  $\text{Ni}^{3+}$ , thereby reducing the  $\text{Li}^+/\text{Ni}^{2+}$  mixing and increasing the structural stability of LNCA samples.  $\text{Ce}^{4+}$  cation doping can impede  $\text{Li}^+/\text{Ni}^{2+}$  mixing of LNCA cathode materials upon the long-term cycles. Both rate performance and long-term cyclability of  $\text{Li}[\text{Ni}_{0.8}\text{Co}_{0.15}\text{Al}_{0.05}]_{0.97}\text{Ce}_{0.03}\text{O}_2$  (LNCA-Ce0.03) sample are significantly improved. Besides, a practical pouch cell based on the cathode presents sufficient gravimetric energy density ( $\approx 300 \text{ Wh kg}^{-1}$ ) and cycling stability (capacity retention of 81.3% after 500 cycles at 1 C).

## 1. Introduction

Among the Ni-rich cathodes for lithium-ion batteries (LIBs) with high energy density and durable cycling capability,  $\text{LiNi}_{0.8}\text{Co}_{0.15}\text{Al}_{0.05}\text{O}_2$  (LNCA) is now receiving growing attention due to its high specific capacity (200 mAh g<sup>-1</sup>) and economic viability.<sup>[1]</sup> However, the drawbacks concerning structural instability, poor rate capability and inadequate cycle performance are still the huge obstacle for its further commercial utilization. One of the reasons is attributed to the  $\text{Li}^+/\text{Ni}^{2+}$  mixing phenomenon, caused by similar ion radii of  $\text{Li}^+$  and  $\text{Ni}^{2+}$ (0.76 and 0.69 Å), which seriously hinders the migration of  $\text{Li}^+$  and increases the kinetics barrier for  $\text{Li}^+$  diffusion, resulting in limited rate capability.<sup>[2]</sup>

In order to tackle these challenges, many efforts have been taken to relieve  $\text{Li}^+/\text{Ni}^{2+}$  mixing of Ni-rich layered materials.<sup>[3]</sup> On the one hand, the Ni-rich cathodes are directly modified by regulating Li, Ni ratio, and surface coating.<sup>[4]</sup> On the other hand, the pre-treatment is often performed on the precursor synthesis. The oxidants such as  $\text{Na}_2\text{S}_2\text{O}_8$ ,<sup>[5]</sup>  $\text{KMnO}_4$ ,<sup>[6]</sup> and

$\text{Mn}(\text{NO}_3)_2$ <sup>[7]</sup> are used to tune the ratio of  $\text{Ni}^{3+}/\text{Ni}^{2+}$  and suppress  $\text{Li}^+/\text{Ni}^{2+}$  cation disordering, consequently achieving enhanced cyclability for layered Ni-rich cathode materials.<sup>[7]</sup> Accordingly, the increased ratio of  $\text{Ni}^{3+}$  content in precursor can relieve  $\text{Li}^+/\text{Ni}^{2+}$  mixing of final Ni-rich cathodes.<sup>[8]</sup> Furthermore, these oxidants can remain in the precursor to form additional effect of elemental doping, which can permanently regulate the degree of  $\text{Li}^+/\text{Ni}^{2+}$  mixing. Previous studies have confirmed that the appropriate doping with cations (Nb, Ca, Ti, Zr, and Zn) in the transition metal (TM) layer could impede  $\text{Li}^+/\text{Ni}^{2+}$  mixing during the long-term cycles and alleviate the structural degradation, thereby promoting the  $\text{Li}^+$  transport kinetics.<sup>[9]</sup> Therefore, the combination of the precursors pre-oxidation and element doping is expected to stabilize the LNCA structure.

The ionic radius of  $\text{Ce}^{4+}$  is 0.87 Å, larger than  $\text{Co}^{3+}$ (0.545 Å),  $\text{Ni}^{2+}$ (0.69 Å),  $\text{Al}^{3+}$ (0.535 Å), and  $\text{Li}^+$ (0.76 Å).<sup>[10]</sup> Meanwhile,  $\text{Ce}^{4+}$  with the strong oxidation can substitute into the bulk structure, which can promote the oxidation of  $\text{Ni}^{2+}$  to  $\text{Ni}^{3+}$ .<sup>[11]</sup> Therefore, the introduction of  $\text{Ce}^{4+}$  can be assumed to be effective in improving the electrochemical performance of Ni-rich

Q. Ma, Y. Wang, F. Lai, S. Dmytro, L. Zhou, M. Yang, Q. Zhang, S. Zhong

Key Laboratory of Power Battery and Materials  
Faculty of Materials Metallurgy and Chemistry  
Jiangxi University of Science and Technology  
Ganzhou 341000, China

E-mail: zhongshw@jxust.edu.cn

Q. Ma

Far East Battery  
FEB Research Institute  
Yichun 336000, China

J. Meng

School of Physics and Electronics  
Gannan Normal University  
Ganzhou 341000, China  
E-mail: jxmeng@buaa.edu.cn

S. Dmytro

The Institute of Bioorganic Chemistry and Petrochemistry  
National Academy of Sciences of Ukraine  
Murmanska, 1, Kyiv-94 02094, Ukraine

 The ORCID identification number(s) for the author(s) of this article can be found under <https://doi.org/10.1002/smtd.202200255>.

DOI: 10.1002/smtd.202200255



## Full Length Article

Crystal growth, first-principle calculations, optical properties and laser performances toward a molybdate  $\text{Er}^{3+}:\text{KBaGd}(\text{MoO}_4)_3$  crystal

Yi Yu <sup>a,b,\*</sup>, Kai Shao <sup>a</sup>, Chonghui Niu <sup>b</sup>, Liucheng Liu <sup>a,b</sup>, Xiurong Zhu <sup>a,b</sup>, Zhibin Wang <sup>a</sup>, Zuju Ma <sup>c</sup>, Guofu Wang <sup>d</sup>

<sup>a</sup> School of Physics and Electronic Information, Gannan Normal University, Ganzhou, 341000, China

<sup>b</sup> Research Center for Rare Earth Materials and Applications, Gannan Normal University, Ganzhou, 341000, China

<sup>c</sup> School of Environmental and Materials Engineering, Yantai University, Yantai, 264005, PR China

<sup>d</sup> Chinese Academy of Sciences Fujian Institute of Research on the Structure of Matter, Fuzhou, 350002, China

## ARTICLE INFO

## Keywords:

Crystal growth

Theoretical calculation

Optical spectra

Up-conversion

1.55 μm Laser performance

## ABSTRACT

A well-shaped  $\text{Er}^{3+}:\text{KBaGd}(\text{MoO}_4)_3$  ( $\text{Er}^{3+}:\text{KBGM}$ ) crystal with the size of  $48 \times 38 \times 15 \text{ mm}^3$  was grown by the flux method and its structure, morphology and optical properties were studied. The first principal calculations on the band structure and density of states of the crystal were also conducted. The important spectroscopic parameters of the  $\text{Er}^{3+}:\text{KBGM}$  crystal were calculated and analyzed by Judd-Ofelt theory. The polarized stimulated emission spectra were investigated by F-L method. The results of up-conversion spectra analysis revealed that two intense green fluorescence bands centered at 533 nm and 554 nm and a broadened weak red fluorescence band at 665 nm were observed when excited at 981 nm. According to the spectroscopic studies, as well as the analysis of decay time of the  ${}^4\text{I}_{13/2}$  state, the specific energy transfer mechanism of  $\text{Er}^{3+}$  ion in this crystal was elucidated. Laser experiment aiming at 1.55 μm continuous-wave laser was conducted in a plane-plane cavity and, when the optimized transmittance of output couplers was 3%, a maximum of 1.05 W laser emission was acquired with the corresponding slope efficiency of 15.36%. With the combination of all the studies,  $\text{Er}^{3+}:\text{KBGM}$  crystal was proved to be a prominent crystal for the 1.55 μm laser.

## 1. Introduction

1.55 μm laser emission not only is safe to human eyes but also has good thermal effect and transmittance to various materials, making it has a variety of applications in many areas, such as remote sensing, range finding, optical communication, and medical treatment [1–3].  $\text{Er}^{3+}$  is an eminent laser-active ion that has attracted considerable interest and been extensively explored to demonstrate laser emissions with the wavelength around 1.55 μm, associated with the  ${}^4\text{I}_{13/2} \rightarrow {}^4\text{I}_{15/2}$  transition. In recent decays, many  $\text{Er}^{3+}$ -doped laser crystals, such as  $\text{Er}^{3+}:\text{Y}_3\text{Al}_5\text{O}_{12}$  [4],  $\text{Er}^{3+}:\text{YVO}_4$  [5],  $\text{Er}^{3+}:\text{KLu}(\text{WO}_4)_2$  [6],  $\text{Er}^{3+}:\text{LiGd}(\text{MoO}_4)_2$  [7], and  $\text{Na}_{0.04}\text{K}_{0.96}\text{Y}(\text{WO}_4)_2$  [8], have been reported as promising 1.55 μm laser crystals. Nevertheless, few of them can meet the various requirements from industries. This is because they have no good enough mechanical or optical properties, and as a result, a great deal of research is still sorely needed until the society is ready for 1.55 μm  $\text{Er}^{3+}$ -doped lasers with excellent comprehensive properties.

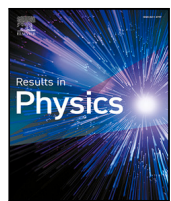
In the process of exploring new inorganic solid-state laser materials,

molybdate crystals have become a kind of attractive host matrix because of their good properties, including chemical and physical stability, good mechanical properties, excellent transmittance in a large wavelength range, as well as relatively large absorption and emission cross-sections when activating ions were introduced into the crystal lattices. Thus, many researchers have been investigating various  $\text{Er}^{3+}$ -doped molybdate laser crystals as 1.55 μm laser media for the purpose of versatile applications in different fields [9–12].

Recent years, a new series of triple-molybdate compounds  $\text{MNRe}(\text{MoO}_4)_3$  ( $\text{M} = \text{Li}, \text{K}; \text{N} = \text{Mg}, \text{Ba}; \text{Re} = \text{Al}, \text{La}-\text{Lu}, \text{Y}$ ) has been drawing much attention because of their attractive characteristics since it was first reported [13]. More and more reports on this type of crystals suggest that it has a huge potential in manifesting laser emissions with different output wavelengths ranging from visible to mid-infrared region when rare-earth metals were doped [14–19].  $\text{KBaGd}(\text{MoO}_4)_3$  ( $\text{KBGM}$ ) also belongs to this family and its structure, as well as the optical properties with  $\text{Nd}^{3+}$  ions doped were first investigated by X. M. Meng et al. in detail [19]. In the KBGM crystal structure, the co-occupation by

\* Corresponding author. School of Physics and Electronic Information, Gannan Normal University, Ganzhou, 341000, China.

E-mail address: [yuyignnu@163.com](mailto:yuyignnu@163.com) (Y. Yu).



# Enhancing the teleportation of quantum Fisher information under correlated generalized amplitude damping noise

Yan-Ling Li <sup>a</sup>, Cai-Hong Liao <sup>a</sup>, Lin Yao <sup>a</sup>, Xing Xiao <sup>b,\*</sup>

<sup>a</sup> School of Information Engineering, Jiangxi University of Science and Technology, Ganzhou 341000, China

<sup>b</sup> College of Physics and Electronic Information, Gannan Normal University, Ganzhou 341000, China

## ARTICLE INFO

### Keywords:

Quantum teleportation  
Quantum Fisher information  
Weak measurement  
Environment-assisted measurement  
Correlated generalized amplitude damping noise

## ABSTRACT

The generalized amplitude damping (GAD) noise models the dynamical map of a qubit in contact with a non-zero temperature bosonic reservoir. When two qubits successively pass through the same GAD channel, correlation effects should be taken into account. Therefore, the dynamical map is modeled as correlated GAD (CGAD) noise. In this paper, we investigate the teleportation of quantum Fisher information (QFI) under CGAD noise. We first show that the correlation effects in CGAD noise can enhance the teleported QFI. We then present two probabilistic schemes to improve the teleportation of QFI in CGAD noise by weak measurement (WM) and environment-assisted measurement (EAM). We find the correlation effects of CGAD noise serve to improve the teleportation of QFI and increase the probability of success. Contrary to intuition, the thermal average photon number  $n$  does not always play a negative role in our probabilistic schemes. Although a larger  $n$  will cause the teleported QFI to decay faster, the corresponding probability of success will be higher. Finally, we introduce a quantity called average QFI to demonstrate that the EAM scheme is superior to the WM scheme with respect to QFI improvement under CGAD noise.

## Introduction

Quantum Fisher Information (QFI) is a measure of the sensitivity of a quantum state to variations in a parameter [1–3]. It is a quantification of how much information can be extracted from the parameter. From the Cramér-Rao bound [2] it is known that the lower bound of the parameter estimation variance is inversely proportional to the square root of the QFI. This means that the accuracy of parameter estimation is proportional to the QFI. With the tremendous theoretical and experimental progress in quantum metrology [4–6], research on single-parameter QFI or multi-parameter QFI matrix has attracted considerable interest in recent years [7–9]. However, from the perspective of quantum remote sensing [10,11], the transmission of the QFI of a single parameter rather than the whole quantum state is a more advisable strategy. For this reason, some research on QFI teleportation has been proposed in recent years [12–22].

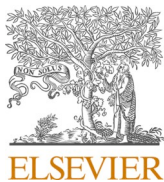
A quantum system inevitably interacts with its environment. These interactions act as noise in quantum information processing systems [23]. A typical noise is amplitude damping noise, which describes the loss of energy from a quantum system. In quantum optics, amplitude damping noise represents the dissipation of a quantum system interacting with a zero-temperature environment [24]. However, the general environment cannot satisfy the condition  $\hbar\omega \gg k_B T$ , where  $\hbar\omega$  is

the transition energy of the quantum,  $k_B$  is the Boltzmann constant and  $T$  is the temperature of the environment. The dissipation process of a quantum system interacting with a finite temperature environment is called generalized amplitude damping (GAD) noise [25]. GAD noise characterizes the noise in superconducting circuit-based quantum computers [26], or losses in linear optical systems in the presence of low-temperature background noise [27], or the  $T_1$  relaxation process in quantum systems coupled to the thermal environment [28]. Furthermore, considering that two or more quantum systems successively pass through the noisy GAD channel, the correlation effects will appear [29,30] if the order of the relaxation time of the channel is comparable to or larger than that of the transmission time through the channel. Such correlated noise cannot be expressed in a tensor product form of the individual GAD noise. Therefore, the correlated generalized amplitude damping (CGAD) noise is introduced to describe the successive uses of the same channel [31,32]. Recently, quantum teleportation in correlated noise has attracted considerable attention from researchers [33–36].

It is well known that almost all quantum information tasks affected by noise degrade their performance (e.g. fidelity or other measures), and teleportation of QFI is no exception. Many methods have been developed to combat noise, ranging from error-correction codes [37],

\* Corresponding author.

E-mail address: [xiaoxing@gnnu.edu.cn](mailto:xiaoxing@gnnu.edu.cn) (X. Xiao).



## Full Length Article

Research on a novel molybdate  $\text{Er}^{3+}:\text{KBaY}(\text{MoO}_4)_3$  crystal as a prominent  $1.55 \mu\text{m}$  laser medium

Yi Yu <sup>a,b,\*</sup>, Kai Shao <sup>a</sup>, Xiurong Zhu <sup>a,b</sup>, Xianke Zhang <sup>a,b</sup>, Huilin Qiu <sup>a</sup>, Shimin Wu <sup>a,b,\*\*</sup>, Guofu Wang <sup>c</sup>

<sup>a</sup> School of Physics and Electronic Information, Gannan Normal University, Ganzhou, 341000, China

<sup>b</sup> Research Center for Rare Earth Materials and Applications, Gannan Normal University, Ganzhou, 341000, China

<sup>c</sup> Fujian Institute of Research on the Structure of Matter, Chinese Academy of Sciences, Fuzhou, 350002, China

## ARTICLE INFO

## ABSTRACT

## Keywords:

Crystal growth  
 $\text{Er}^{3+}$ -doped molybdate crystal  
 $1.55 \mu\text{m}$  laser  
 Optical spectra  
 Up-conversion

An  $\text{Er}^{3+}:\text{KBaY}(\text{MoO}_4)_3$  (denoted  $\text{Er}^{3+}:\text{KBYM}$ ) crystal with excellent optical quality was grown for the first time by the top-seeded-solution growth method (TSSG) from a flux of  $\text{K}_2\text{Mo}_2\text{O}_7$  and its morphology, including concentration of  $\text{Er}^{3+}$  ions was analyzed. The concentration of  $\text{Er}^{3+}$  ion and spectroscopic properties were measured and investigated. Applying the Judd-Ofelt theory, the spectroscopic parameters of  $\text{Er}^{3+}:\text{KBYM}$  crystal, including the oscillator intensity parameters  $\Omega_t$  ( $t = 2, 4, 6$ ), spontaneous emission probabilities, fluorescence branching ratios, and radiative lifetimes, were calculated and analyzed. The stimulated emission cross-sections at around  $1.55 \mu\text{m}$ , corresponding to the  $^4\text{I}_{13/2} \rightarrow ^4\text{I}_{15/2}$  transition were  $1.01 \times 10^{-20} \text{ cm}^2$ ,  $1.32 \times 10^{-20} \text{ cm}^2$  and  $1.10 \times 10^{-20} \text{ cm}^2$  for the X-, Y- and Z-polarizations, respectively. The fluorescence lifetime of the  $^4\text{I}_{13/2}$  state was measured and discussed. The fluorescence decay curve for the  $^4\text{I}_{13/2}$  state exhibited a single exponential behavior and fluorescence lifetime was fitted to be 5.35 ms. Two intense green up-conversion fluorescence bands located at 533 nm and 554 nm and a broadened weak red fluorescence at 665 nm were observed at 984 nm excitation, and the energy transfer mechanism was discussed.

## 1. Introduction

Due to its abundant energy levels,  $\text{Er}^{3+}$  is a well-known laser-active ion that demonstrates laser emissions, which is useful for a variety of different applications. For example, the strong emission around 550 nm is advantageous for applications in data storage, electronic visual displays, and submarine communications [1,2]; Moreover, the  $1.55 \mu\text{m}$  emission band of  $\text{Er}^{3+}$ , which corresponds to the  $^4\text{I}_{13/2} \rightarrow ^4\text{I}_{15/2}$  transition, is safe to the human eyes and close to the minimum wavelength of the optical losses in silica fibers or optical waveguide; Thus it can be applied in range finding, remote sensing, and optical communication [3–5]. In this regard, comprehensive studies on the properties of  $\text{Er}^{3+}$ -doped laser crystals, such as  $\text{Er}^{3+}:\text{Y}_3\text{Al}_5\text{O}_{12}$  [6],  $\text{Er}^{3+}:\text{YVO}_4$  [7],  $\text{Er}^{3+}:\text{KGd}(\text{WO}_4)_2$  [4],  $\text{Er}^{3+}:\text{LiGd}(\text{MoO}_4)_2$  [8], and  $\text{Er}^{3+}:\text{Gd}_3\text{Sc}_2\text{Al}_3\text{O}_{12}$  [9], and their applications in laser emissions with different wavelengths have been conducted in recent decays. Nevertheless, significant amount of research still needs to be performed until the industry is ready for

$\text{Er}^{3+}$ -based lasers. Therefore, development of  $\text{Er}^{3+}$ -doped laser crystals and their applications is necessary and meaningful.

Molybdate crystals are an ideal host material for solid-state lasers because of their excellent chemical stability, high transmittance over a large wavelength range, and strong absorption and emission cross-sections when doped with rare-earth ions in their crystal lattices. Therefore, researchers have been exploring the use of molybdate laser crystals doped with rare earth metals in many different materials, especially  $\text{Er}^{3+}$ , whose spectral properties have been increasingly investigated for various applications in different fields of research [10–13].

Since the first report of a new triple-molybdate crystal with the general formula of  $\text{MNLn}(\text{MoO}_4)_3$  ( $\text{M}=\text{Li}, \text{K}; \text{N}=\text{Mg}, \text{Ba}; \text{Ln}=\text{Al}, \text{La-Lu}, \text{Y}$ ) by N. M. Kozhevnikova et al. [14], significant attention has been paid on the research and development of rare-earth-doped triple-molybdate crystals as laser media due to their attractive characteristics, which suggests that this type of laser crystal is promising for manifesting laser

\* Corresponding author. School of Physics and Electronic Information, Gannan Normal University, Ganzhou, 341000, China.

\*\* Corresponding author. School of Physics and Electronic Information, Gannan Normal University, Ganzhou, 341000, China.

E-mail addresses: [yuyignnu@163.com](mailto:yuyignnu@163.com) (Y. Yu), [wsm0800014@163.com](mailto:wsm0800014@163.com) (S. Wu).



Contents lists available at ScienceDirect



# Neural network modeling based double-population chaotic accelerated particle swarm optimization and diffusion theory for solubility prediction

Mengshan Li\*, Suyun Lian, Fan Wang, Yanying Zhou, Bingsheng Chen, Lixin Guan, Yan Wu

College of Physics and Electronic Information, Gannan Normal University, Ganzhou, 341000, Jiangxi, China

## ARTICLE INFO

### Article history:

Received 29 July 2019

Received in revised form 2

December 2019

Accepted 2 January 2020

Available online 13 January 2020

## ABSTRACT

Solubility is as a key chemical and physical property. Solubility prediction methods are applied in diverse fields including preparation synthesis and modifications of materials. To overcome the shortcomings of existing solubility prediction methods, taking the mass transfer of two-phase system as an example, a solubility prediction model based on the diffusion theory and hybrid artificial intelligence method was proposed in this paper. An improved double-population chaotic accelerated particle swarm optimization (APSO) algorithm combined diffusion theory was developed according to the particle evolution utilizing diffusion energy. The developed algorithm was applied in the training of parameters of the radial basis function artificial neural network and then a model for predicting solubility was developed. The experimental results of supercritical carbon dioxide solubility in 8 polymers were consistent with the predicted values by the model, indicating the high prediction accuracy. The average relative deviation, squared correlation coefficient, and root mean square error were respectively 0.0036, 0.9970, and 0.0152, displaying its higher comprehensive performance. The model may also be applied in other physicochemical fields.

© 2020 Institution of Chemical Engineers. Published by Elsevier B.V. All rights reserved.

## 1. Introduction

Solubility of supercritical carbon dioxide (SCCO<sub>2</sub>) in polymeric compounds is important for the modifications, synthesis, and preparation of new materials (Gong et al., 2017; Rabaeh et al., 2019; Duncan and Pillai, 2015; Khatsee et al., 2018; Ota et al., 2018; Guerin et al., 2019). Under high-temperature and high-pressure supercritical conditions, a solubility experiment is time-consuming and costly and it is not easy to obtain experimental data. Therefore, it is necessary to design a prediction model with high accuracy. The solubility of SCCO<sub>2</sub> in polymers is affected by polarity of molecules, density, temperature, and pressure. These factors show the complicated non-linear associations with the solubility and the relationships among these factors are also

complex. Therefore, traditional prediction methods based on thermodynamic equation of state or other empirical equations cannot provide the satisfactory prediction accuracy (Sun et al., 2017; Baghban et al., 2019; Koszynowski, 2016; Aftab et al., 2018; Cowen et al., 2018; Zhou and Kasuga, 2018). Ziae et al. (2015) predicted carbon dioxide solubility in different polymers with support vector machine and indicated that the proposed models were efficient. Artificial neural network (ANN) possesses the ability of self-organizing, non-linear processing, and fault tolerance and can overcome the challenges of prediction (Lazzus et al., 2017; Lazzus, 2013a; Hosaini-Alvand et al., 2017; Giri Nandagopal and Selvaraju, 2016; Mehdizadeh and Movaghfarnejad, 2011; Qiu et al., 2019; Lashkarbolooki and Bayat, 2018; Li et al., 2018a; Lazzus, 2011; Yao et al., 2018). Bakhtbakhshi (2012) and Hezave et al. (2012) compared

**Abbreviations:** PVT, pressure, volume, temperature; ANN, artificial neural network; RBF, radial basis function; PSO, particle swarm optimization; CAPSO, chaotic accelerated PSO; DP-DT-CAPSO, double population CAPSO based on diffusion theory; PBS, poly(butylene succinate); PBSA, poly(butylene succinate-co-adipate); PP, polypropylene; PS, polystyrene; CPEs, carboxylated polyesters; PLLA, poly(L-lactide); PLGA, poly(D,L-lactide-co-glycolide); HDPE, high-density polyethylene; ARD, average relative deviation; R<sup>2</sup>, squared correlation coefficient; MSE, mean square error; RMSEP, root mean square error of prediction.

\* Corresponding author.

E-mail address: [jcimsli@163.com](mailto:jcimsli@163.com) (M. Li).

<https://doi.org/10.1016/j.cherd.2020.01.003>

0263-8762/© 2020 Institution of Chemical Engineers. Published by Elsevier B.V. All rights reserved.



# Prediction of pK(a) values of neutral and alkaline drugs with particle swarm optimization algorithm and artificial neural network

Bingsheng Chen<sup>1</sup> · Huaijin Zhang<sup>1</sup> · Mengshan Li<sup>1</sup>

Received: 28 August 2018 / Accepted: 18 December 2018 / Published online: 1 January 2019  
© Springer-Verlag London Ltd., part of Springer Nature 2019

## Abstract

A prediction model of pKa values of neutral and alkaline drugs based on particle swarm optimization algorithm and back propagation artificial neural network, called PSO–BP ANN, was established. PSO–BP ANN model was proposed using back propagation artificial neural network trained by particle swarm optimization algorithm, and used to predict the pKa values. The five parameters, including relative N atom number, Randic index (order 3), relative negative charge, relative negative charge surface area and maximum atomic net charge, were selected by particle swarm optimization algorithm and used as input variables of the model. The output variable in the proposed model was pKa values. The experimental results showed that the three layers (5–7–1) prediction model had a good prediction performance. The absolute mean relative error, root mean square error of prediction and square correlation coefficient were 0.5728, 0.0512 and 0.9169, respectively. The pKa values of neutral and alkaline drugs were positively correlated with the value of maximum atomic net charge, but the pKa value decreased with the increase in the other four parameters.

**Keywords** pKa value · Particle swarm optimization · Back propagation · Artificial neural network

## 1 Introduction

pKa constant, called acidity coefficient, is mainly using some genes to regulate protein phosphorylation and make it acid, so that to activate the specific gene to transcribe [1–3]. And pKa constant is also a key point which the drugs generating affect. Therefore, it is necessary to precisely predict the acidity coefficient in the process of drug synthesis.

The structure of a substance determines its activity or properties. Molecular descriptors can represent molecular structures, so molecular descriptors are used to explore the relationship between the molecular structure and the nature or activity of a substance. However, all descriptors are not

necessary for representing the properties of the substance [4–6]. Therefore, it may reduce the effect of important factors and affect the results of the experiment when using more unnecessary descriptors. Thus, it is necessary to develop certain methods to select valid variables. All kinds of swarm intelligent algorithms have been proposed to screen the molecular descriptors, such as artificial fish swarm algorithm [7], genetic algorithm [8, 9], artificial bee colony algorithm [10, 11], ant colony optimization algorithms [12, 13], simulated annealing algorithm [14] and particle swarm optimization (PSO) [15, 16]. PSO is a computational method that optimizes a problem by iteratively trying to improve a candidate solution with regard to a given measure of quality. PSO is a meta-heuristic as it makes few or no assumptions about the problem being optimized and can search very large spaces of candidate solutions [17, 18]. Compared with the other evolutionary algorithm, the most important advantages of PSO are the few parameters needed to adjust and the easy implementation. In this paper, we use PSO to screen the molecular structure descriptors screened.

A pKa value is a vital parameter, but its determination experiments are cumbersome. Therefore, it is important to develop a pKa prediction model with high accuracy [19].

✉ Bingsheng Chen  
bscheng@gnnu.edu.cn

Mengshan Li  
lms@gnnu.edu.cn; jcimsli@163.com

Huaijin Zhang  
xjxie@gnnu.edu.cn

<sup>1</sup> College of Physics and Electronic Information, Gannan Normal University, Ganzhou, China

**OPEN**

# Prediction Model of Organic Molecular Absorption Energies based on Deep Learning trained by Chaos-enhanced Accelerated Evolutionary algorithm

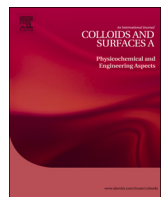
Mengshan Li<sup>1</sup>\*, Suyun Lian<sup>1</sup>, Fan Wang, Yanying Zhou, Bingsheng Chen, Lixin Guan & Yan Wu

As an important physical property of molecules, absorption energy can characterize the electronic property and structural information of molecules. Moreover, the accurate calculation of molecular absorption energies is highly valuable. Present linear and nonlinear methods hold low calculation accuracies due to great errors, especially irregular complicated molecular systems for structures. Thus, developing a prediction model for molecular absorption energies with enhanced accuracy, efficiency, and stability is highly beneficial. By combining deep learning and intelligence algorithms, we propose a prediction model based on the chaos-enhanced accelerated particle swarm optimization algorithm and deep artificial neural network (CAPSO BP DNN) that possesses a seven-layer 8-4-4-4-4-4-1 structure. Eight parameters related to molecular absorption energies are selected as inputs, such as a theoretical calculating value  $E_c$  of absorption energy (B3LYP/STO-3G), molecular electron number  $N_e$ , oscillator strength  $O_s$ , number of double bonds  $N_{db}$ , total number of atoms  $N_a$ , number of hydrogen atoms  $N_h$ , number of carbon atoms  $N_c$ , and number of nitrogen atoms  $N_N$ ; and one parameter representing the molecular absorption energy is regarded as the output. A prediction experiment on organic molecular absorption energies indicates that CAPSO BP DNN exhibits a favourable predictive effect, accuracy, and correlation. The tested absolute average relative error, predicted root-mean-square error, and square correlation coefficient are 0.033, 0.0153, and 0.9957, respectively. Relative to other prediction models, the CAPSO BP DNN model exhibits a good comprehensive prediction performance and can provide references for other materials, chemistry and physics fields, such as nonlinear prediction of chemical and physical properties, QSAR/QAPR and chemical information modelling, etc.

As an important physical property of molecules, the absorption energy contains internal structural information and electronic performance of molecules. The accurate prediction of absorption energies is an important direction in the field of computational chemistry with great research value and significance<sup>1,2</sup>. Many linear and nonlinear computational methods such as linear regression, density functional theory, support vector machine, and artificial neural network have been applied to examine the absorption energies of organic molecules<sup>3–5</sup>.

Hutchison *et al.*<sup>6</sup> used ZINDO/CIS, ZINDO/RPA, HF/CIS, HF/RPA, TDDFT/TDA, and TDDFT to predict the absorption energies of 60 organic molecules and identified that the linear regression achieved superior combined performances for TDDFT/CIS and TDDFT/RPA. However, for complicated molecules or a large system, these kinds of methods fall short in performance. Gao *et al.*<sup>7,8</sup> used the least squares support vector machine to reduce the errors of absorption energies of 160 organic molecules, the multiple linear regression method to seek for characteristic space and select the main molecular physical parameters, and the least squares support vector machine to establish a nonlinear model. Results showed that the least squares support vector machine was a more accurate and effective correction method in the field of physical chemistry than the other methods. Li *et al.*<sup>9</sup>

College of Physics and Electronic Information, Gannan Normal University, Ganzhou, Jiangxi, 341000, China. \*email: jcimsli@163.com



## Sandwiched CNT@SnO<sub>2</sub>@PPy nanocomposites enhancing sodium storage

Jujun Yuan<sup>a,1</sup>, Youchen Hao<sup>b,c,1</sup>, Xianke Zhang<sup>a</sup>, Xifei Li<sup>b,c,\*</sup>

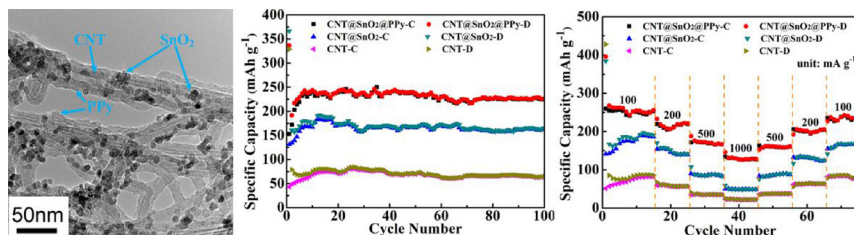
<sup>a</sup> School of Physics and Electronics, Gannan Normal University, Ganzhou, 341000, China

<sup>b</sup> Institute of Advanced Clean Energy, Xi'an University of Technology, Xi'an, 710048, China

<sup>c</sup> Energy & Materials Engineering Centre, College of Physics and Materials Science, Tianjin Normal University, Tianjin, 300387, China

### GRAPHICAL ABSTRACT

CNT@SnO<sub>2</sub>@PPy nanocomposites were designed by combining liquid-phase deposition (LPD) and in-situ chemical-polymerization method for sodium-ion battery anodes. Sandwiched CNT@SnO<sub>2</sub>@PPy electrode exhibits excellent rate capability and high capacity retention with a reversible capacity of 226 mAh g<sup>-1</sup> after 100 cycles.



### ARTICLE INFO

#### Keywords:

Sodium ion batteries  
Anode  
CNT@SnO<sub>2</sub>nanocomposites  
PPy  
Coating

### ABSTRACT

CNT@SnO<sub>2</sub>@PPy nanocomposites were designed by combining liquid-phase deposition (LPD) and in-situ chemical-polymerization method for sodium-ion battery anodes. CNT@SnO<sub>2</sub>@PPy nanocomposites maintain one-dimensional structure of CNT in diameters of about 35–45 nm, moreover, the thickness of PPy coating is about 6–8 nm. Sandwiched CNT@SnO<sub>2</sub>@PPy electrode exhibits excellent rate capability and high capacity retention with a reversible capacity of 226 mAh g<sup>-1</sup> after 100 cycles at the current density of 100 mA g<sup>-1</sup>. The improved electrochemical performance may be assigned to the synergistic effects among CNT, SnO<sub>2</sub>, and PPy. It may enhance electrical conductivity, avoid the pulverization of electrode material, and prevent the aggregation of Sn during the charge/discharge processes.

### 1. Introduction

Lithium-ion batteries (LIBs) have been widely utilized for portable devices as well as electrical vehicles because of their advantages of high energy density, long cycle life, and environmental benignity [1–3]. However, the limited lithium resources have become the obstacles for the large scale application of LIBs with high cost [4,5]. As a result, sodium-ion batteries (SIBs) may be considered as one of the most attractive candidates for LIBs for large-scale energy storage system, due to

their low price and abundant sodium resources [6]. Compared with lithium-ion (0.59 Å), sodium-ion has a larger radius (1.02 Å), which leads to limited electrochemical activity of sodium-ion insertion/extraction into/from the graphite interlayer. Hence, some effort has been focused on developing anode materials with high performance including hard carbon [7,8], metal oxides [9–11], alloy materials [12,13], metal sulfides [14,15], etc.

Among metal oxides anode materials of SIBs, SnO<sub>2</sub> has gained much attention owing to the high theoretical capacity of 667 mAh g<sup>-1</sup>

\* Corresponding author at: Institute of Advanced Clean Energy, Xi'an University of Technology, Xi'an, 710048, China.

E-mail address: [xfl@xaut.edu.cn](mailto:xfl@xaut.edu.cn) (X. Li).

<sup>1</sup> These authors contributed equally to this work and should be considered co-first authors.

# SCIENTIFIC REPORTS



OPEN

## Prediction of pKa Values for Neutral and Basic Drugs based on Hybrid Artificial Intelligence Methods

Received: 4 September 2017

Accepted: 21 February 2018

Published online: 05 March 2018

Mengshan Li , Huaijing Zhang, Bingsheng Chen, Yan Wu & Lixin Guan

The pKa value of drugs is an important parameter in drug design and pharmacology. In this paper, an improved particle swarm optimization (PSO) algorithm was proposed based on the population entropy diversity. In the improved algorithm, when the population entropy was higher than the set maximum threshold, the convergence strategy was adopted; when the population entropy was lower than the set minimum threshold the divergence strategy was adopted; when the population entropy was between the maximum and minimum threshold, the self-adaptive adjustment strategy was maintained. The improved PSO algorithm was applied in the training of radial basis function artificial neural network (RBF ANN) model and the selection of molecular descriptors. A quantitative structure-activity relationship model based on RBF ANN trained by the improved PSO algorithm was proposed to predict the pKa values of 74 kinds of neutral and basic drugs and then validated by another database containing 20 molecules. The validation results showed that the model had a good prediction performance. The absolute average relative error, root mean square error, and squared correlation coefficient were 0.3105, 0.0411, and 0.9685, respectively. The model can be used as a reference for exploring other quantitative structure-activity relationships.

As an important step in drug design, the quantitative structure-activity relationship (QSAR) study has become one of the most active branches because it can improve the efficiency of drugs by computer simulation and provide ideas for designing new drugs<sup>1</sup>. The QSAR study is also important in computer science, chemistry, pharmacy and life sciences<sup>2</sup>. The acidity of drugs is mainly achieved by activating the acidity coefficient, which is called pKa constant and denotes the capability of an acid to dissociate hydrogen ions<sup>3,4</sup>. The pKa value is an important parameter in drug design and determines pharmacological activity. The experimental measurement method of pKa value is relatively cumbersome and time-consuming. Therefore, it is necessary to establish an accurate and efficient pKa prediction model<sup>5,6</sup>.

Model establishment is one of the key steps in QSAR research. The traditional model establishment methods include linear regression and least square method<sup>7,8</sup>. The modern computing methods consist of support vector machines (SVM)<sup>9</sup>, artificial neural networks (ANN)<sup>10-13</sup>, and various intelligent algorithms<sup>14,15</sup>. Polanski<sup>16</sup> proposed a model utilizing ANN and partial least squares (PLS) to study the relationship between molecular surface area and pKa value and predicted the pKa values of aromatic acids and alkyl acids. Luan<sup>17</sup> proposed a pKa prediction model based on the heuristic method (HM) and radial basis function artificial neural network (RBF ANN) and obtained the better prediction performance. Previous studies confirmed that the ANN model had the better performance in QSAR modelling<sup>18,19</sup>, but the performance of ANN depended on its training algorithm. The training algorithm plays a decisive role in RBF ANN model and various evolutionary algorithms have been successfully applied in the training of RBF ANN<sup>20-23</sup>.

The selection of molecular descriptors largely determines the quality of QSAR model<sup>24-26</sup>. There are many selection methods of molecular descriptors, which can be mainly divided into two categories: traditional step-wise selection methods (including the PLS method and its variants) and the modern search algorithm based on optimization strategy<sup>27,28</sup>. The first category is simple, direct, and efficient, but it fails to achieve the global optimum, especially in the complex data sets. The second category is a global optimal method and shows significant advantages. It is easy to search the optimal solution and suitable to deal with complex large data sets. Therefore, the second category has become one of the hotspots<sup>29</sup>.

College of Physics and Electronic Information, Gannan Normal University, Ganzhou, Jiangxi, 341000, China.  
Correspondence and requests for materials should be addressed to M.L. (email: [jcimsli@163.com](mailto:jcimsli@163.com))

# Detection of Chylous Plasma Based on Machine Learning and Hyperspectral Techniques

Applied Spectroscopy  
 2024, Vol. 78(4) 365–375  
 © The Author(s) 2024  
 Article reuse guidelines:  
[sagepub.com/journals-permissions](http://sagepub.com/journals-permissions)  
 DOI: 10.1177/00037028231214802  
[journals.sagepub.com/home/asp](http://journals.sagepub.com/home/asp)



Yafei Liu<sup>1</sup> , Jianxiu Lai<sup>2</sup>, Liying Hu<sup>2</sup>, Meiyuan Kang<sup>2</sup>, Siqi Wei<sup>1</sup>, Suyun Lian<sup>1</sup>,  
 Haijun Huang<sup>1</sup>, Hao Cheng<sup>1</sup>, Mengshan Li<sup>1</sup>, and Lixin Guan<sup>1</sup>

## Abstract

Chylous blood is the main cause of unqualified and scrapped blood among volunteer blood donors. Therefore, a diagnostic method that can quickly and accurately identify chylous blood before donation is needed. In this study, the GaiaSorter “Gaia” hyperspectral sorter was used to extract 254 bands of plasma images, ranging from 900 nm to 1700 nm. Four different machine learning algorithms were used, including decision tree, Gaussian Naive Bayes (GaussianNB), perceptron, and stochastic gradient descent models. First, the preliminary classification accuracies were compared with the original data, which showed that the effects of the decision tree and GaussianNB models were better; their average accuracies could reach over 90%. Then, the feature dimension reduction was performed on the original data. The results showed that the effects of the decision tree were better with a classification accuracy of 93.33%. The classification of chylous plasma using different chylous indices suggested that the accuracies of the decision trees model both before and after the feature dimension reductions were the best with over 80% accuracy. The results of feature dimension reduction showed that the characteristic bands corresponded to all kinds of plasma, thereby showing their classification and identification potential. By applying the spectral characteristics of plasma to medical technology, this study suggested a rapid and effective method for the identification of chylous plasma and provided a reference for the blood detection technology to achieve the goal of reducing wasting blood resources and improving the work efficiency of the medical staff.

## Keywords

Chylous plasma, hyperspectral techniques, decision tree, Gaussian Naive Bayes, GaussianNB, perceptrons, stochastic gradient descent

Date received: 23 March 2023; accepted: 27 May 2023

## Introduction

Currently, the lifespan of modern people is constantly improving, but the lifestyle is getting unhealthy. A large amount of high-fat content food is being consumed in daily life, which in combination with a lack of exercise results in a large amount of fat accumulation in the body,<sup>1</sup> thereby increasing the fat content in blood.<sup>2</sup> The increase in blood fat contents makes the blood plasma appear milky white or cloudy, thereby forming chylous blood.<sup>3</sup> Chylous blood should not be used for clinical purposes.<sup>4</sup> Its injection into the patients causes adverse reactions, such as allergy, fever, and fat embolism,<sup>5</sup> thereby further harming the patient. Therefore, a convenient and fast method for differentiating between chylous and normal healthy blood should be urgently developed.<sup>6</sup>

Currently, the direct and accurate method for differentiating between chylous and normal healthy blood includes the detection of plasma components and identification of chylous

blood by components. Although the results are very accurate, it is a time-consuming process. The detection of a single component takes about 5 min, thereby greatly reducing the detection efficiency and failing to meet the current detection requirements.<sup>7</sup> However, the detection methods for chylous blood, which are based on machine vision and image analysis, have also been widely used and can improve detection efficiency. However, the detection method based on image analysis is limited to the calculation of image grayscale values and can easily be affected by background noise, resulting in

<sup>1</sup>College of Physics and Electronic Information, Gannan Normal University, Ganzhou, Jiangxi, China

<sup>2</sup>Central Blood Station of Ganzhou City in Jiangxi Province, Ganzhou, Jiangxi, China

## Corresponding author:

Lixin Guan, College of Physics and Electronic Information, Gannan Normal University, Ganzhou, 341000, Jiangxi, China  
 Email: [lxguan@gnnu.edu.cn](mailto:lxguan@gnnu.edu.cn); [84955441@qq.com](mailto:84955441@qq.com)



## Studies on a novel Ho<sup>3+</sup>:KBGM crystal toward the ~2 μm laser applications

Yi Yu <sup>a,b,\*</sup>, Chonghui Niu <sup>a,b</sup>, Kai Shao <sup>a,b</sup>, Mingjie Dan <sup>a,b</sup>, Zhibin Wang <sup>a</sup>, Yingying Wang <sup>a</sup>, Jie Chen <sup>a</sup>, Jiani Luo <sup>a</sup>

<sup>a</sup> School of Physics and Electronic Information, Gannan Normal University, Ganzhou 341000, China

<sup>b</sup> Research Center for Rare Earth Materials and Applications, Gannan Normal University, Ganzhou 341000, China



### ARTICLE INFO

#### Keywords:

- A1. Crystal structure
- A1. Polarized spectra properties
- A2. Top-seeding solution growth method
- B1. Molybdate crystal
- B2. 2 μm laser

### ABSTRACT

A Ho<sup>3+</sup>:KBGM crystal with good quality and large size was successfully grown via TSSG method. The crystal's structure, ambient-temperature polarized absorption and emission spectra and fluorescence lifetime were studied. The J-O theory was adopted to analyze the absorption spectra and results show that crystal exhibits relatively large intensity parameters  $\Omega_2$  and spectroscopic quality factor which is up to 3.12. At 453 nm, the absorption band is the strongest, and the corresponding cross-sections are  $21.94 \times 10^{-20} \text{ cm}^2$ ,  $26.66 \times 10^{-20} \text{ cm}^2$  and  $18.56 \times 10^{-20} \text{ cm}^2$  for the -X, -Y and -Z polarizations, respectively. The emission spectra also demonstrate the broad and strong emission band at 2030 nm. The FWHMs and cross-sections are 74 nm,  $0.37 \times 10^{-20} \text{ cm}^2$ , 50 nm,  $0.68 \times 10^{-20} \text{ cm}^2$ , and 49 nm  $0.52 \times 10^{-20} \text{ cm}^2$  for the three polarizations, respectively. In addition, the crystal has a superior quantum efficiency which is as high as 97.1%. Taking all the analyses into account, it is reasonable to assert that the Ho<sup>3+</sup>:KBGM crystal an ideal candidate for ~2 μm laser applications in many areas.

### 1. Introduction

As laser emissions at around 2 μm are within the eye-safe spectral region, solid-state lasers with wavelength at around 2 μm have great application potential in various fields, such as medicine, optical communication, remote sensing, etc. Recent years, with the development of science and technology in our society, the urgent need for ~2 μm lasers has prompted a lot of passion on the research of laser crystal with wavelength in this region. Due to abundant energy levels with rich corresponding emission spectral lines ranging from ultraviolet to mid-infrared region, Ho<sup>3+</sup> is one of the ideal elements to generate the emission at the desired wavelength at around 2.0 μm which is corresponding to the  $5I_7 \rightarrow 5I_8$  transition, and consequently, various of Ho<sup>3+</sup>-doped laser crystals have attracted much attention and been investigated as gain materials in this region, such as [1–7]. Molybdate crystals are of importance hosts due to good properties, including the aspects of physical stability, mechanical properties, etc. Thus, many kinds of Ho<sup>3+</sup>-based molybdate crystals which have been extensively investigated are regarded as prominent laser media and it is of great interest to explore more novel Ho<sup>3+</sup>-doped molybdate laser crystals with excellent comprehensive properties for both continuous-wave (CW) and mode-locked (ML) lasers at ~2 μm [8–12].

In the past years, many researchers have been focusing on a series of

triple-molybdate compounds denoted by the formula of MNRe(MoO<sub>4</sub>)<sub>3</sub> (M = Li, K; N = Mg, Ba; Re = Al, La-Lu, Y) which were first reported in 1990 [13]. Advantageous crystal structure, moderate mechanical properties and excellent optical performances have been demonstrated in this type of crystals doped with variety of rare-earth ions [14–17]. KBaGd(MoO<sub>4</sub>)<sub>3</sub> (KBGM) belongs to this family and our previous works based on this crystal indicated its huge potential as laser material [18]. Revealed by X. M. Meng et al, this crystal is monoclinic with the space group of C2/c and the unit cell parameters are  $a = 17.401(13)$  Å,  $b = 12.226(8)$  Å,  $c = 5.324(4)$  Å,  $\beta = 106.19(1)$  Å. In addition, the structure of KBGM crystal possesses several merits that can be taken advantage to fulfill the aim of improving the performance of activating ions introduced in the host lattice [19]. One of the interested features of the KBGM structure is the local disorder originated from the co-occupation at one site by K and Ba atoms, forming a distorted dodecahedron with eight adjacent oxygen atoms. For the Mo-O units, there are [MoO<sub>4</sub>] tetrahedrons and [MoO<sub>6</sub>] octahedrons, both of which exhibit different bond lengths and bond angles. Consequently, the eight-coordinate [GdO<sub>8</sub>] dodecahedrons were also distorted. Profile of the KBGM crystal structure and the distorted polyhedrons with bond lengths assigned were depicted in Fig. 1. Taking the advantage of these crystal structure features, it is highly possible to modulate the crystal field for the doped rare-earth ions as the activating centers and thereby improve their optical

\* Corresponding author.

E-mail address: [yuyignnu@163.com](mailto:yuyignnu@163.com) (Y. Yu).



Cite this: RSC Adv., 2023, 13, 31785

## Dual-emission center ratiometric optical thermometer based on $\text{Bi}^{3+}$ and $\text{Mn}^{4+}$ co-doped $\text{SrGd}_2\text{Al}_2\text{O}_7$ phosphor

Yi Yu, †<sup>a,b</sup> Kai Shao, †<sup>ab</sup> Chonghui Niu, <sup>ab</sup> Mingjie Dan, <sup>ab</sup> Yingying Wang, <sup>a</sup> Xiourong Zhu, <sup>abc</sup> Xianke Zhang <sup>a</sup> and Yeqing Wang<sup>\*d</sup>

In recent years, more and more attention has been paid to optical temperature sensing, and how to improve its accuracy is the most important issue. Herein, a new temperature sensing material,  $\text{SrGd}_2\text{Al}_2\text{O}_7:\text{Bi}^{3+},\text{Mn}^{4+}$ , based on fluorescence intensity ratio was designed in this work. It has both blue-purple and red luminescence under 300 nm excitation, and the dual-emitting centers with distinct colors, the different thermal sensitivities of  $\text{Bi}^{3+}$  and  $\text{Mn}^{4+}$ , and the energy transfer between  $\text{Bi}^{3+}$  and  $\text{Mn}^{4+}$  give it excellent signal resolution and accurate temperature detection. The  $S_a$  of  $\text{SrGd}_2\text{Al}_2\text{O}_7:0.04\text{Bi}^{3+},0.003\text{Mn}^{4+}$  phosphor reaches a maximum value of  $8.573\% \text{ K}^{-1}$  at 473 K, and the corresponding  $S_r$  is  $1.927\% \text{ K}^{-1}$ , both of which are significantly better than those of most other reported optical temperature sensing materials. Taking all the results into account, the  $\text{SrGd}_2\text{Al}_2\text{O}_7:0.04\text{Bi}^{3+},0.003\text{Mn}^{4+}$  phosphor can be regarded as a prominent FIR-type temperature sensing material.

Received 2nd September 2023  
Accepted 19th October 2023

DOI: 10.1039/d3ra05988j

rsc.li/rsc-advances

### 1. Introduction

Temperature is a physical quantity that shows how hot or cold something is. It is a fundamental and important physical quantity in daily life, industrial applications, scientific research, etc. Currently, thermometers can be divided mainly into contact type and non-contact type. The working principle of the contact type is based mainly on the thermocouple characteristics or the Seebeck effect, the latter relying on temperature-dependent optical properties.<sup>1</sup>

Traditional contact thermometers have limitations in application to biological tissue, or in a corrosive or strongly magnetic environment. For example, in the outbreak of the novel coronavirus pneumonia from December 2019, the virus is highly contagious, and the use of contact temperature measuring instruments greatly increases the risk of virus transmission, so non-contact measurement is an ideal choice to resolve this problem. Even in a variety of other fields, non-contact temperature measurement is still preferred. However, although many kinds of non-contact temperature sensors are

emerging in the market at present, most of them are greatly affected by the environment, resulting in low measurement accuracy and large error, which makes the test results less repeatable. An optical temperature sensor can not only easily realize non-contact measurement, but also maintain high measurement accuracy in a special measurement environment. It also has incomparable advantages over traditional contact temperature sensors in terms of volume, response speed and sensitivity. Therefore, research on optical temperature sensors has attracted more and more attention.<sup>2</sup>

Owing to their abundant and complex energy levels and temperature-sensitive optical behavior, lanthanide-ion-based fluorescence intensity ratio (FIR)-type temperature measurement materials are taking a leading role in the field of temperature sensing materials. However, their band gaps are often relatively narrow, leading to problems, including overlap of two transmitted signals, large detection deviation and poor resolution. These drawbacks in turn limit their ability to measure temperature with high accuracy.<sup>3,4</sup> In order to overcome these shortcomings, temperature sensing materials based on multiple emission centers with different thermal sensitivities, such as rare earth/rare earth (Re/Re) or transition metal/rare earth (Tr/Re) ion co-doped materials, have been designed in recent years. Among these co-doped materials,  $\text{Eu}^{3+}/\text{Tb}^{3+}$ ,  $\text{Eu}^{3+}/\text{Bi}^{3+}$ , and  $\text{Eu}^{3+}/\text{Dy}^{3+}$  groups have revealed excellent temperature sensing ability.<sup>5–7</sup> However, there are few reports on temperature sensing materials doped by double transition group metal elements. The luminescence properties of  $\text{Bi}^{3+}$  ions are easily affected by the crystal field environment where the ions reside. Based on their adjustable luminescence,  $\text{Bi}^{3+}$  ions are often selected as efficient

<sup>a</sup>School of Physics and Electronic Information, Gannan Normal University, Ganzhou 341000, China. E-mail: yuyignnu@163.com

<sup>b</sup>Advanced Energy Storage & Photoelectric Materials Research Center, Gannan Normal University, Ganzhou 341000, China

<sup>c</sup>Shanghai Key Laboratory of Special Artificial Microstructure Materials & Technology, Department of Physics, Tongji University, Shanghai 200092, China

<sup>d</sup>Department of Applied Physics, East China Jiaotong University, Nanchang, 330013, Jiangxi, China. E-mail: jxdxmeng@126.com

† These authors contributed equally to this work.

## ACCEPTED MANUSCRIPT

# Compared discharge characteristics and film modifications of atmospheric pressure plasma jets with two different electrode geometries

To cite this article before publication: Xiong Chen *et al* 2023 *Chinese Phys. B* in press <https://doi.org/10.1088/1674-1056/ace768>

## Manuscript version: Accepted Manuscript

Accepted Manuscript is “the version of the article accepted for publication including all changes made as a result of the peer review process, and which may also include the addition to the article by IOP Publishing of a header, an article ID, a cover sheet and/or an ‘Accepted Manuscript’ watermark, but excluding any other editing, typesetting or other changes made by IOP Publishing and/or its licensors”

This Accepted Manuscript is © 2023 Chinese Physical Society and IOP Publishing Ltd.



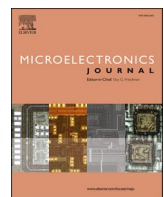
During the embargo period (the 12 month period from the publication of the Version of Record of this article), the Accepted Manuscript is fully protected by copyright and cannot be reused or reposted elsewhere.

As the Version of Record of this article is going to be / has been published on a subscription basis, this Accepted Manuscript will be available for reuse under a CC BY-NC-ND 3.0 licence after the 12 month embargo period.

After the embargo period, everyone is permitted to use copy and redistribute this article for non-commercial purposes only, provided that they adhere to all the terms of the licence <https://creativecommons.org/licenses/by-nc-nd/3.0>

Although reasonable endeavours have been taken to obtain all necessary permissions from third parties to include their copyrighted content within this article, their full citation and copyright line may not be present in this Accepted Manuscript version. Before using any content from this article, please refer to the Version of Record on IOPscience once published for full citation and copyright details, as permissions may be required. All third party content is fully copyright protected, unless specifically stated otherwise in the figure caption in the Version of Record.

View the [article online](#) for updates and enhancements.



## A high efficiency buck converter based on PLL for frequency stabilization

Huang-Hong Yang, Hua Wu <sup>\*</sup>, An-An Zhang, Xian-Guo Cao

Gannan Normal University, China

### ARTICLE INFO

**Keywords:**

Buck converter  
Phase-locked loop(PLL)  
Frequency stabilization  
Adaptive on time(AOT)  
High conversion efficiency

### ABSTRACT

A high efficiency Buck converter circuit based on Phase-locked loop (PLL) to achieve frequency stabilization is proposed to solve the problems of reduced converter efficiency, unstable output and high electromagnetic interference caused by unstable switching frequency. Since the increase of load current increases the switching frequency in the conventional adaptive on-time (AOT) control, a phase-locked loop is designed to achieve the switching frequency stabilization by forming a negative feedback. In addition, a bootstrap high-voltage gate driver circuit is designed to drive the dual NMOS power tubes in order to achieve high conversion efficiency and optimize the chip area. The proposed Buck circuit is simulated and verified based on SMIC 0.18 μm CMOS 2P4M process, with an input voltage of 2.5V–5.5V, an output voltage of 0.8V–4V, a switching frequency variation rate of only 8.5 kHz/A over the load range of 0.5A–3A, and a peak efficiency of 94.8 % over the full load range is achieved, and the undershoot/overshoot recovery time of the load transient response is only 5.4μs and 6.9μs.

### 1. Introduction

Among the many control methods of DC-DC power supply, AOT control, as a simple and effective control technology, is one of the widely used control methods at present; it has the advantages of output stabilization, fast dynamic response, and strong anti-jamming ability, etc. In the traditional AOT control mode, when the load current or input/output voltage changes, the control loop needs to adaptively adjust the switching frequency to maintain the stability of the output voltage. However, the change of switching frequency not only causes the transient response of the output voltage to become slower or unstable, affecting the ability of the system to dynamically respond to the load changes; it also changes the inductor current and the charging and discharging time of the output capacitor, which affects the ripple size of the output voltage or current. In addition, changes in switching frequency cause additional switching losses that affect the overall efficiency, and also lead to serious noise and electromagnetic interference problems.

To overcome these problems, several control techniques have been proposed, such as predictive control and current mode control, etc.; these techniques can reduce the effects of input voltage, output voltage and load current fluctuations on switching frequency. For example, in 2016 Chien-Hung Tsai [1] proposed Sensor-less load current correction (SLCC) and dynamic tolerance window (DTW) control techniques, which can reduce the frequency variations caused by conduction losses

and have the advantage of simple circuit structure. However, the switching frequency varies drastically in the load range of 800mA–1000mA, and the conversion efficiency

does not exceed 70 % in this load range. In 2021 Keng Chen [2] proposed an accurate frequency prediction method based on constant on-time (COT) buck converter, which can be used for point-of-load (POL) regulation with fast load transient requirements and wide load variation range. However, a 470 μF output capacitor is required, which takes up more chip area and increases cost. In 2023, Hamed Abbasi Zadeh [3] designed has been a novel multilevel hybrid plug-and-play dc-dc converter, which improves the performance of the conventional COT converter by proposing solutions to the key issues such as switching frequency variation, output spurious and ripple. However, the efficiency needs to be improved due to the increased switching loss by the implementation method of using multiple fly capacitors. In 2021, Jing-xiang Zhao [4] used the reference frequency compensation (RFC) technique to stabilize the converter and eliminate the problem of switching frequency variation of the low ESR output capacitors without adding external components or integrating clock control circuits and RC filters. However, the low switching frequency may not be suitable for high precision voltage stabilization applications.

However, frequency locking using PLL is the most reliable and effective measure for switching frequency variations, which will effectively improve system stability, transient response, etc. For example, in 2018, Chen Jiann-Jong [5] proposed a novel fast-response current-type

\* Corresponding author.

E-mail address: [wh1125@126.com](mailto:wh1125@126.com) (H. Wu).



## A High-Order Curvature Compensated CMOS Bandgap Reference Without Resistors

Xiuping Feng<sup>1,2</sup> · Hua Wu<sup>1</sup> · Libin Huang<sup>1</sup> · Jia Yao<sup>1</sup> · Wei Zeng<sup>1</sup> ·  
Xianguo Cao<sup>2</sup>

Received: 22 February 2023 / Revised: 9 June 2023 / Accepted: 10 June 2023 /

Published online: 24 June 2023

© The Author(s), under exclusive licence to Springer Science+Business Media, LLC, part of Springer Nature 2023

### Abstract

This paper presents a resistor-less high-order curvature compensation bandgap voltage reference. A high-order curvature compensation is based on generating successive  $V_{GS}$  voltages with different temperature characteristics, which are used to cancel thermal nonlinearity the first- and higher-order terms of the transistor voltage  $V_{EB}$ . At the same time, a piecewise-linear curvature compensation circuit is used to broaden the temperature range of the whole circuit and achieve low-temperature coefficient. The proposed bandgap reference was designed using standard CSMC 0.18- $\mu\text{m}$  CMOS technology. Simulation results indicate that the proposed bandgap reference achieves the best temperature coefficient of 2.37 ppm/ $^{\circ}\text{C}$  from  $-40$  to  $125\ ^{\circ}\text{C}$  with a supply voltage of 5 V. The BGR output is about 1.1881 V and a  $-60.7$ -dB PSRR at 10 kHz while only consuming 200  $\mu\text{W}$ .

---

✉ Hua Wu  
wh1125@126.com

Xiuping Feng  
1635129692@qq.com

Libin Huang  
3316628870@qq.com

Jia Yao  
1323695117@qq.com

Wei Zeng  
768548257@qq.com

Xianguo Cao  
1127232408@qq.com

<sup>1</sup> College of Physics and Electronic Information, Gannan Normal University, Ganzhou 341000, China

<sup>2</sup> Sichuan Xinsheng Xinguo Technology Co., Ltd., Chengdu 610000, China

# Biological Activity Predictions of Ligands Based on Hybrid Molecular Fingerprinting and Ensemble Learning

Mengshan Li,\* Ming Zeng, Hang Zhang, Huijie Chen, and Lixin Guan


Cite This: *ACS Omega* 2023, 8, 5561–5570


Read Online

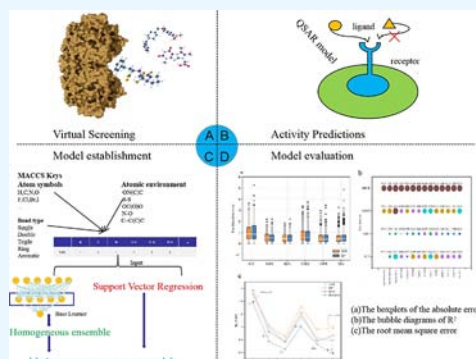
ACCESS |

Metrics &amp; More

Article Recommendations

Supporting Information

**ABSTRACT:** The biological activity predictions of ligands are an important research direction, which can improve the efficiency and success probability of drug screening. However, the traditional prediction method has the disadvantages of complex modeling and low screening efficiency. Machine learning is considered an important research direction to solve these traditional method problems in the near future. This paper proposes a machine learning model with high predictive accuracy and stable prediction ability, namely, the back propagation neural network cross-support vector regression model (BPCSVR). By comparing multiple molecular descriptors, MACCS fingerprint and ECFP6 fingerprint were selected as inputs, and the stable prediction ability of the model was improved by integrating multiple models and correcting similar samples. We used leave-one-out cross-validation on 3038 samples from six data sets. The coefficient of determination, root mean square error, and absolute error were used as the evaluation parameters. After comparing the multiclass models, the results show that the BPCSVR model has stable prediction ability in different data sets, and the prediction accuracy is higher than other comparison models.



## 1. INTRODUCTION

Ligand biological activity is an important parameter for receptors and ligand binding, and it is also the primary factor in the drug screening process.<sup>1</sup> By predicting ligand biological activity, the number of compounds to be screened can be reduced so as to improve the efficiency of the drug screening process, reduce the cost, and increase the positive rate of drug screening.<sup>2</sup> In summary, ligand biological activity prediction is a popular and valuable research topic in the field of drug screening.

The most common approach for the prediction of biological activity based on ligands is the quantitative structure–activity relationship (QSAR) proposed by Hansch et al.,<sup>2,3</sup> which is based on the principle that ligand activity is correlated with molecular structure and the activity value can be predicted by establishing a mathematical model based on the molecular structure of ligands.<sup>4,5</sup> The Hansch equation is the first one implemented in QSAR. This equation was formed by Hansch and Fujita, and it uses ED<sub>50</sub> as the activity parameter and the electrical parameter, steric parameters, and hydrophobic parameters as variables for linear regression analysis.<sup>6</sup> Guided by the Hansch equation, 4-quinolone antibacterial drugs such as norfloxacin have been successfully designed, and it proves the validity of the Hansch equation.<sup>7</sup> However, the Hansch equation has many parameters that make the modeling process difficult. During the same period as when the Hansch equation was formed, Freeman-Cook et al. proposed the Free–Wilson method,<sup>8</sup> which is a method to quantitatively express the relationship between the chemical structure and the biological

activity of drugs by mathematical formulas. The Free–Wilson method can reduce the modeling difficulty, but it is not as accurate as the Hansch equation and has not been widely used. It is generally considered that the more data characteristic parameters, the more accurate the model prediction. But the more data characteristic parameters, the more difficult it is to establish and solve the model. Due to the accumulation of a large number of experimental data, more and more researchers had been attempting to use machine learning methods to build models to predict the activity of compounds. The advantage of the machine learning method is that parameters are automatically learned according to the given data, which can reduce the difficulty of modeling and improve the efficiency of model solving. The more information contained in the data features of the machine learning model, the higher the prediction accuracy. For the activity prediction problem, we need a molecular descriptor that we can use for machine learning.

A variety of descriptors have been developed over the past few decades.<sup>9–11</sup> Molecular descriptors can be simply divided into two categories, namely, two-dimensional descriptors and high-dimensional descriptors. The two-dimensional molecular

Received: October 27, 2022

Accepted: December 23, 2022

Published: February 1, 2023





# A lncRNA-disease association prediction model based on the two-step PU learning and fully connected neural networks

Hou Biyu, Tan GuangWen, Zeng Ming, Guan Lixin, Li Mengshan <sup>\*</sup>

College of Physics and Electronic Information, Gannan Normal University, Ganzhou, Jiangxi, 341000, China

## ARTICLE INFO

**Keywords:**  
PU learning  
Two-step approach  
lncRNA-disease association  
Deep learning

## ABSTRACT

Long non-coding RNAs (lncRNAs) have been shown to play a regulatory role in various processes of human diseases. However, lncRNA experiments are inefficient, time-consuming and highly subjective, so that the number of experimentally verified associations between lncRNA and diseases is limited. In the era of big data, numerous machine learning methods have been proposed to predict the potential association between lncRNA and diseases, but the characteristics of the associated data were seldom explored. In these methods, negative samples are randomly selected for model training and the model is prone to learn the potential positive association error, thus affecting the prediction accuracy. In this paper, we proposed a cyclic optimization model of predicting lncRNA-disease associations (COPTLDA in short). In COPTLDA, the two-step training strategy is adopted to search for the samples with the greater probability of being negative examples from unlabeled samples and the determined samples are treated as negative samples, which are combined together with known positive samples to train the model. The searching and training steps are repeated until the best model is obtained as the final prediction model. In order to evaluate the performance of the model, 30% of the known positive samples are used to calculate the model accuracy and 10% of positive samples are used to calculate the recall rate of the model. The sampling strategy used in this paper can improve the accuracy and the AUC value reaches 0.9348. The results of case studies showed that the model could predict the potential associations between lncRNA and malignant tumors such as colorectal cancer, gastric cancer, and breast cancer. The predicted top 20 associated lncRNAs included 10 colorectal cancer lncRNAs, 2 gastric cancer lncRNAs, and 8 breast cancer lncRNAs.

## 1. Introduction

The high-throughput sequencing technology allows researchers to glimpse the full picture of species' genes. The human genome contains about 3.16 billion DNA base pairs, but the number of exons only accounts for 1–2% of the total length of the genome and the remaining 98% cannot be encoded as protein sequences. According to the size, non-coding RNAs are divided into large non-coding RNAs and small non-coding RNAs [1,2]. Long non-coding RNA (lncRNA) is a large non-coding RNA with a length of more than 200 nucleotides and the largest subspecies of non-coding RNA with the important genetic role, but it was initially thought to be only a short copy of DNA [3,4]. More evidences have shown that lncRNA can change mRNA splicing through the interaction with splicing factors, regulate the epigenetic state through chromosome remodeling proteins, promote or block transcription factors to affect gene

\* Corresponding author. Gannan Normal University, China.

E-mail address: [msli@gnnu.edu.cn](mailto:msli@gnnu.edu.cn) (L. Mengshan).

# Prediction of the Aqueous Solubility of Compounds Based on Light Gradient Boosting Machines with Molecular Fingerprints and the Cuckoo Search Algorithm

Mengshan Li,\* Huijie Chen, Hang Zhang, Ming Zeng, Bingsheng Chen, and Lixin Guan



Cite This: ACS Omega 2022, 7, 42027–42035



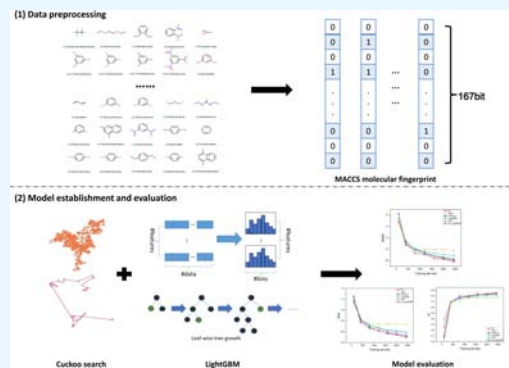
Read Online

ACCESS |

Metrics &amp; More

Article Recommendations

**ABSTRACT:** Aqueous solubility is one of the most important physicochemical properties in drug discovery. At present, the prediction of aqueous solubility of compounds is still a challenging problem. Machine learning has shown great potential in solubility prediction. Most machine learning models largely rely on the setting of hyperparameters, and their performance can be improved by setting the hyperparameters in a better way. In this paper, we used MACCS fingerprints to represent the structural features and optimized the hyperparameters of the light gradient boosting machine (LightGBM) with the cuckoo search algorithm (CS). Based on the above representation and optimization, the CS-LightGBM model was established to predict the aqueous solubility of 2446 organic compounds and the obtained prediction results were compared with those obtained with the other six different machine learning models (RF, GBDT, XGBoost, LightGBM, SVR, and BO-LightGBM). The comparison results showed that the CS-LightGBM model had a better prediction performance than the other six different models. RMSE, MAE, and  $R^2$  of the CS-LightGBM model were, respectively, 0.7785, 0.5117, and 0.8575. In addition, this model has good scalability and can be used to solve solubility prediction problems in other fields such as solvent selection and drug screening.



## 1. INTRODUCTION

Aqueous solubility of compounds is a key physicochemical property in drug development because it affects drug absorption, distribution, metabolism, excretion, and toxicity (ADMET properties).<sup>1–3</sup> Therefore, the accurate and efficient prediction of the aqueous solubility of compounds is significant in reducing drug development costs and avoiding development failures.

Since the last century, a series of methods based on mechanistic models have been proposed to predict the aqueous solubility of compounds,<sup>4,5</sup> including general solubility equations (GSEs), Monte Carlo (MC) simulation, and COSMO-RS.<sup>6–10</sup> However, these methods rely on mathematical equations or physical constants, so they have certain limitations and require a great deal of calculation. Due to the high diversity of compound drugs, the poor variability of fitting equations, and the high fitting cost in terms of time and manpower, these methods are not ideal or efficient.

To replace traditional mechanistic models, many researchers turned to the quantitative structure–property relationship (QSPR) model.<sup>11–13</sup> In QSPR, the quantitative relationship among the physicochemical properties, biological properties, and molecular structures of compounds is explored with various statistical methods and mathematical models.<sup>14,15</sup> Usually, the molecular descriptors were selected as inputs of the models.<sup>16</sup> In previous studies, the main methods used in the QSPR model

include multivariable linear regression (MLR), artificial neural network (ANN), Gaussian process (GP), and support vector machine (SVM).<sup>17,18</sup> However, the complex correlation between molecular descriptors and high-dimensional nonlinear data required for dissolution prediction poses great difficulties in traditional machine learning methods.<sup>19</sup>

Advanced machine learning methods expand the application scope of the QSPR model.<sup>20–23</sup> In recent years, ensemble learning methods, especially random forest (RF)<sup>24</sup> and light gradient boosting machine (LightGBM), have yielded satisfactory results in dissolution prediction.<sup>25,26</sup> In 2021, Ye et al.<sup>27</sup> predicted the solubility of compounds in organic solvents with the LightGBM algorithm, which showed better generalization ability compared to deep learning and other traditional machine learning algorithms.

In previous studies, a single model was generally used and the hyperparameters were set through exhaustive search. It is worth noting that the performance of the model is directly related to

Received: June 21, 2022

Accepted: October 18, 2022

Published: November 8, 2022





## Automatic quality inspection system for discrete manufacturing based on the Internet of Things

Bingsheng Chen<sup>\*</sup>, Huijie Chen, Mengshan Li

College of Physics and Electronic Information, Gannan Normal University, Ganzhou, Jiangxi 341000, China



### ARTICLE INFO

Editor: Dr. M. Malek

**Keywords:**

Internet of Things technology  
Discrete manufacturing  
Manufacturing execution system  
Quality inspection system

### ABSTRACT

With the development of information technology and the wide application of embedded technology and automatic detection technology, the requirements for equipment productivity and production process stability are also increasing. The purpose of this research is to use Internet of Things technology to design an automated quality inspection system for discrete manufacturing MESs and analyse its performance. In this study, a manufacturer's inspection system is used as the research experiment object. The products are checked and scanned one by one, and defective products with quality problems are found and returned to the production workshop. The experimental results show that the number of failures detected by the MES quality inspection system is reduced from 150 s to 79 s. This shows that the functions of the MES automated quality inspection system are significantly improved over traditional systems.

### 1. Introduction

China's manufacturing industry is currently facing a series of problems, such as high manufacturing costs, low production efficiency, low added value of products, low manufacturing quality, poor manufacturing technology, enterprises' lack of independent innovation ability, and lack of core competitiveness of enterprises. The manufacturing industry is the main body of China's national economy, the foundation of the country, the tool of national activation and the foundation of a powerful country. China both is and is not a manufacturing country. The most important point in solving the problems faced by enterprises in the process of development and establishing competitive advantages is to establish leading information and promote the scientific development mode of informatization through industrialization and industrialization.

In researching automatic inspection systems for discrete manufacturing, Song D.'s purpose was to define the reliability of automatic quality inspection systems and to improve the reliability of quality inspection data. Through a correlation analysis and feature selection, a method was proposed to improve the detection accuracy and efficiency in the auto parts thermal image quality automatic detection system based on a support vector machine. He applied the proposed method to the dispensing process of sealing machines in automobile manufacturing and analysed the optimal feature selection in the quality analysis results to show the effectiveness of the method. Since thermal imaging technology is susceptible to environmental interference, such as noise, using this method to improve detection accuracy and efficiency gives unstable results [1]. To realize the non-destructive testing of pipeshell welding defects, a visual-based automatic inspection system for a pipe shell welding quality is proposed. Based on the principle of laser triangulation, a

Reviews processed and recommended for publication by Guest Editor Dr. Neeraj Kumar .

\* Corresponding author.

E-mail address: [chenbingsheng@gmu.edu.cn](mailto:chenbingsheng@gmu.edu.cn) (B. Chen).



## Models for the solubility calculation of a CO<sub>2</sub>/polymer system: A review

Mengshan Li<sup>a,\*</sup>, Jiale Zhang<sup>b</sup>, Yanying Zou<sup>a</sup>, Fan Wang<sup>a</sup>, Bingsheng Chen<sup>a</sup>, Lixin Guan<sup>a</sup>, Yan Wu<sup>a</sup>

<sup>a</sup>College of Physics and Electronic Information, Gannan Normal University, Ganzhou, Jiangxi, 341000, China

<sup>b</sup>College of Life Science and Technology, Nanyang Normal University, Nanyang, Henan, 473061, China



### ARTICLE INFO

**Keywords:**

Multiscale  
Computational chemistry  
Molecular dynamics  
Solubility big data

### ABSTRACT

Multiscale models are modeled at different time and spatial scales to achieve the spans among the micro-, meso-, and macroscales. The multiscale study of solubility is the most effective way to reveal its essence, which is widely used in the extraction, separation, material modification, and preparation of new materials. In this article, the progress of solubility-calculation models for CO<sub>2</sub>/polymer systems at the micro-, meso-, and macroscales is surveyed. The research situation of the thermodynamic-calculation model and modern computer simulation at the macroscale is discussed, and the calculation model of molecular dynamics and particle dynamics at the micro- and mesoscales are analyzed. Focus is also given on the development trend of solubility-calculation models at different scales, particularly the mechanism and interpretability of solubility calculation at the macroscopic scale. The possible development directions of solubility big data, such as acquisition, storage, search, sharing, mining, and analysis under the background of big data, are proposed. The authors further describe the development directions of particle dynamics, coarse-grained method, and translink method on the basis of evolutionary algorithm at the micro- and mesoscales. The multiscale methods mentioned in this paper can serve as a reference in many fields, such as polymer self-assembly, phase rheological property, phase separation of block copolymers, amphiphilic molecular self-assembly into membranes, transformation and separation of vesicle morphology, and kinetic analysis. Multiscale research of solubility big data combined with deep learning and artificial intelligence may become important research directions in the future.

### 1. Introduction

Solubility is one of the important physical properties that refer to the capability of substance absorption in solvents. Solubility is widely used in the fields of the extraction and separation, material modification, and preparation of new materials [1–6]. The solubility of supercritical CO<sub>2</sub>/polymer system is extremely important in the processing and forming of the polymer materials, especially in foaming material preparation, and has important theoretical research and application value. Solubility research contains experimental and computer simulation. Given the difficulty of the experiment under high temperature and pressure, especially in the formation process with stirring, vibration, and shear aim to accelerate the solubility, the solubility experiment, which promotes the development of computer simulation, is difficult [7–9]. At present, multiscale simulation is increasingly favored by academic and industrial researchers. The 2013 Nobel Prize in chemistry was awarded to Martin Karplus, Michael Levitt, and Arieh Warshel for the development of multiscale models for complex chemical systems [10]. The multiscale method uses different time and space scales to study a common problem in detail from the micro-,

meso-, and macrospatial scales and from the femto-, nano-, and millisecond time scales [11–16]. Fig.1 plots the models and methods of multiscale model.

With the supercritical conditions of high temperature and pressure, the solubility shows the characteristics of nonlinearity, nonequilibrium, dynamic, and criticality. The solubility at the macroscale and solubility rate at the micro-, meso-, and macroscales presents the challenges to the traditional research methods. The multiscale solubility study is the most effective way to reveal the nature of dissolving and expected to provide scientific reference for process parameter selection at the multiscale level. The multiscale solubility study also has a good application prospect in the fields of self-assembly, phase rheology, and dynamic analysis of polymers and possesses important research significance in theory and application [17–19]. In terms of the macroscopic solubility calculation model, literature [20] reviewed the calculation model of the artificial neural network, and there is no relevant literature report under the micro and mesoscopic. Therefore, this article focuses on the multiscale calculation model of solubility in CO<sub>2</sub>/polymer systems; summarizes the research situations of calculation models at the micro-, meso-, and macroscales; and analyses the development trends of

\* Corresponding author.

E-mail address: [jcimsli@163.com](mailto:jcimsli@163.com) (M. Li).



# A facile route for constructing porous Ni-Mn-oxide film on Ni foam with high lithium storage performance

Jujun Yuan<sup>1,2,\*</sup> Weidong Lai<sup>1,2</sup>, Xiaofan Li<sup>1,2</sup>, Xiaokang Li<sup>1,2,\*</sup>, Xianke Zhang<sup>1</sup>, Junxia Meng<sup>1</sup>, and Huajun Yu<sup>1</sup>

<sup>1</sup> Gannan Normal University, College of Physics and Electronics, Ganzhou 341000, PR China

<sup>2</sup> Gannan Normal University, College of Chemistry and Chemical Engineering, Ganzhou 341000, PR China

Received: 18 August 2020

Accepted: 1 November 2020

Published online:

6 November 2020

© Springer Science+Business Media, LLC, part of Springer Nature 2020

## ABSTRACT

Porous Ni-Mn-oxide film on Ni foam was fabricated through electrostatic spray deposition (ESD) and subsequently calcination under argon atmosphere. The porous Ni-Mn-oxide architecture was composed of  $\text{Mn}_2\text{O}_3$  and  $\text{NiMnO}_3$  composite structure. When used as lithium-ion battery (LIB) anode, the Ni-Mn-oxide electrode exhibits superior cycleability ( $902 \text{ mAh g}^{-1}$  after 100 cycles at  $400 \text{ mA g}^{-1}$ ) and good rate capacity. The superior electrochemical property for the porous Ni-Mn-oxide film on Ni foam can be associated with the unique architecture, which can offer enough void space to buffer volume change in the charge/discharge process and provide more reactive sites in the electrochemical reaction.

## 1 Introduction

LIBs now represent an effective energy-storage system for various portable electronic devices, and are considered as hopeful energy sources in upcoming high energy area [1–6]. As one of promising alternates, manganese-based transitional metal oxides including  $\text{Mn}_2\text{O}_3$  [7],  $\text{ZnMn}_2\text{O}_4$  [8],  $\text{NiMn}_2\text{O}_4$  [9],  $\text{NiMnO}_3$  [10], etc., have drawn notable attentions for LIBs anodes because of their high theoretical capacities and natural abundance. Amidst them, Ni-containing manganese-based oxides with different atomic ratio of Ni and Mn have been proved that exhibited superior electrochemical properties for LIBs anodes owing to their rich redox reactions and better electrical conductivity [11]. Nevertheless, the

practical applications for Ni-Mn oxides are hampered by their rapid capacity attenuation owing to the large volume change in the lithiation/delithiation processes.

In order to resolve this problem, an effective strategy is to fabricate porous/hollow Ni-Mn oxides architectures, which own the advantages of providing enough empty space to buffer the volume change during the lithiation/delithiation processes, and offering large numbers of redox active sites in the electrochemical reaction [12, 13]. For instance,  $\text{Ni}_{0.14}\text{Mn}_{0.86}\text{O}_{1.43}$  hollow microspheres fabricated by coprecipitation method showed sustainable capacity ( $553 \text{ mAh g}^{-1}$  during 150 cycles at  $0.2 \text{ A g}^{-1}$ ) [12]. The hierarchical porous  $\text{NiMn}_2\text{O}_4$  microspheres synthesized through hydrothermal method could

Address correspondence to E-mail: yuanjujun123@163.com; gnnulxk@163.com

# Improving cycling stability and suppressing voltage fade of layered lithium-rich cathode materials via $\text{SiO}_2$ shell coating

Junxia Meng<sup>1</sup> & Quanxin Ma<sup>2</sup> & Lishuang Xu<sup>1</sup> & Zicheng Wang<sup>1</sup> & Huaizhe Xu<sup>1</sup> & Shichao Zhang<sup>3</sup>

Received: 15 May 2018 / Accepted: 27 July 2018  
# Springer-Verlag GmbH Germany, part of Springer Nature 2018

## Abstract

Li-rich layered metal oxide ( $\text{Li}_{1.2}\text{Mn}_{0.56}\text{Ni}_{0.16}\text{Co}_{0.08}\text{O}_2$ , denoted as LLMO) cathode materials with  $\text{SiO}_2$  coating have been successfully synthesized by using a wet chemical method combined with high temperature annealing. Scanning electron microscopy (SEM) and high-resolution transmission electron microscopy (HRTEM) analyses revealed that an amorphous  $\text{SiO}_2$  coating layer has formed on the surface of the LLMO electrode. Electrochemical analysis demonstrated that an optimal  $\text{SiO}_2$  coating amount on the surface of LLMO particles can effectively improve the cycling stability, suppress the voltage and capacity decay, and enhance the thermal stability of these electrodes. An optimal  $\text{SiO}_2$  coating amount of 0.5 wt% on an LLMO electrode (S-LLMO-0.5 wt%) improved the capacity retention to 82.6% after 200 cycles at 25 °C (67.0% for the pristine LLMO electrode) and 68.8% after 100 cycles at 60 °C (56.3% for the pristine LLMO electrode), respectively. Besides, the voltage drop of the S-LLMO-0.5 wt% sample (46.8 mV/53.6 mV) was lower than that of the pristine LLMO sample (366.1 mV/60.3 mV) after 200 cycles at 3.2 V/3.8 V, confirming that 0.5 wt%  $\text{SiO}_2$  coating can reduce the capacity loss and slower the voltage degradation rate of LLMO electrodes. In addition, the exothermic reaction of the pristine LLMO (denoted as P-LLMO from now on) electrode can be delayed by  $\text{SiO}_2$  coating while the decomposition temperature of the S-LLMO-0.5 wt% sample is significantly higher than that of the P-LLMO. These results are attributed to a uniform amorphous  $\text{SiO}_2$  coating layer that not only blocks the highly active oxygen release from the bulk material but also prevents the direct contact of the electrolyte to the positive electrodes, suppressing structural transition from a layered phase to a spinel-like one.

**Keywords** Li-rich layered metal oxide ·  $\text{SiO}_2$  shell coating · Cycling stability · Voltage fade

## Introduction

With the development of mobile electronics and electric vehicles, lithium-ion batteries (LIBs) have been considered as the

**Electronic supplementary material** The online version of this article (<https://doi.org/10.1007/s11581-018-2673-5>) contains supplementary material, which is available to authorized users.

\* Huaizhe Xu  
hxxu@buaa.edu.cn

<sup>1</sup> School of Physics and Nuclear Energy Engineering, Beihang University, Beijing 100191, China

<sup>2</sup> School of Materials Science and Engineering, Key Laboratory of Power Battery and Materials, Jiangxi University of Science and Technology, Ganzhou 341000, China

<sup>3</sup> School of Materials Science and Engineering, Beihang University, Beijing 100191, China

best energy source. However, traditional  $\text{LiCoO}_2$  cathode materials used in LIBs cannot meet the requirements of large-scale applications partially because of their low capacity and high costs. Therefore, there is a great demand for developing alternative cathode materials with high capacity and low cost [1–6]. In recent years, Li-rich Mn-based layered oxides  $x\text{Li}_2\text{MnO}_3 \cdot (1-x)\text{LiMO}_2$  ( $M = \text{Mn, Ni, Co}$ ), which are composed of two components, monoclinic  $\text{Li}_2\text{MnO}_3$  (C/2 m) and hexagonal a- $\text{NaFeO}_2$ -structured  $\text{LiMO}_2$  (R-3 m), have been regarded as a promising candidate for cathode materials because of their higher specific capacity (about 260 mAh g<sup>-1</sup>) and higher energy density (about 1000 Wh kg<sup>-1</sup>) [7–10] compared with those of commercial cathode materials. Unfortunately, Li-rich Mn-based compounds suffer from poor cycling stability, severe voltage decay, and poor thermal stability at high voltages [11–13], among which the voltage decay is recognized as a key issue hindering their commercial applications. It is widely accepted that the voltage decay during cycling is largely related to the intrinsic phase

# *Three-dimensionally porous CoMn<sub>2</sub>O<sub>4</sub> thin films grown on Ni foams for high-performance lithium-ion battery anodes*

**Jujun Yuan, Chunhui Chen, Yong Hao, Xianke Zhang, Richa Agrawal, Chunlei Wang, Xifei Li, Youchen Hao, Bingbing Liu, Quanjun Li, et al.**

**Journal of Materials Science**  
Full Set - Includes 'Journal of Materials Science Letters'

ISSN 0022-2461  
Volume 52  
Number 10

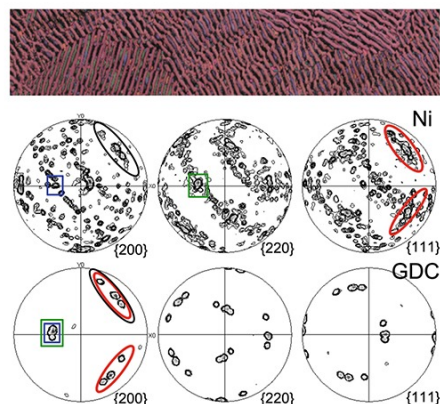
J Mater Sci (2017) 52:5751–5758  
DOI 10.1007/s10853-017-0810-6

Volume 52 • Number 10  
May 2017

## **Journal of Materials Science**

Special Section: Eutectics

Guest Editors: Elizabeth C. Dickey, Dorota A. Pawlak, Marie-Hélène Berger, Rosa I. Merino, and Ali Sayir



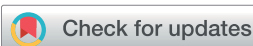
jMS

10853-52(10) 5475-6146 (2017)  
ISSN 0022-2461 (Print)  
ISSN 1573-4803 (Electronic)

Springer

 Springer

## REVIEW



Cite this: RSC Adv., 2017, 7, 35274

Received 13th April 2017  
Accepted 8th July 2017

DOI: 10.1039/c7ra04200k

rsc.li/rsc-advances

## Solubility prediction of gases in polymers based on an artificial neural network: a review

Li Mengshan,<sup>a</sup> Wu Wei,<sup>a</sup> Chen Bingsheng,<sup>a</sup> Wu Yan<sup>a</sup> and Huang Xingyuan<sup>b</sup>

As an important physical chemistry property, solubility is still a popular research topic. Its theoretical calculation method has developed rapidly. In particular, the artificial neural network (ANN) has attracted the attention of researchers because of its unique nonlinear processing ability. This review provides a brief explanation of the ANN approaches that are most commonly applied to predict gas solubility in polymers, and states the implementation principle, progress, and performance analysis of hybrid ANNs based on the intelligence algorithm. The prospect of solubility prediction based on current research trends is then proposed. This review attempts to analyze the solubility calculation method and provides an insight into and reference for the application of the artificial intelligence method in chemistry and material fields, and can expand in the future because of the increasing number of solubility prediction approaches being introduced.

### 1 Introduction

The solubility of gases in polymers is an important physico-chemical property, it is widely applied in the fields of material extraction and separation, material modification, and new



Li Mengshan received his Ph.D. in 2014. He is currently working at the Gannan Normal University (in the College of Physics and Electronic Information). He has coauthored more than 40 publications that include articles in peer-reviewed international journals, communications at national and international conferences. His research interests include polymer materials processing, polymer theoretical calculation and simulation, polymer physical chemistry, artificial intelligence, swarm intelligence algorithm and its application, and quantitative structure–activity relationship.

Wu Wei is currently a senior student at Gannan Normal University (in the College of Physics and Electronic Information). She has published about 10 peer reviewed journal articles. Her current

research interests include a swarm intelligence algorithm and its application.

Chen Bingsheng is currently working as Assistant Professor at Gannan Normal University (in the College of Physics and Electronic Information). His current research interests include polymer theoretical calculation and simulation, artificial intelligence and quantitative structure–activity relationship. He has published over 10 peer reviewed journal articles.

Wu Yan is currently working at the Gannan Normal University (in the College of Mathematics and Computer Science). She has published over 20 peer reviewed journal articles. Her current research interests include polymer theoretical calculation and simulation, swarm intelligence algorithm and its application, and quantitative structure–activity relationship.

Huang Xingyuan received his Ph.D. in 2007. He is currently working as a Professor at Nanchang University (in the College of Mechanical and Electric Engineering). He has coauthored more than 100 publications that include articles in peer-reviewed international journals and communications at national and international conferences. His research interests include polymer chemistry, polymer modification, polymer materials processing, microcellular plastics, and polymer theoretical calculation and simulation.



Cite this: RSC Adv., 2017, 7, 49817

## Prediction of supercritical carbon dioxide solubility in polymers based on hybrid artificial intelligence method integrated with the diffusion theory

Li Mengshan, \*<sup>a,b</sup> Liu Liang,<sup>a</sup> Huang Xingyuan,<sup>b</sup> Liu Hesheng,<sup>b</sup> Chen Bingsheng,<sup>a</sup> Guan Lixin<sup>a</sup> and Wu Yan<sup>a</sup>

Solubility is one of important research hotspots of physical chemistry properties and is widely utilized in the modification, synthesis and preparation of a lot of materials. To avoid the defects of traditional thermodynamic dissolution forecasting methods, according to the mass transfer features of a two-phase system, the dissolution process is simulated. In this paper, the diffusion theory is integrated into the improvement of particle swarm optimization (PSO) so that the particles in the algorithm evolve along with the diffusion energy. In this way, the improved PSO of dual-population diffusion is obtained and used to train the parameters of the radial basis function artificial neural network. Then, a prediction model for supercritical carbon dioxide solubility in polymers is proposed. The solution experiments of 8 polymers indicate that the predicted values with the model are consistent with the experimental results. The prediction accuracy is higher and the correlation is significant. The average relative error, mean square error and square correlation coefficient are respectively 0.0043, 0.0161, and 0.9954. The prediction model has a high comprehensive performance and provides the basis for the prediction, analysis and optimization of other physical and chemical fields.

Received 28th August 2017  
Accepted 18th October 2017

DOI: 10.1039/c7ra09531g  
[rsc.li/rsc-advances](http://rsc.li/rsc-advances)

### 1. Introduction

The solubility property of supercritical carbon dioxide ( $\text{ScCO}_2$ ) in a polymer is widely utilized in the modification and synthesis of materials, the preparation of new materials, and other fields.<sup>1–6</sup> Under the supercritical conditions of high temperature and high pressure, dissolution experiments are characterized by the relatively difficult operation procedure, high cost, long time, and high manpower requirements and it is not easy to get solubility data.<sup>7,8</sup> Therefore, it is of great significance to establish the precise dissolution prediction model.<sup>9,10</sup>

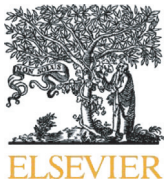
The dissolution of  $\text{ScCO}_2$  in polymers is influenced by many factors, such as temperature, pressure, density and the polarity of polymer molecules. These factors represent the extremely complex nonlinear relationships with the dissolution and are correlated with each other. Therefore, traditional thermodynamic state equation and empirical equation cannot provide the satisfactory prediction accuracy of the solubility.<sup>5,11,12</sup> Artificial neural network (ANN) has the better self-organization, tolerance and nonlinear processing abilities, which make it especially suitable for solving the problem of solubility prediction.<sup>13–16</sup> Bakhtbakhshi<sup>17</sup> and Lashkarbolooki<sup>18</sup> *et al.* compared the

solubility prediction results obtained with ANN and equations of state and indicated that ANN method was superior to the equations of state in the prediction accuracy and correlation. Gharagheizi *et al.*<sup>19</sup> predicted the solubility of various compounds in  $\text{ScCO}_2$ , indicating that the prediction accuracy and correlation of ANN were satisfactory. Eslamimanesh *et al.*<sup>20</sup> indicated that ANN had the superior prediction performance in the solubility experiment of  $\text{ScCO}_2$ . Pahlavanzadeh *et al.*<sup>21</sup> predicted the solubility with ANN and Deshmukh–Mather method and indicated that ANN was superior to the traditional thermodynamic prediction methods.

Prediction reliability and accuracy of ANN depend on its training algorithm for the optimizing the model structure and parameters. Various optimization algorithms had been developed for ANN training. Evolution algorithms are the most widely used,<sup>22</sup> including genetic algorithm,<sup>23</sup> simulated annealing algorithm, particle swarm optimization algorithm (PSO),<sup>24–26</sup> and ant colony algorithm.<sup>27</sup> Liu *et al.*<sup>28</sup> used the PSO algorithm and online strategy to train the fuzzy neural network and successfully predicted the melt index. Lazzus *et al.*<sup>29</sup> precisely predicted the phase equilibrium data of  $\text{ScCO}_2$  with PSO algorithm. The solubility prediction method of radial basis function artificial neural network and adaptive fuzzy nervous system proposed by Khajeh *et al.*<sup>30</sup> is superior to the traditional method in prediction accuracy and correlation. Hussain *et al.*<sup>31</sup> proposed the mixed neural network solution calculation model by combining Kent–Eisenberg with ANN and realized the better

<sup>a</sup>College of Physics and Electronic Information, Gannan Normal University, Ganzhou, 341000, Jiangxi, China. E-mail: jcimsli@163.com

<sup>b</sup>College of Mechanical and Electric Engineering, Nanchang University, Nanchang, 333001, Jiangxi, China



## A facile synthetic strategy to three-dimensional porous ZnCo<sub>2</sub>O<sub>4</sub> thin films on Ni foams for high-performance lithium-ion battery anodes



Jujun Yuan <sup>a,b,\*</sup>, Chunhui Chen <sup>b</sup>, Yong Hao <sup>b</sup>, Xianke Zhang <sup>a,b</sup>, Shiyong Gao <sup>c</sup>, Richa Agrawal <sup>b</sup>, Chunlei Wang <sup>b</sup>, Zuzhou Xiong <sup>a</sup>, Huajun Yu <sup>a</sup>, Yingmao Xie <sup>a</sup>

<sup>a</sup> School of Physics and Electronics, Gannan Normal University, Ganzhou 341000, PR China

<sup>b</sup> Department of Mechanical & Materials Engineering, Florida International University, Miami, FL 33174, USA

<sup>c</sup> School of Materials Science and Engineering, Harbin Institute of Technology, Harbin 150001, PR China

### ARTICLE INFO

#### Article history:

Received 1 November 2016

Received in revised form 21 January 2017

Accepted 24 January 2017

Available online 27 January 2017

#### Keywords:

ZnCo<sub>2</sub>O<sub>4</sub> film

Electrostatic spray deposition

Porous structure

Anode material

Lithium-ion battery

### ABSTRACT

Three-dimensional (3D) porous ZnCo<sub>2</sub>O<sub>4</sub> thin films on nickel foam substrates have been fabricated through a facile strategy of electrostatic spray deposition (ESD) followed by annealing in Ar atmosphere for lithium-ion battery anodes. The obtained ZnCo<sub>2</sub>O<sub>4</sub> films on Ni foams show excellent cycling performance with a reversible capacity of over 1726 mAh g<sup>-1</sup> after 100 cycles at 400 mA g<sup>-1</sup>. The ZnCo<sub>2</sub>O<sub>4</sub> electrodes also present good rate capability with 811 mAh g<sup>-1</sup> at 5 A g<sup>-1</sup>. The improved electrochemical performances should be ascribed to 3D porous ZnCo<sub>2</sub>O<sub>4</sub> architecture directly grown on Ni foam current collector, due to the synergistic advantages of offering more reaction sites, effective void space to the volume variation during cycling, and improving of electron transport. It is proposed that this facile strategy of ESD technique can be extended to synthesize other 3D porous mixed transition-metal oxide materials.

© 2017 Elsevier B.V. All rights reserved.

## 1. Introduction

In the past few years, lithium-ion batteries (LIBs) have been widely utilized as main power sources for numerous portable electronic devices and become promising energy storage systems for use in upcoming high energy area including electric vehicles (EVs), hybrid electric vehicles (HEVs), and so on [1,2]. To meet the ever-growing large energy requirements, many efforts have been devoted to develop high-performance anode materials [3–5] for replacing traditional graphene based materials with low theoretical capacity of 372 mAh g<sup>-1</sup>. Recently, transition metal oxides (TMO) such as SnO<sub>2</sub> [6], Co<sub>3</sub>O<sub>4</sub> [7,8], Mn<sub>3</sub>O<sub>4</sub> [9], and Fe<sub>3</sub>O<sub>4</sub> [10] have been widely researched for high-performance LIB anodes. Particularly, Co<sub>3</sub>O<sub>4</sub> has been considered as one of the most promising anode candidates in view of its high capacity and good rate capability [11,12]. However, the practical application of cobalt oxides is hindered owing to their disadvantages of high cost and toxicity for cobalt. Thus, partially replacing cobalt in Co<sub>3</sub>O<sub>4</sub> by cost-effective and environment-friendly metals (Zn, Mn, Ni, Cu, etc) to constitute the mixed transition-metal oxides (MTMOs) [13–20], has been regarded as ideal LIB anode materials.

Among the above MTMOs, ZnCo<sub>2</sub>O<sub>4</sub> is a quite attractive candidate for substitution of the Co<sub>3</sub>O<sub>4</sub> anode in LIBs. ZnCo<sub>2</sub>O<sub>4</sub> presents many

advantages such as lower cost, low toxicity, and high theoretical capacity (975 mAh g<sup>-1</sup>), which could be assigned to both conversion and alloying mechanisms [21,22]. Nevertheless, ZnCo<sub>2</sub>O<sub>4</sub> still suffers from fast capacity fading because of large volume variation in the process of lithiation/delithiation. Up to now, many ZnCo<sub>2</sub>O<sub>4</sub> micro/nanostructures such as nanowires [23–25], nanosheets [26,27], and hollow or porous architectures [28–34], have been synthesized to improve the cycle life and rate capability of ZnCo<sub>2</sub>O<sub>4</sub> for LIB anodes. It should be pointed that hollow or porous architecture has shown promising results for enhancing electrochemical performance of LIBs owing to the advantages of offering more reaction sites and effective void space to the volume variation during cycling. Porous and hollow ZnCo<sub>2</sub>O<sub>4</sub> structures have been fabricated through different strategies including solvothermal process [27–29], electrospinning technique [30,31], template-assistant synthesis [32,33], co-precipitation [34,35], and so on. The common weakness of hollow or porous power materials is that the electrodes were prepared through mixing carbon and polymer binder with these active materials, and fastening on current collectors, leading to an increase of “dead surface”, reduction of the reaction sites, and decrease of the electrical conductivity. It is proposed that synthesizing hollow or porous ZnCo<sub>2</sub>O<sub>4</sub> structures directly on the current collector will be promising method to resolve the problem.

Electrostatic spray deposition (ESD) technique has been regarded as a simple and facile method for fabricating binder-free film of metal oxide electrodes with porous structures for LIBs [36–38]. However, there are few researches on the preparation of MTMOs film using ESD

\* Corresponding author at: School of Physics and Electronics, Gannan Normal University, Ganzhou 341000, PR China

E-mail addresses: [yuanjyun@aliyun.com](mailto:yuanjyun@aliyun.com) (J. Yuan), [Wangc@fiu.edu](mailto:Wangc@fiu.edu) (C. Wang).



## Retrieval of leaf chlorophyll content in Gannan navel orange based on fusing hyperspectral vegetation indices using machine learning algorithms

**Suyun Lian<sup>1</sup> Lixin Guan<sup>1\*</sup> Zhongzheng Peng<sup>2</sup> Gui Zeng<sup>1</sup> Mengshan Li<sup>1</sup> Yin Xu<sup>1</sup>**

<sup>1</sup>Intelligent Control Engineering & Technology Research Center, Gannan Normal University, 341000, Ganzhou, China. E-mail: lxguan@gnnu.edu.cn.

\*Corresponding author.

<sup>2</sup>Nanjing University of Information Science and Technology, Nanjing, China.

**ABSTRACT:** Estimating leaf chlorophyll contents through leaf reflectance spectra is efficient and nondestructive. The literature base regarding optical indices (particularly chlorophyll indices) is wide ranging and extensive. However, it is without much consensus regarding robust indices for Gannan navel orange. To address this problem, this study investigated the performance of 19 published indices using RDS (raw data spectrum), FDS (first derivative data spectrum) and SDS (second derivative data spectrum) for the estimation of chlorophyll content in navel orange leaves. The single spectral index and combination of multiple spectral indices were compared for their accuracy in predicting chlorophyll *a* content ( $Chl_a$ ), chlorophyll *b* content ( $Chl_b$ ) and total chlorophyll content ( $Chl_{tot}$ ) content in navel orange leaves by using partial least square regression (PLSR), adaboost regression (AR), random forest regression (RFR), decision tree regression (DTR) and support vector machine regression (SVMR) models. Through the comparison of the above data in three datasets, the optimal modeling data set is RDS data, followed by FDS data, and the worst is SDS data. In modeling with multiple spectral indices, good results were obtained for  $Chl_a$  (NDVI750, NDVI800),  $Chl_b$  (Datt, DD, Gitelson 2) and  $Chl_{tot}$  (Datt, DD, Gitelson2) by corresponding index combinations. Overall, we can find that the AR is also the best regression method judging by prediction performance from the results of single spectral index models and multiple spectral indices models. In comparison, result of multiple spectral indices models is better than single spectral index models in predicting  $Chl_a$  and  $Chl_{tot}$  content using FDS data and SDS data, respectively.

**Key words:** chlorophyll content, spectral index, regression, Gannan navel orange.

## Recuperação do teor de clorofila de folhas em laranja do umbigo Gannan com base na fusão de índices de vegetação hiperespectral usando algoritmos de inteligência artificial

**RESUMO:** Estimar os teores de clorofila foliar através de espectros de refletância foliar é eficiente e não destrutivo, a base da literatura sobre índices ópticos (principalmente índices de clorofila) é ampla e extensa. No entanto, não há muito consenso sobre índices robustos para a laranja de Gannan. O estudo investigou o desempenho de 19 índices publicados usando RDS (espectro de dados brutos), FDS (espectro de dados de primeira derivada) e SDS (espectro de dados de segunda derivada) para a estimativa do teor de clorofila em folhas de laranja de umbigo. Os índices espectrais foram comparados quanto à sua precisão na previsão do teor de clorofila *a* ( $Chla$ ), teor de clorofila *b* ( $Chlb$ ) e teor de clorofila total ( $Chltot$ ) em folhas de laranja de umbigo usando regressão dos mínimos quadrados parcial (PLSR), regressão adaboost (AR), modelos de regressão de floresta aleatória (RFR), regressão de árvore de decisão (DTR) e regressão de máquina de vetor de suporte (SVMR). Através da comparação dos dados acima em três conjuntos de dados, o conjunto de dados de modelagem ideal são os dados RDS, seguidos pelos dados FDS, e o pior são os dados SDS. Na modelagem com vários índices espectrais, bons resultados foram obtidos para  $Chla$  (NDVI750, NDVI800),  $Chlb$  (Datt, DD, Gitelson 2) e  $Chltot$  (Datt, DD, Gitelson2) por combinações de índices correspondentes. No geral, podemos descobrir que o AR também é o melhor método de regressão a julgar pelo desempenho de previsão dos resultados de modelos de índice espectral único e modelos de índices espectrais múltiplos. Em comparação, o resultado de modelos de índices espectrais múltiplos é melhor do que os modelos de índices espectrais únicos na previsão do conteúdo de  $Chla$  e  $Chltot$  usando dados FDS e dados SDS, respectivamente.

**Palavras-chave:** teor de clorofila, índice espectral, regressão, Gannan laranja umbigo.

## INTRODUCTION

Gannan navel orange is a national geographical indication product of China. It is of high quality, rich in essential nutrients and enjoys the reputation of Chinese famous fruit. As a major indicator of nutrients, chlorophyll content is involved

in various biochemical and physiological processes that are vital for navel orange production. Real-time and non-destructive assessment of navel orange chlorophyll content is important for evaluating crop productivity and improving the precise management of N(LI et al., 2016). Although, traditional measurement of chlorophyll content via wet chemistry methods



# Cold atmospheric plasma: an effective approach for fast benazoxystrobin degradation via generating reactive oxygen species

Yuxiang Wang<sup>a,b</sup>, Xingquan Wang<sup>b</sup> and Xiaofeng Dai<sup>a</sup>

<sup>a</sup>Wuxi School of Medicine, Jiangnan University, Wuxi, China; <sup>b</sup>School of Physics and Electronic Information, Gannan Normal University, Ganzhou, China

## ABSTRACT

Cold atmospheric plasma (CAP) has demonstrated its efficacy in degrading organophosphorus or organochlorine pesticide residues without generating secondary pollution. Yet its potential in degrading triazole pesticides and methoxyacrylate pesticides that are gaining popularities in more and more countries remains unexplored. Using benazoxystrobin as the modelling molecule to be degraded, we demonstrated in this paper that CAP could effectively degrade triazole or methoxyacrylate pesticides, with the efficacy being influenced by many factors such as the voltage, flow rate, and frequency. Specifically, CAP could effectively degrade benazoxystrobin via destroying the benzene ring structure; the degradation efficacy can reach 90%, with 'ionized oxygen', '60 V voltage' '2 L min<sup>-1</sup> oxygen flow rate' and '9 min treatment duration' being associated with the optimal degradation effect; active CAP articles capable of degrading benazoxystrobin are enriched with ROS, where more oxygen is needed to degrade higher concentration of benazoxystrobin. Our study, for the first time, showed the efficacy of CAP in degrading triazole and methoxyacrylate type of pesticides, providing experimental support for its industrial translation.

## ARTICLE HISTORY

Received 8 September 2021  
Accepted 25 October 2021

## KEYWORDS

Benazoxystrobin; cold atmospheric plasma; pesticide degradation; solubility

## 1. Introduction

Pesticides are natural or synthetic chemicals used in agricultural production to control harmful insects [1,2]. The use of pesticides could be dated back before Christ when sulphur fumigation was used to kill agricultural pests in ancient Greece. Pesticides were firstly commercialised in Europe, and widely used globally in the 1940s. Nowadays, most pesticides used are organic synthetic pesticides due to their wide spectrum of targeted insects and efficacy in rapid insets killing [3]. Although these pesticides play prominent roles in protecting crops from insect damage, natural pollutions imposed by residual pesticides raised significant global concern since the mid-20<sup>th</sup> century [4]. It has been gradually recognised that pesticide residues are harmful to human liver and the nervous system [5], and may impose greater threat to human health if they flowed into the sewer. In January 2021, Switzerland [6], being one of the largest global pesticide exporters,

**CONTACT** Xiaofeng Dai  [xiaofeng.dai@jiangnan.edu.cn](mailto:xiaofeng.dai@jiangnan.edu.cn); [xiaofengteam@163.com](mailto:xiaofengteam@163.com)

This article has been republished with minor changes. These changes do not impact the academic content of the article.

© 2021 Informa UK Limited, trading as Taylor & Francis Group

**Materials Science inc. Nanomaterials & Polymers**

# Prediction of Carbon Dioxide Solubility in Polymers Based on Adaptive Particle Swarm Optimization and Least Squares Support Vector Machine

Huijie Chen, Ming Zeng, Hang Zhang, Bingsheng Chen, Lixin Guan, and Mengshan Li<sup>\*[a]</sup>

Solubility is a significant physical and chemical property. The solubility of carbon dioxide( $\text{CO}_2$ ) in polymers is an important application of green chemistry. Aimed at the problem of insufficient precision of the existing prediction model, a solubility prediction model based on the adaptive particle swarm optimization algorithm and the least-squares support vector machine(APSO-LSSVM) is proposed. Different from the traditional particle swarm algorithm, APSO algorithm improves the problem of easily falling into local optimal solution. The regularization parameters and kernel function tuning parameters of the LSSVM were optimized by APSO and then use this model to predict the solubility of  $\text{CO}_2$  in eight polymers within

a wide range of temperatures and pressures. APSO-LSSVM model has great prediction ability, with a good correlation between prediction data and experimental data, high prediction accuracy, short calculation time and strong stability. Compared with back propagation artificial neural network(BP ANN), back propagation-particle swarm optimization algorithm artificial neural network(BP-PSO ANN) and LSSVM, APSO-LSSVM has better comprehensive performance. The average absolute relative deviation(AARD), root mean square error(RMSE), determination coefficient( $R^2$ ) were respectively 0.2130, 0.0120, 0.9853. In addition, the model has good expansibility and can be applied to other fields such as chemistry and medicine.

## 1. Introduction

Polymer plays an important role in industrial production and is an essential part of our daily life.  $\text{CO}_2$  is easy to prepare, often used in polymer synthesis and processing,<sup>[1]</sup> and shows strong potential in green chemistry.<sup>[2,3]</sup> Therefore, the solubility of  $\text{CO}_2$  in polymers has been a hot research topic.

In the past few decades, there have been many methods to calculate and predict the solubility of  $\text{CO}_2$  in polymers. Firstly, there are some methods based on theoretical calculations, such as perturbation hard chain theory, lattice fluid theory and cubic equation of state, etc.<sup>[4-6]</sup> and many scientists calculate solubility by experimental methods, such as phase separation, chromatography, gravimetric methods, volumetric methods, pressure attenuation methods, etc.<sup>[7,8]</sup> However, under the limited conditions of high temperature and high pressure, it is difficult for the experimental equipment and technology to meet the requirements of the experiment, resulting in inaccurate experimental results, low efficiency, and a waste of economic and time costs. In addition, the solubility of  $\text{CO}_2$  in polymers is affected by many factors, and the relationship between dissolution factors and dissolution behavior is nonlinear. Therefore, traditional methods have been unable to meet the needs.

In recent years, scientists have made great efforts to solve this problem by using advanced intelligent algorithms instead

of traditional methods. Khajeh et al.<sup>[9]</sup> proposed an adaptive neuro-fuzzy reasoning system (ANFIS) for predicting the solubility of  $\text{CO}_2$  in six different polymers and proved that this method has better accuracy than traditional methods. Eslamimanesh and Gharagheizi et al.<sup>[10,11]</sup> put forward an optimized three-layer feedforward neural network to predict the solubility of supercritical carbon dioxide(SCCO<sub>2</sub>) in 24 commonly used ionic liquids and 21 commonly used industrial solid compounds, respectively. The results showed that the prediction ability of this model is better than the traditional thermodynamic model. Lashkarbolooki et al.<sup>[12]</sup> established a feed-forward multilayer perceptron neural network (MLPNN) model to predict the solubility of SCCO<sub>2</sub> in aromatic hydrocarbons and other compounds. It proved that the prediction effect of the artificial neural network model is more accurate than the state equation. Soleimani et al.<sup>[13]</sup> proposed a new solubility prediction model based on decision tree called random gradient lifting algorithm, which predicted the solubility of  $\text{CO}_2$  in 13 different polymers. Compared with 17 different machine learning algorithms and equation of state models, it was found that the proposed model had higher accuracy than other methods.

The training process of the neural networks can be considered as a classical optimization problem. The emergence of the swarm intelligence optimization algorithm makes the neural network model have a broader development space. As an algorithm with strong global search ability in swarm intelligence optimization algorithm, PSO algorithm has the advantages of few parameters and easy to implement, which is used and improved by the majority of researchers. Ahmadi et al.<sup>[14]</sup> proposed a reservoir asphaltene precipitation predic-

[a] H. Chen, M. Zeng, H. Zhang, Dr. B. Chen, Dr. L. Guan, Dr. M. Li  
College of Physics and Electronic Information,  
Gannan Normal University,  
Ganzhou, Jiangxi 341000, China  
E-mail: jcimsli@163.com

To read the full version of this content please select one of the options below:

[Add to cart](#)

¥260.00 (excl. tax)  
30 days to view and  
download

[Access through your institution](#)[Access and purchase options ▾](#)

## A half-bridge IGBT drive and protection circuit in dielectric barrier discharge power supply

[Xingquan Wang, Xiuyuan Lu, Wei Chen, Fengpeng Wang, Jun Huang, Lingli Liu, Mengchao Li, Kui Lin](#) ▾

[Circuit World](#)

ISSN: 0305-6120

Article publication date: 29 July 2021

[Reprints & Permissions](#)

Issue publication date: 24 November 2022

### DOWNLOADS



42

## Abstract

### Purpose

This paper aims to improve the general circuit of driving and protection based on insulated gate bipolar transistor (IGBT) in dielectric barrier discharge power supply by designing a novel half-bridge inverter circuit with discrete components.

### Design/methodology/approach

With one SG3524 chip, the structure based on discrete components is used to design the IGBT drive circuit. The driving waveform is isolated and sent out by photo-coupler 6N137. The protection circuit is realized by Hall sensor directly detecting the main circuit current, supplemented by a few components, including diodes, resistors, capacitors and triodes. It improves the reliability of the protection circuit.

### Findings

In the driving circuit, the phase difference of signals from two channels are 180°. Moreover, when the duty cycle is set at 40%, it can ensure sufficient pulse width modulation response time. In the protection circuit, when over-current occurs, an intermittent output signal is automatically sent out. Furthermore, the over-current response time can be controlled independently. The peak voltage can be adjusted continuously from 0 to 30 kV with its frequency from 8 to 25 kHz and the power output up to 150 W.

### Originality/value

The novel circuit of driving and protection makes not only its structure simpler and easier to be realized but also key parameters, such as frequency, the duty cycle and the driving voltage, continuously adjustable. Moreover, the power supply is suitable for other discharges such as corona discharge and jet discharge.

## Keywords

[IGBT](#)[Dielectric barrier discharge](#)[Drive circuit](#)[Inverter power supply](#)[Protection circuit](#)



Paper

# DOA Estimation of Multipath Signals in the Presence of Gain-Phase Errors Using an Auxiliary Source

Zhangsheng Wang\*, Non-member

Wei Xie\*\*<sup>a</sup>, Non-member

Qun Wan\*, Non-member

In this paper, we address the problem of direction-of-arrival (DOA) estimation of multipath signals in the presence of gain-phase uncertainties using an auxiliary source (AS) with uniform rectangular array. Based on the assumption that the waveform of the AS is a known prior, and the signal of the AS impinges on the array without multipath propagation, a two-step algorithm is proposed to estimate the DOAs along with the fading coefficients and gain-phase errors. First, a coarse estimation is obtained by extending the traditional spatial smoothing-based ESPRIT algorithm. Second, in order to overcome the performance deterioration due to a reduction of the effective array aperture, an alternate iterative algorithm is proposed. Meanwhile, the relevant stochastic Cramér-Rao bound (CRB) is also derived. Simulation results show that the proposed method is capable of approaching the stochastic CRB when the signal-noise ratio (SNR) of the AS is large enough and is greater than the SNR of the unknown source. © 2019 Institute of Electrical Engineers of Japan. Published by John Wiley & Sons, Inc.

**Keywords:** direction-of-arrival estimation; uniform rectangular array; multipath propagation; coherent signals; sensor gain-phase uncertainties

Received 5 June 2018; Revised 24 October 2018

## 1. Introduction

The problem of direction-of-arrival (DOA) estimation using an array of antennas is frequently encountered in many application areas, such as radar, sonar and wireless communications [1]. Over the last few decades, numerous high-resolution techniques, such as the subspace methods (see Ref. [1] and references therein), sparse representation methods [2–5] and maximum likelihood (ML) algorithms [6,7], have been proposed for estimating the DOAs of multiple narrowband far-field signals. However, most of the high-resolution methods may fail to work in real environments when the sensor gain-phase responses are not precisely known and/or there exist coherent incident signals due to multipath propagation.

Most of the sparse representation methods [2–5] and the ML methods [6,7] apply to the coherent signals, but they are limited by off-grid problem, parameter selection problem or high computational complexity. Although some attempts [8–10] have been made to overcome these limitations, they are not capable of coping with large sensor gain-phase uncertainties. Compared with the ML methods and the sparse representation methods, the subspace methods have attained considerable attention because of their good compromise between estimation performance and computational complexity. Numerous effective subspace methods have been proposed to solve the coherency problem or the problem of sensor gain-phase uncertainties. In solving the rank deficiency problem, the forward/backward spatial smoothing (FBSS) preprocessing [11] is a simple but efficient technique. Based on smoothed array data, all the high-resolution algorithms can be directly used to solve the DOA estimation problem. For sensor gain-phase uncertainties, there are two categories, the precalibration methods [12,13] and

the autocalibration techniques [14–20]. The precalibration methods commonly use auxiliary sources (ASs) with known DOAs. If the DOAs are precisely known, these methods can achieve excellent estimation performance. The autocalibration methods jointly estimate the parameters of DOAs and sensor gain-phase errors. The methods in [14–19], designed for non-uniform linear array (ULA) with certain conditions [21], estimate these parameters based on the eigenstructure of (modified) array covariance, where the iterative methods [16–19] apply to small array perturbations, and the non-iterative methods [14,15] apply to a small number of incident signals regardless of the degree of array perturbations. The methods specially designed for ULA [18,19] or uniform rectangular array (URA) [20] do not need iteration and are capable of handling large perturbations (there is an unidentifiable rotation factor for estimating sensor phase errors and DOAs (see [22] for a ULA case and [20] for a URA case).

While the problems of coherent signals and sensor gain-phase uncertainties have been extensively studied, the DOA estimation problem of coherent signals in the presence of sensor gain-phase uncertainties has not been given enough concern and research. In this paper, we propose to use an AS to cope with the problem of coexistence of coherent signals and sensor gain-phase uncertainties, and one-dimensional (1-D) DOA estimation using a URA is considered. Other than the DOA, the waveform of AS is assumed to be a known prior as an accurate DOA is not easily available in the real environment. Based on the known waveform, a modified FBSS-based ESPRIT algorithm is presented for estimating the DOAs. It is noted that the proposed DOA estimator is independent from the sensor gain-phase errors, and the DOAs are obtained in closed-form. Meanwhile, the unambiguity condition is also analyzed. To solve the performance deterioration caused by FBSS preprocessing, an alternate iteration method is presented. The fading coefficients and sensor gain-phase errors are obtained along with the refined DOAs. Finally, we also derive the corresponding stochastic Cramér-Rao bound (CRB) to which we compare the performance of the proposed method. Numerical examples are provided to verify the effectiveness of the proposed

<sup>a</sup> Correspondence to: Wei Xie. E-mail: raysheik@foxmail.com

\*Department of Electronic Engineering, University of Electronic Science and Technology of China, Chengdu 611731, China

\*\*Department of aerospace, Southwest China Institute of Electronic Technology, Chengdu 610036, China